Molecular analysis of vesicle biogenesis during autophagy

Dissertation

zur Erlangung des Doktorgrades
der Mathematisch-Naturwissenschaftlichen Fakultät
der Georg-August-Universität zu Göttingen

vorgelegt von

Sebastian Bremer

aus Hannover

Göttingen 2009

Members of the thesis committee:
Advisor: Prof. Dr. M. Thumm
Institut für Biochemie II, Zentrum Biochemie und Molekulare Zellbiologie
Georg-Auguts-Üniversität, Göttingen

Co-advisor: Prof. Dr. G. H. Braus
Institut fr Mikrobiologie und Genetik
Georg-Auguts-Üniversität, Göttingen

Dr. D. Fasshauer
Abteilung Neurobiologie
Max-Planck-Institut für biophysikalische Chemie, Göttingen

I hereby declare that this thesis has been written independently and with no other sources and aids than quoted.

I. Contents

II. List of figures

III. List of tables

IV. Abbreviations

Abbreviation	
- HIS	Without histidine
- LEU	Without leucine
- URA	Without uracil
+ KAN	Containing kanamycin
+ NAT	Containing nourseotricine
°C	Degree Celsius
aa	Amino acid(s)
Amp	Ampicillin
Ape1p	Aminopeptidase 1
APS	Ammonium persulfate
ATP	Adenosine 5`-triphosphate
BSA	Bovine serum albumine
clonNAT	Nourseotricine
CMAC	7-amino-4-chloromethylcoumarin
CPY	Carboxypeptidase Y (Pcr1)
ct	Control
ddH$_2$O	Double distilled water
DMSO	Dimethylsulfoxide
DNA	Deoxyribonucleic acid
dNTPs	Deoxynucleosidetriphosphate (dATP, dGTP, dCTP, dTTP)
DTT	Dithiothreitol
E. coli	*Echerichia coli*
e.g.	for example
EDTA	Ethylenediamintetraacetate-Disodium salt
ER	Endoplasmic Reticulum
EtOH	Ethanol
Fig.	Figure
g	Gram
g	Gravity

Abbreviation

GFP	Green fluorescent protein
Gluc	Glucose
h	Hour(s)
HRP	Horseradish-Peroxidase
Ig	Immunoglobulin
IPTG	Isopropyl-α-D-Thiogalactopyranoside
KAc	Potassium acetate
kbp	Kilobase pair(s)
kDa	Kilodalton
l	Liter
M	Molar
mA	Milliampere
mg	Milligram
min	Minute(s)
MIPA	Micropexophagy-specific membrane apparatus
ml	Milliliter
mM	Millimolar
MVB	Multi vesicular body
NAT	Nourseotricine (clonNAT)
NLS	Nuclear localization sequence
nm	Nanometer
NSF	N-ethylmaleimide-sensitive factor
NV-junction	Nucleus-vacuole junction
OD	Optical density
PAGE	Poly-acrylamide gel electrophoresis
pApe1	Precursor aminopeptidase I
PAS	pre- autophagosomal structure
PCR	Polymerase chain reaction
PE	Phosphatidylethanolamine
pH	Negative logarithm of H^+ concentration
PMSF	Phenylmethylsulfonylfluoride

Abbreviation	
PVDF	Polyvinylidene Fluoride
RAPA	Rapamycine
rpm	Rounds per minute
rt	Room temperature
S. cerevisiae	*Saccharomyces cerevisiae*
SDS	Sodium Dodecyl Sulfate
sec	Second(s)
sec	Secretory pathway
SED	Standard Error of the Difference
SMP	Skim milk powder
SNARE	Soluble NSF attachment receptors
sup	Supernatant
TAE	Tris-acetate-EDTA-buffer
TBS	Tris buffer saline
TCA	Trichloroacatic acid
TEMED	N,N,N´,N´-Tetramethylethylenediamine
TGN	Trans Golgi network
TOR	Target of rapamycin
U	Units
UV	Ultraviolet
V	Volt
v / v	(Volume/volume)
w / o	Without
w / v	(Weight/volume)
wt	Wild type
YPD	Yeast Peptone Dextrose
μ	Micro

1. Summary

Autophagy in *Saccharomyces cerevisiae* comprises diverse processes that transport cytoplasm and even organelles into the vacuolar lumen for degradation. During macroautophagy out of the pre- autophagosomal structure (PAS) autophagosomes are formed that fuse with the vacuole for degradation. During microautophagy cargo is directly engulfed by the vacuolar membrane.

One aim of this study was to identify membrane sources needed for the formation of autophagosomes out of the PAS. Atg9 a transmembrane protein has been proposed to cycle between the PAS and a peripheral pool that may serve as a membrane source. In *S. cerevisiae* this pool has been described to colocalize in part with mitochondria. This was questioned in mammalian cells where this peripheral pool colocalizes with the trans Golgi network and endosomes.

Another suitable candidate to follow the membrane flow is Atg8 that is covalently coupled to membranes via phosphatidylethanolamine (PE).

This study describes for the first time a peripheral pool of Atg8 located at endosomes. Its formation is dependent on Atg1 and Atg27 as described for the Atg9 peripheral pool. Atg8 is conjugated to PE at the peripheral pool.

Micronucleophagy (piecemeal microautophagy of the nucleus; PMN) occurs at nucleus-vacuole (NV) junctions and results in the pinching-off and release of nonessential portions of the nucleus into the vacuole. In contrast to previous published results Krick et al. showed in a recent publication that PMN requires the core macroautophagy genes. They analysed the degradation of the PMN marker protein GFP-Osh1 by quantifying the release of hydrolase resistant free GFP in the vacuole using immuno-western blot analysis. In this study a microscopic assay was established which supports the finding that PMN is efficiently inhibited in *atg* mutant cells. A nuclear resident fluorescent protein (NLS-mCherry) is used as marker protein. Part of this fluorescent protein pinch-off the nucleus dependent on the autophagic machinery and is degraded in the vacuole.

The release of PMN vesicles at the NV-junctions requires at least three membrane fusion events. Krick et al. reported that the standard homotypic vacuolar fusion machinery is not required for the formation of PMN vesicles. This study indicates the requirement of Cdc48 and its major substrate-recruiting factor Shp1 for efficient PMN

as well as macroautophagy. The human homologues of Cdc48 / Shp1 p97 / p47 are involved in human mitotic Golgi reassembly. This p97 / p47 complex is thought to extract a monoubiquitylated fusion inhibitor out of membranes and thereby mediate fusion. In this study the involvement of monoubiquitin in PMN as well as macroautophagy could be shown in *S. cerevisiae*.

The ubiquitin deconjugation enzyme Ubp3 and its cofactor Bre5 are also required for PMN but not for the Cvt-pathway or autophagy. The *vps* class E genes *vps27* and *vps28* are also exclusively required for PMN.

So far the fusion of the edges of double-membrane structures leading to autophagosomes was dubious, since neither NSF / Sec18 nor t-SNARES are required. Therefore a novel membrane fusion machinery requiring the Atg proteins has been proposed. In contrast this work supports the function of the previously excluded AAA$^+$ ATPase Cdc48 in autophagic membrane fusion events.

2. Introduction

2.1 Yeast as model organism

The baker's yeast *Saccharomyces cerevisiae* belongs to the budding fungi. It is a single cell organism that has the typical compartment structure of eukaryotic cells like endoplasmic reticulum (ER), Golgi apparatus, peroxisomes, mitochondria, nucleus and vacuole (a homologue to the animal lysosome). *S. cerevisiae* cells have a simple lifespan. Two haploid yeast cells with different mating type (a and α) can mate and form a diploid cell. The diploid cells use mitotic division to bud. Under starvation conditions a meiotic cell division occurs. In this step asci are formed containing 4 haploid spores. These asco-spores are more resistant to environmental influences. A change of growth conditions leads to budding of the spores as haploid yeast cells (Fig. 1).
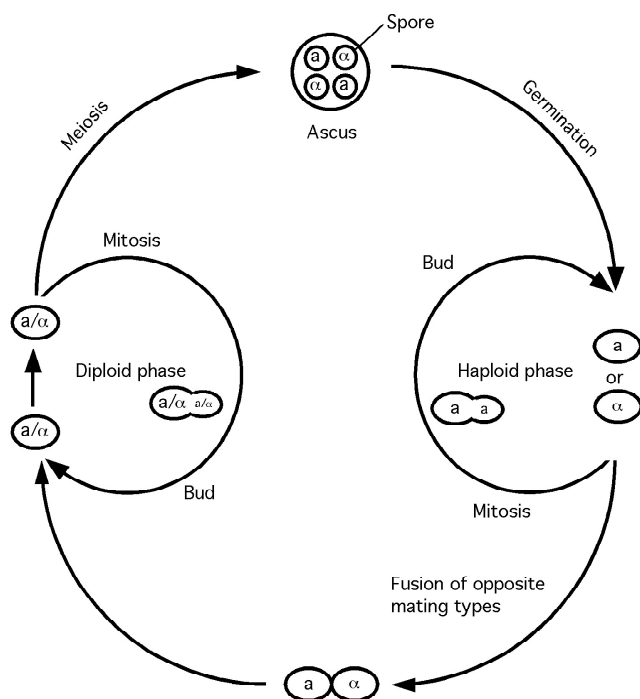
Fig. 1 Life cycle of *Saccharomyces cerevisiae*

S. cerevisiae has 16 chromosomes consisting of 14 million basepairs with about 6000 open reading frames (Goffeau, 1996). It is an ideal model organism for molecular genetics because of its haploid genome that can be easily modified genetically, its structured cellular compartments and only 90 min doubling time. Information gained in *S. cerevisiae* can often be transferred to higher eukaryotes.

2.2 The yeast vacuole

The yeast vacuole is analogue to lysosomes in mammalian cells. It has an acetic pH and is rich in hydrolases. The yeast vacuole is the biggest organelle, occupying up to 60% of the cell volume.

It is involved in a wide variety of physiological processes, including pH and osmoregulation of the cell. During nitrogen starvation, amino acids are obtained by protein degradation in the vacuole. Diploid yeast cells lacking protease activities fail to sporulate. This indicates the importance of vacuolar proteolysis for survival and differentiation (Raymond, 1992).

2.3 Delivery of proteins to the vacole

Proteins can reach the vacuole by four transport routes: secretory pathway, endocytosis, multivesicular body (MVB) and autophagic pathways. Vacuolar resident proteins are either transported by the secretory, the MVB or the cytoplasm to vacuole targeting (Cvt) pathway, a selective variant of autophagy. Endocytosis and autophagic processes transport proteins and whole organelles destined for degradation to the vacuole.

2.4 The secretory pathway

In eukaryotic cells the secretory pathway is used to sort and transport proteins from their site of synthesis to several intracellular organelles, the plasma membrane or the periplasm. Proteins are synthesized on ER-bound ribosomes and translocated into the lumen of the ER. These proteins have an amino terminal clevage or non-cleavage internal hydrophobic signal which targets the proteins to the ER membrane (Rapoport, 1996). Cleavage of the signal sequence releases the proteins into the ER lumen. N-liked carbohydrate addition occurs co-translationally. Proteins are then transported via vesicles to the Golgi complex, where they undergo additional post-translational modifications of the carbohydrate side chains before their transport to the trans-Golgi network.

2.5. Autophagy

In eukaryotes autophagy is a highly conserved process. It has been morphologically identified in the 1960s in mammalian cells. One breakthrough studying the molecular basis of autophagy was the identification of the first genes involved in this process (Tsukada and Ohsumi, 1993) (Thumm, 1994) in *S. cerevisiae*. These genes were termed autophagy-related (ATG) genes (Klionsky, 2003). Further ATG genes have been discovered studying cytoplasm to vacuole targeting (Cvt) pathway and pexophagy (peroxisome degradation) in *S. cerevisiae* and *Pichia pastoris* (Harding, 1995) (Yuan, 1997).

Up to now 31 ATG genes have been identified and most of them are required for all autophagic processes (except chaperone-mediated autophagy).

2.5.1 Relevance of autophagy in eukaryots

Cellular growth and cell development require well regulated protein synthesis as well as degradation. Eukaryotic cells have two different protein degradation pathways: the ubiquitin-proteasome degradation system and autophagy. Proteasomal degradation is constantly active and degrades short-lived proteins, which are polyubiquitinated. Autophagy in contrast is induced by nutrient limitation and degrades unselective cellular proteins and whole organelles. The recycling of these non-essential protein components allows the cell to synthesize proteins that are essential for survival under nutrient limited conditions. Besides cellular homeostasis (Yorimitsu and Klionsky, 2005), autophagy is involved in cellular processes like autophagic programmed cell death (Yu, 2006), organelle homeostasis (Monastyrska and Klionsky, 2006), developmental processes (Ma, 2007) or ageing (Levine and Kroemer, 2009) (Mariño and López-Otín, 2008).

Autophagy is also implicated in many human diseases, like breast, ovarian and prostate cancer (Chen and Karantza-Wadsworth, 2009), pathogen infections (Orvedahl and Levine, 2009), fungal pathogens (Palmer, 2008), cardiomyopathy (Nishida, 2009) and neurodegenerative diseases like Alzheimer´s, Parkinson´s and Huntington´s (Rubinsztein, 2005).

2.5.2 Autophagic processes

Autophagic processes can be divided in three fundamentally different subtypes (Fig. 2): microautophagy, macroautophagiy and chaperone-mediated autophagy. For macroautophagic processes double membrane-layered vesicles are formed which contain diverse cargos (chapter 3.5.11). By fusion with the vacuolar membrane, a still monolayered vesicle is released into the vacuole, where it is degraded (chapter 3.5.12.).

During microautophagic processes invaginations of the vacuolar membrane are formed (chapter 3.5.15, 3.5.16 and 3.5.18). Chaperone-mediated autophagy is a mechanism allowing the degradation of cytosolic proteins via a protein complex in the lysosomal membrane (chapter 3.5.14) (Massey, 2004), (Majeski and Dice, 2004).
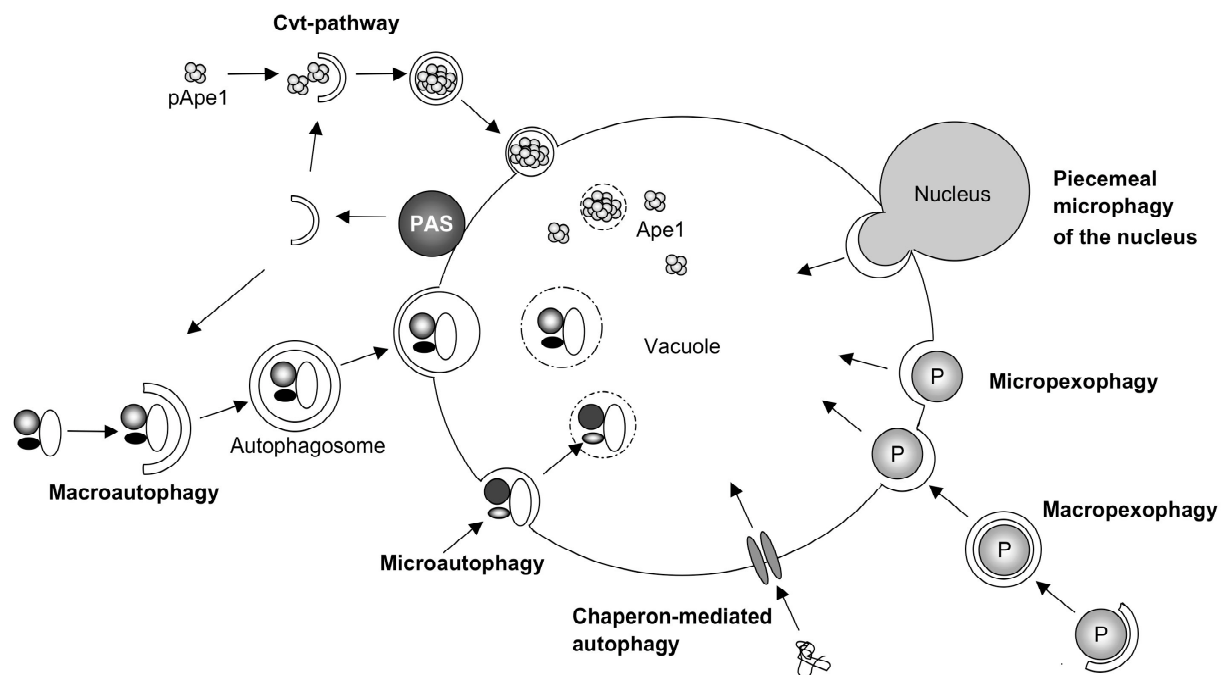
Fig. 2 Schematic diagram of autophagy-related pathways
((Huang and Klionsky, 2007) (Mühe, 2007); modified)

2.5.3 The autophagic machinery

The molecular machinerie of autophagy identified in yeast is also conserved in other eukaryotic cells. In *S. cerevisiae* the autophagic process can be separated into different steps: induction, vesicle nucleation, cargo recognition (for specific types of autophagy) and packaging, vesicle expansion and completion, Atg protein cycling, vesicle fusion with the vacuole, vesicle breakdown and cargo recycling. For example,

the Atg1 kinase complex is involved in induction, Atg11 and Atg19 are required for cargo recognition, Atg8 and Atg12 ubiquitin like conjugation systems are involved in vesicle formation and Atg23 and Atg27 are proteins participating in the Atg9 cycling step (Yorimitsu and Klionsky, 2005) (Xie and Klionsky, 2007).

2.5.4 The pre-autophagosomal structure (PAS)

Fluorescence microscopy has shown that most Atg proteins localize to the pre-autophagosomal structure (PAS), which is considered to be the site of Cvt vesicle and autophagosome formation (Suzuki, 2001) (Suzuki, 2007). 16 ATG genes are essential for autophagosome formation (Atg1-Atg18 except Atg11 and Atg15) and all of these proteins show a PAS localization.

2.5.5 Regulation and induction of autophagy

Autophagy occurs at a basal level in growing cells but is induced by nutrient starvation, including nitrogen and carbon depletion. The protein kinase target of rapamycin (Tor) is a regulator that responds to the nitrogen level. Under nutrient-rich conditions, Tor kinase is active and inhibits autophagy, whereas Tor is inactive under nutrient-deficient conditions and autophagy is induced (Fig. 3). Tor kinase regulates the phosphorylation state of Atg13, which is important for the formation of the Atg1-Atg13 complex. Atg13 is required for autophagy but not necessary for the Cvt-pathway (Funakoshi, 1997) in contrast Atg1, a serine / threonine protein kinase, is essential for both, the Cvt-pathway and autophagy. For Atg1 and its kinase activity a more regulatory (Kamada, 2000) or structural role (Abeliovich, 2003) has been proposed, but this is still under debate. The Atg1-Atg13 complex interacts with several proteins as Vac8, Atg11, Atg20, Atg24 and Atg17, that is only strictly required for autophagy. But in *atg17Δ* cells the size of the vesicles is reduced from 300 - 600 nm to 200 nm, causing a dramatic reduction in bulk autophagy because Atg17 acts as a scaffold protein in PAS organization (chapter 3.5.10 and 3.5.11) (Kabeya, 2005) (Cheong, 2005) (Suzuki, 2007). The interaction of Atg1-Atg13-Atg17 seems to be involved in size determination of the vesicles (Yorimitsu and Klionsky, 2005). The interaction of Atg17 with Atg29 and Atg31, both autophagy specific genes, has an

essential function in the organisation of the PAS for autophagosome formation (Kawamata, 2008). Atg11 is only required for the Cvt-pathway.
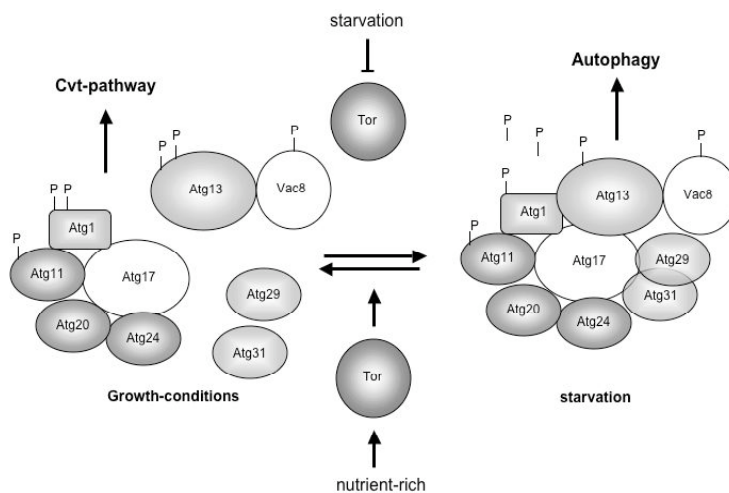
Fig. 3 Regulatory complex for autophagy induction
Atg20, Atg24, Atg11 and Vac8 might also be involved in autophagic induction, but a complete holo-complex has not been identified. ((Yorimitsu and Klionsky, 2005); modified)

2.5.6 The two ubiquitin like conjugation systems

Both ubiquitin like conjugation systems are highly conserved in eukaryots and required for the biogenesis of autophagosomes.

2.5.6.1 The Atg8-phosphatidylethanolamine conjugation system

Atg8 consists of 117 amino acids and has a molecular weight of 13.6 kDa. Homologues of Atg8 are found from yeast to human (Lang, 1998) (Elazar, 2003). The structures of the mammalian homologues revealed that Atg8 family members contain two domains: an N-terminal helical domain (NHD; aa 1 - 24) and a C-terminal ubiquitin-like domain (ULD; aa 24 -117) (Fig. 4) (Paz, 2000) (Coyle, 2002) (Sugawara, 2004) (Nakatogawa, 2007).
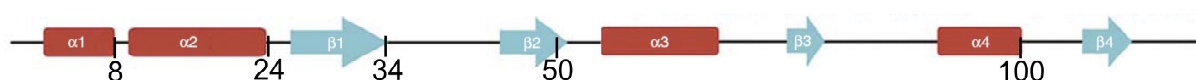
Fig. 4 Model of the three-dimensional structure of Atg8
((Amar, 2006); modified)

Atg8 is coupled via an ubiquitine like reaction to phosphatidylethanolamine (PE) (Ichimura, 2000). The cystein protease Atg4 removes a C-terminal arginine residue of Atg8, exposing a glycine that is now accessible to the E1-like Atg7. Atg7 activates Atg8, that is then transferred to the E2 like Atg3 and in a second step covalently coupled to PE through an amide bond. Atg8-PE is located to the inside and outside of the forming and completed autophagosomes but the coupling of Atg8 to PE is a reversible event. Atg8 can be cleaved of from the outer membrane of the completed vesicle by Atg4 and be reused (Fig. 5). Atg8 is used as marker protein for autophagosomes.

Atg21 is required for the efficient conjugation of Atg8 to PE under Cvt conditions whereas the specificity depends on the intracellular milieus such as cytosolic pH and acidic phospholipids (Strømhaug, 2004) (Oh-oka, 2008).

In an *in vitro* system Atg8 mediates the tethering and hemifusion of membranes, what is modulated by the deconjugation enzyme Atg4. These membrane-tethering and hemifusion activities of Atg8 are required for the expansion of the autophagosomal membranes (Nakatogawa, 2007).

2.5.6.2 The Atg12-Atg5 conjugation sytem

During the coupling of Atg12 to Atg5 an irreversible isopeptide bond is formed (Mizushima, 1998). Two additional proteins are required for its formation. The E1 like Atg7 and Atg10 which functions like an E2 ubiquitin-conjugating enzyme. The Atg12-Atg5 conjugate binds Atg16 and forms a homo-oligomer, which is functionally important for autophagy (Fig. 5) (Kuma, 2002).
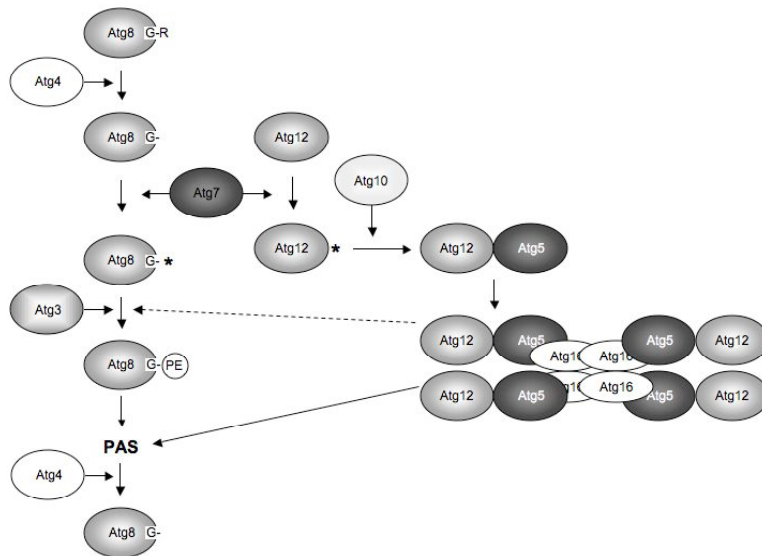
Fig. 5 The two conjugation machineries
((Yorimitsu and Klionsky, 2005); modified)

2.5.7 The two phosphatidylinositol-3-kinase (PI3K) complexes

Vps34, the only phosphatidylinositol 3-phosphate (PtdIns(3)P)-kinase in yeast, is required for autophagy. It formes two complexes: Complex I and Complex II (Kihara, 2001). Complex I consists of Vps34, Atg14, Atg6/Vps30 and Vps15 and is required for the Cvt-pathway as well as autophagy. Complex II contains the same proteins, except that Atg14 is replaced by Vps38 (Fig. 6). *Vps38Δ* cells show defects in carboxypeptidase Y (CPY; Pcr1) sorting and the MVB-pathway, but no autophagic defects (Kihara, 2001).
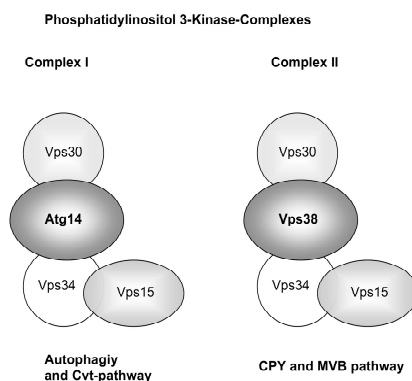
Fig. 6 The two Vps34 complexes in yeast
((Yorimitsu and Klionsky, 2005); modified)

2.5.8 The Atg18, Atg21 and Ygr223c protein family

Atg18, Atg21 and Ygr223c are highly homologous proteins, but have distinct functions in autophagy. Atg18 is essential for macroautophagy, the Cvt-pathway and micronucleophagy, while the function of Atg21 is restricted to the Cvt-pathway and micronucleophagy (Barth, 2001) (Barth, 2002). Ygr223c, a third member of this family of homologous proteins, is only required for efficient micronucleophagy (Krick, 2008a). All three proteins have a WD-40 repeat and are expected to fold as seven bladed ß-propellers. As a common function WD-repeat proteins are thought to regulate the assembly of multiprotein complexes (Smith, 1999). All three homologues bind preferentially to PtdIns(3)P and PtdIns(3,5)P$_2$ (Krick, 2006) (Krick, 2008a).

Atg2 and Atg18 form a complex, that is dependent on PtdIns(3)P, Atg1, Atg9, Atg13 and the recruitment of Atg17 to the PAS (Suzuki, 2007). This complex then recruits further Atg proteins to the PAS (Fig. 7) (Obara, 2008b).

2.5.9 Atg9 cycling

The integral membrane protein Atg9, containing 6 predicted transmembrane domains, cycles in *S. cerevisiae* between the PAS and a peripheral pool. Its origin is still under debate. In yeast the peripheral pool has in part been localized to mitochondria (Reggiori, 2005) but in contrast to the yeast system, mammalian Atg9 cycles between the TGN (trans Golgi network) and late endosomes (Young, 2006) but not mitochondria (Yamada, 2005).

In yeast the anterograde transport from mitochondria to the PAS depends on Atg11, Atg23, Atg27, a functional VTF complex, the early secretory pathway and actin. The retrograde transport requires the Atg1-Atg13-complex, a functional Vps34 kinase complex I and the Atg2-Atg18 complex (Fig. 7) (Reggiori and Klionsky, 2006) (He, 2006) (Yen, 2007). This shuttling of Atg9 could contribute to the delivery of membrane material to the PAS (Reggiori, 2005).
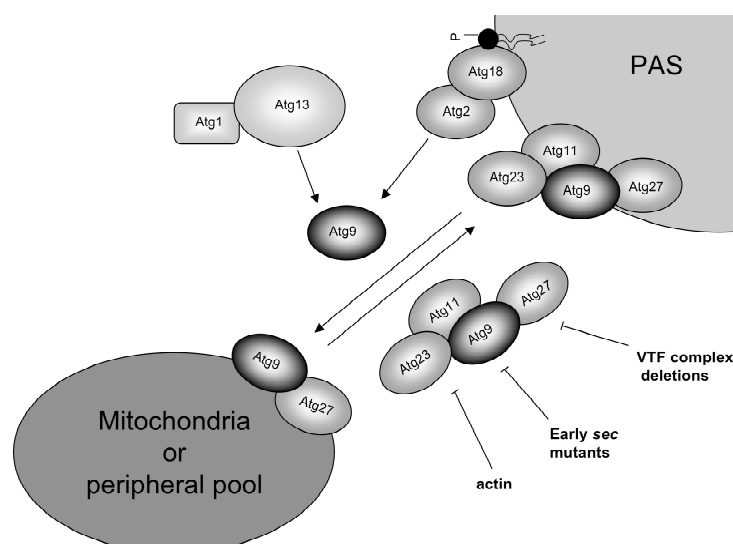
Fig. 7 Cycling of *S. cerevisiae* Atg9 between the PAS and a peripheral pool
((He, 2006) (Reggiori and Klionsky, 2006) (Yen, 2007); modified)

Atg27 was described as an effector of Vps34, the only PtdIns 3-kinase in *S. cerevisiae* (Wurmser and Emr, 2002). Due to a sequencing error in the *Saccharomyces* Genome Database, the full length Atg27 contains 75 additional amino acids at the N terminus and is a transmembrane protein described to locate at the PAS, the mitochondria and the Golgi complex (Yen, 2007). The earlier detected PtdIns(3)P binding site of Atg27 does either not bind PtdIns(3)P or is at least not required for its localization (Yen, 2007). In *atg1Δ atg27Δ* double mutant cells the localization of Atg9 to a peripheral pool, which corresponds in part to mitochondria, is increased (Yen, 2007).

2.5.10 The Cvt-pathway

The Cvt-pathway is a selective transport pathway process of at least two specific cargoes the resident vacuolar hydrolases, aminopeptidase I (Ape1) and α-mannosidase (Ams1) (Scott, 1997) (Hutchins and Klionsky, 2001). The Ape1 protein is synthesized as a pro form (pApe1) in the cytosol, where it forms a dodecameric complex that further assembles to a large oligomeric structure, called Ape1-complex. The Ape1-receptor protein Atg19 binds to the Ape1-complex to form the Cvt-complex, which is dependent on Atg11 dependent recruited to the PAS (pre-autophagosomal structure). This complex is sequestered within a double membrane layered vesicle. These vesicles are formed at the PAS and have a consistent size of 140 - 160 nm in diameter and exclude bulk cytosolic material (Baba, 1997) (Fig. 2).

The Cvt vesicles fuse with the vacuole and a single-membrane vesicle (Cvt body) is released into the vacuolar lumen. The Cvt body is lysed and pApe1 is matured (mApe1).

2.5.11 Macroautophagy

Macroautophagy is a starvation induced degradative protein transport pathway. Autophagosomes are also formed at the PAS, but in contrast to the selective Cvt-pathway, autophagosomes contain unspecific cytosolic material and whole organelles. Completed autophagosomes, measuring 300 – 900 nm in diameter, fuse with the vacuole and a single-membrane vesicle (autophagic body) is released into the lumen and degraded (Baba, 1994).

2.5.12 Fusion and breakdown of vesicles in the vacuole

The fusion of autophagosomes as well as Cvt vesicles with the vacuole requires the homotypic vacuolar fusion machinery. The degradation of the monolayered vesicles in the vacuole is dependent on two vacuolar proteases (Pep4 and Prb1) and an acidification of the vacuole (Takeshige, 1992) (Nakamura, 1997). Additionally the transmembrane protein Atg15 is required for the lysis step (Epple, 2001). Atg15 has a conserved lipase motive and is transported to the vacuole via the multi vesicular body (MVB) pathway (Epple, 2003).

The autophagosomal cargo is degraded, recycled and reused for the synthesis of proteins essential for survival.

Atg22 was described to be involved in the lysis step (Suriapranata, 2000). Recent reports point to an indirect role of Atg22 in the breakdown of the autophagic bodies inside the vacuole. Indeed Yang et al. demonstrated that Atg22 is a partially redundant vacuolar effluxer, that mediates the efflux of leucine resulting from autophagic degradation (Yang, 2006). The supply of amino acids by autophagy allows the maintenance of protein synthesis and viability during nitrogen starvation. Cells respond to nitrogen starvation by up-regulation of genes, including those for vacuolar proteases (such as Pep4, Prb1, and Prc1) (Gasch, 2000). Therefore *atg22Δ* cells lack leucine for the production of these proteases leading to indirect stabilization of the vesicles (Yang, 2006).

2.5.14 Chaperon-mediated autophagy

Chaperone-mediated autophagy allows the degradation of cytosolic proteins that contain a particular pentapeptide consensus motif (KFERQ) via a protein complex in the lysosomal membrane (Massey, 2004), (Majeski and Dice, 2004) (Fig. 2). In human cell lines chaperone-mediated autophagy modulates the neuronal survival machinery. Dysregulation of this pathway is associated with Parkinson's disease (Yang, 2009). At present chaperone-mediated autophagy has only been discovered in mammalian cells. There is no similar process described in *S. cerevisiae* so far (Klionsky, 2007).

2.5.15 Microautophagy

During microautophagy, cytosolic components are directly engulfed by the vacuole by invagination of the organelle´s limiting membrane (Fig. 2).

2.5.16 Pexophagy

Peroxisomes are cell organelles important for the lipid metabolism. Peroxisomes differ in size and number dependent on physiological conditions of the cell. A shift from methanol to glucose containing medium induces the selective microautophagic degradation of peroxisomes. Micropexophagy is best characterized in the methylotrophic yeast *Pichia pastoris* (Farré and Subramani, 2004) (Dunn, 2005) (Sakai, 2006) and has not been described in *S. cerevisiae* so far.

Macroautophagy and micropexophagy are morphologically very different processes (Fig. 2), but both depend on the same set of core Atg proteins. Micropexophagy requires an additional set of specific Atg proteins (e.g. Atg25, Atg26, Atg28, Atg30, Gcn1-3 and Pfk1) (Dunn, 2005) (Farré, 2008). During engulfment arm like extensions of the vacuolar membrane are formed around the peroxisome. The MIPA (micropexophagy-specific membrane apparatus), a double membrane cap-like structure, containing Atg8 and Atg26, is formed at the far end of the encircled peroxisome, where it is thought to mediate the vacuolar membrane fusion event (Dunn, 2005).

2.5.17 Mitophagy

Mitophagy is a selctive variant of autophagy that degrades defective mitochondria and is reported to be involved in the cell death process (Tal, 2007). The mitochondrial protein Uth1 is selectively involved in mitophagy (Kissová, 2004). Additionally, Aup1 is required for efficient mitophagy. It localizes to the mitochondrial intermembrane space and may be part of a signal transduction mechanism that marks mitochondria for sequestration into autophagosomes (Tal, 2007). Primarily, Aup1 was identified in a screen for protein phosphatase homologues that functionally interact with Atg1 in yeast.

2.5.18 Micronucleophagy (PMN)

Piecemeal microautophagy of the nucleus (PMN) is a microautophagic process and was therefore named micronucleophagy (Krick, 2009).

Micronucleophagy occurs at nucleus vacuole (NV) junctions, that are formed by interactions between Vac8 in the vacuolar membrane and Nvj1 in the inner and outer nuclear membrane (Pan, 2000) (Roberts, 2003) (Millen, 2008). During PMN a portion of the nucleus is extruded along the NV junctions into an invagination of the vacuolar membrane, forming a tethered bleb. Scission of the ER and fusion of the vacuolar membrane then releases a PMN vesicle into the vacuolar lumen, where it is degraded by resident hydrolases (Kvam and Goldfarb, 2007). The intravacuolar PMN vesicles are limited by three membrane layers. The outer membrane is derived from the vacuolar membrane, and the two inner layers from the nuclear envelope (Fig. 8).
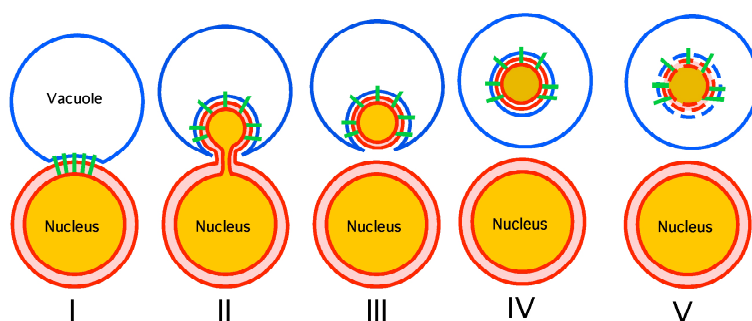
Fig. 8 Schematic illustration of PMN
In stage I nucleus-vacuole (NV) junctions form. Then the nuclear ER bulges into invaginations of the vacuolar membrane (stage II), followed by fission of an ER-deduced vesicle (stage III). After fusion at the tips of the vacuolar membrane extensions (stage IV), a PMN vesicle is released into the vacuolar lumen, where it is finally degraded (stage V) ((Krick, 2008b); modified)
.

PMN is induced by nutrient depletion and degrades nonessential portions of the nucleus (Krick, 2008b). Nvj1 recruits at least two additional proteins to the NV junctions: Tsc13 an enoyl-CoA reductase required for the synthesis of very-longchain fatty acids and Osh1 a homologoue to mammalian oxysterol-binding protein (OSBP) that may function in nonvesicular lipid trafficking (Fig. 9) (Kvam, 2005) (Kvam and Goldfarb, 2004).
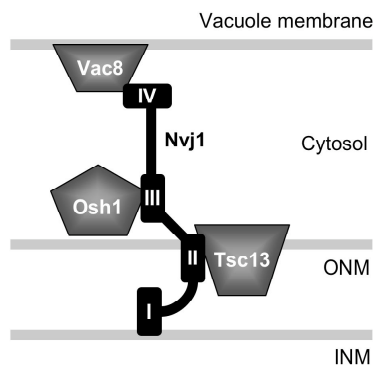
Fig. 9 Model of molecular composition of NV-junctions
The hydrophobic N-terminus of Nvj1p links the inner- and outer-nuclear membranes by direct insertion (Millen, 2008). ONM = outer nuclear membrane; IMN = inner nuclear membrane ((Kvam and Goldfarb, 2006a); modified)

PMN has been categorized as an autophagic process based on morphological criteria and its induction under starvation conditions (Kvam and Goldfarb, 2007). First analysis by the Goldfarb lab neglected the involvement of the autophagic machinery in PMN. They measured the degradation of Nvj1-EYFP by western blot. Wild type and *atg7Δ* cells showed a slight reduction in the Nvj1-EYFP band but in *pep4Δ* Nvj1-EYFP was stabilized (Roberts, 2003).

In contrast Krick et al. showed using two independent biochemical assays that the efficient production of PMN vesicles depends on the core Atg proteins (Krick, 2008b). They used Nvj1-GFP and GFP-Osh1 as marker proteins and followed their degradation in the vacuole by detection of free GFP. Free GFP accumulates in the vacuole because of its resistance to vacuolar hydrolases.

2.6 Membrane fusion

Eukaryotic cells contain membrane-enclosed organelles that exchange proteins and lipids through vesicular transport.

SNAREs (soluble *N*-ethylmaleimide-sensitive factor attachment protein receptor)

have been identified as key components to drive membrane fusion. They localize to the vesicle and the acceptor membrane. During fusion the SNAREs on both membranes form a four helix bundle. The energy required for membrane fusion is provided by the free energy released during formation of the bundle (Jahn and Scheller, 2006).

SNAREs contain a 60 - 70 amino acids conserved SNARE motif. At their C-terminal ends most SNAREs have a single transmembrane domain that is connected to the SNARE motif by a short linker. Dependent on the presence of arginine or glutamine in the SNARE motif they are called R- or Q-SNAREs (Fasshauer, 1998). Functional SNARE complexes are hetero-oligomeric, parallel four-helix bundles, requiring one of each Qa-, Qb-, Qc- and R-SNAREs (Jahn and Scheller, 2006).

After fusion SNARE complexes exist in a biologically inactive configuration until the complex is dissociated. This recycling of SNARE complexes is mediated by the AAA$^+$ (ATPases associated with various cellular activities) protein NSF (*N*-ethylmaleimide-sensitive factor) by the dissociation of the helical bundle. To interact with SNAREs NSF requires a cofactor, the soluble NSF attachment protein (α-SNAP) (Fig. 10).

In yeast the homologue of NSF is the Sec18 protein and Sec17 the corresponding α-SNAP.

Cis-SNARE complex   **Disassembly complex**   **Free SNARE clusters**
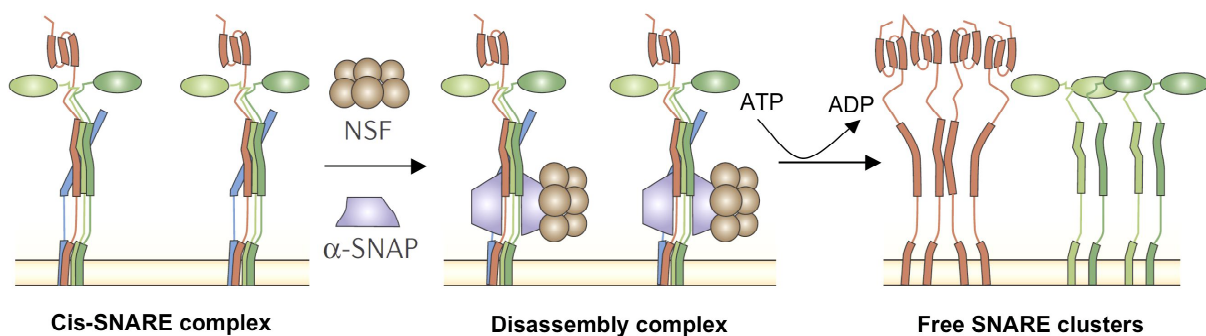
Fig. 10 SNARE disassembly after fusion
During fusion, the *trans*-complex relaxes into a *cis*-configuration. *Cis*-complexes are disassembled by the AAA+ (ATPases associated with various cellular activities) protein NSF (*N*-ethylmaleimide-sensitive factor) together with SNAPs (soluble NSF attachment proteins) that function as cofactors. ((Jahn and Scheller, 2006); modified)

2.6.1 Cdc48 dependent membrane fusion

Cdc48 (the homologue of p97 in mammals) belongs to the family of AAA$^+$ ATPases (ATPases associated with various cellular activities). It is a highly conserved protein involved in many different cellular processes, including ubiquitin-dependent protein degradation, fusion of homotypic membranes, nuclear envelope reassembly and cell cycle progression (Schuberth, 2004) (Wang, 2004a) (Woodman, 2003).

The molecular mechanism of Cdc48/p97 action in all these processes is believed to be its "segregase" activity (Braun, 2002). Cdc48/p97 uses the energy provided by ATP hydrolysis to extract substrate proteins from protein complexes or lipid membranes (Schuberth and Buchberger, 2008).

In order to provide specificity for its various cellular functions, Cdc48/p97 activity is tightly regulated by numerous different cofactors in the cell (Tab. 1).

Tab. 1 Classification of Cdc48 cofactors in yeast

Type of cofactor	Identified proteins	Function
Substrate-recruiting - major	Ufd1-Npl4 Shp1	Decision between major cellular pathways: protein degradation versus membrane fusion (and others)
Substrate-recruiting - additional	Ubx2, Ubx5, Dfm1*, Der1*	Co-adaptors for specific pathways: improve substrate binding and/or provide additional spatial regulation
Substrate-processing	Otu1, Ufd2, Ufd3	Additional enzymatic activities; Regulation of substrate fate: stabilization versus degradation

*protein with functional human homologues   ((Schuberth and Buchberger, 2008); modified)

The UBX proteins are one family of such cofactors. The UBX domain is a general Cdc48/p97-binding module (Decottignies, 2004) (Hartmann-Petersen, 2004). Cdc48/p97 can either bind directly to ubiquitin or the UBX domain, which turned out to be a close structural homologue of ubiquitin itself (Buchberger, 2001). In yeast there are seven UBX proteins and three of them possess an amino-terminal UBA domain, which binds ubiquitylated proteins *in vivo* (Schuberth, 2004) (Fig. 11).
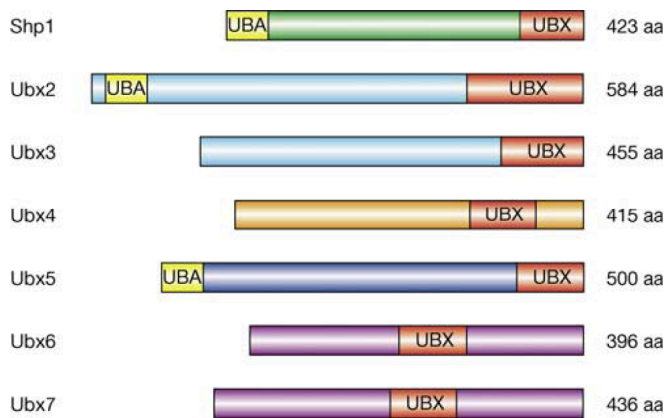
Fig. 11 UBX proteins of *S. cerevisiae*
UBX (red) and UBA (yellow) domains are labelled. Significant homology outside these domains
is indicated by similar colours. Shp1 (alias Ubx1); Ubx2 (alias Sel1); (taken from (Schuberth, 2004))

During the homotypic fusion of Golgi and ER membranes, Cdc48/p97 was suggested
to act on mono- ubiquitinated substrates during the remodeling of SNARE complexes
and/or their regulators (Latterich, 1995) (Rabouille, 1998) (Wang, 2004b). The
required cofactor of the mamalian p97 is p47 (Fig. 12) (Kondo, 1997) and the
corresponding yeast homologue is Shp1.
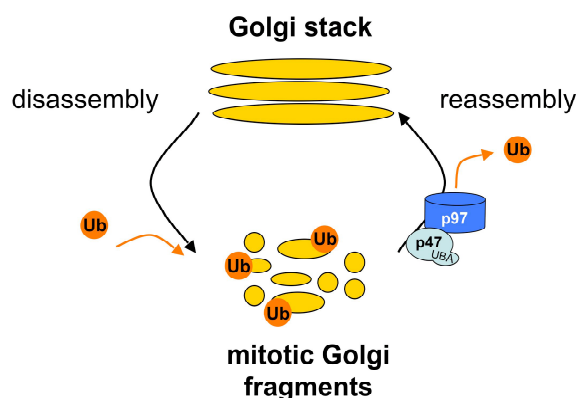
Fig. 12 p97 - Golgi membrane reassembly in humans
((Meyer, 2005); modified)

For the degradation of ubiquitinated protein substrates out of the ER Cdc48/p97
interacts with the heterodimeric substrate-recruiting cofactor Ufd1/Npl4.
Simultaneous binding of Cdc48-Ufd1-Npl4 to the ER-membrane protein complex and
the poly-ubiquitin chain on the substrate seems to trigger the segregase activity of
Cdc48 which pulls substrates out of the ER (Braun, 2002) (Meyer, 2000) (Ye, 2001)
(Jarosch, 2002) (Raasi and Wolf, 2007).
In the literature these two major functional distinct CDC48 complexes have been
described.

In contrast to the previously described function in membrane fusion *shp1Δ* cells have been found to exhibit defects in ubiquitin-dependent degradation pathways (Schuberth, 2004). Furthermore the p97 Ufd1-Npl4 complex is involved in the reformation of the nuclear envelope double-membrane structure after mitosis (Anderson and Hetzer, 2007).

2.7 Aim of the study

I. Autophagy starts at the pre- autophagosomal structure (PAS). Out of this structure double membrane layered vesicles are formed and transported to the vacuole, where their outer membranes fuse with the vacuole, releasing a monolayered vesicle into the vacuolar lumen. The PAS is believed to be an organelle-like membrane structure. The origin of the membrane source for the formation of Cvt- and autophagic vesicles is still unclear. The transmembrane protein Atg9 is supposed to be involved in the transport of membranes from a peripheral pool to the PAS, where the vesicles are formed. Aim of this study was to investigate the localization and characteristics of this peripheral pool.

II. Micronucleophagy occurs at nucleus-vacuole (NV) junctions and results in the pinching-off and degradation of nonessential portions of the nucleus in the vacuole. In contrast to previous published results biochemical data from the Thumm lab indicated a strict requirement of the autophagic machinery in PMN. Therefore in this study a microscopy based assay should be established to support these results. Furthermore the molecular machinery for the membrane fusion events in autophagy and PMN should be analysed.

3. Materials and Methods

3.1 Materials

3.1.1 *Saccharomyces cerevisiae* strains

Tab. 2 *S. cerevisiae* strains used in this study

Strain	Genotype	Source
atg1Δ atg27Δ	WCG4a MATα *atg1*Δ::KAN *atg27*Δ::HIS3	This study
atg1Δ atg27Δ cGFP-Atg8	WCG4a MATα *atg1*Δ::KAN *atg27*Δ::HIS3 cGFP-Atg8	This study
atg1Δ atg27Δ Snf7-RFP	WCG4a MATa *atg1*Δ::KAN *atg27*Δ::HIS3 snf7-RFP::KAN	This study
atg1Δ atg4Δ	WCG4a MATα *atg1*Δ::KAN *atg4*Δ::HIS5	
atg1Δ atg4Δ atg27Δ	WCG4a MATα *atg1*Δ::KAN *atg4*Δ::NAT *atg27*Δ::HIS3	This study
atg1Δ cGFP-Atg8	WCG4a MATa *atg1*Δ::KAN cGFP-Atg8	This study
atg1Δ vps4Δ atg27Δ	WCG4a MATα *atg1*Δ::KAN *vps4*Δ::NAT *atg27*::HIS3	This study
atg27Δ	WCG4a MATα *atg27*Δ::HIS3	This study
atg4Δ atg27Δ	WCG4a MATα *atg4*Δ::KAN *atg27*Δ::HIS3	This study
atg8Δ	WCG4a MATα *atg8*Δ::KAN	AG Thumm
aut5delta	WCG4a MATα *atg15*Δ::KAN	AG Thumm
BY4741	*MATa his3*Δ1 *leu2*Δ0 *met15*Δ0 *ura3*Δ0	Euroscarf
cdc48.3 BY	BY4741 CDC48.3 temperature sensitive at 36°C	T. Prick u. E. Welter
cdc48.3 WCG	WCG4a CDC48.3 temperature sensitive at 38°C	This study
cdc48-3	pep4Δ::URA3 cdc48-3 temperature sensitive at 36°C	F. Madeo
Snf7	S288C MATa Snf7-RFP::KAN	Falvo

Strain	Genotype	Source
WCG4	*WCG4a MATα his3-11,15 leu2-3,112 ura3*	W. Heinemeyer, Stuttgart
wt cGFP-Atg8	WCG4a MATα cGFP-Atg8	This study
Y00379	BY4741 MATa *myo4Δ*::KAN	Euroscarf
Y00399	BY4741 MATa *spo7Δ*::KAN	Euroscarf
Y00560	BY4741 MATa *sel1Δ*::KAN	Euroscarf
Y01375	BY4741 MATa *ubx6Δ*::KAN	Euroscarf
Y01481	BY4741 MATa *ice2Δ*::KAN	Euroscarf
Y02763	BY4741 MATa *vps28Δ*::KAN	Euroscarf
Y03084	BY4741 MATa *shp1Δ*::KAN	Euroscarf
Y03269	BY4741 MATa *she3Δ*::KAN	Euroscarf
Y03298	BY4741 MATa *ifa38Δ*::KAN	Euroscarf
Y03341	BY4741 MATa *der1Δ*::KAN	Euroscarf
Y03592	BY4741 MATa *rtn1Δ*::KAN	Euroscarf
Y03698	BY4741 MATa *ubx5Δ*::KAN	Euroscarf
Y03788	BY4741 MATa *ubx3Δ*::KAN	Euroscarf
Y03888	BY4741 MATa *ufd2Δ*::KAN	Euroscarf
Y04004	BY4741 MATa *doa4Δ*::KAN	Euroscarf
Y04247	BY4741 MATa *dfm1Δ*::KAN	Euroscarf
Y04980	BY4741 MATa *she2Δ*::KAN	Euroscarf
Y05063	BY4741 MATa *doa1Δ*::KAN	Euroscarf
Y05281	BY4741 MATa *elo3Δ*::KAN	Euroscarf
Y05381	BY4741 MATa *vps27Δ*::KAN	Euroscarf
Y05447	BY4741 MATa *yop1Δ*::KAN	Euroscarf
Y05721	BY4741 MATa *ubx7Δ*::KAN	Euroscarf
Y05763	BY4741 MATa *elo2Δ*::KAN	Euroscarf
Y06078	BY4741 MATa *bre5Δ*::KAN	Euroscarf
Y06119	BY4741 MATa *scs2Δ*::KAN	Euroscarf
Y06148	BY4741 MATa *ubp3Δ*::KAN	Euroscarf
Y06200	BY4741 MATa *ubx4Δ*::KAN	Euroscarf
YCV9	WCG4a MATα *atg4Δ*::KAN *atg8Δ*::KAN	C. Voss
YHB 1	WCG4a MATα *atg18Δ*::KAN	H. Barth
YHB 4	WCG4a *atg21Δ*::KAN	H. Barth

Strain	Genotype	Source
YMS30K1	WCG4a MATa *atg1*Δ::KAN	AG Thumm
YMTA	WCG4a MATa *pep4*Δ::HIS3	M. Thumm
YSR3	WCG4a MATa *aut9*Δ::KAN	S. Reiche
YUE105-1B	BY4741 MATa *bsd2*Δ::KAN *tul1*Δ::KAN	U. Epple
YUE37	WCG4a MATα *atg1*Δ::KAN *atg15*Δ::KAN	U. Epple
YUE40	WCG4a MATa *atg1*Δ::KAN *pep4*Δ::HIS3	U. Epple
YWO 0377	BWG1-7a MATa ura3-52 leu2-3,112 his4-519 ade1-100	C. Taxis
YWO1018	BWG1-7a MATa ufd1_1 pcr1_1	C. Taxis
YYH6	W303 MATa	T. Rapoport
YYH75	W303 CDC48.3 temperature sensitive at 34°C	T. Rapoport
YYW09	WCG4a MATα *vac8*Δ::HIS3	Y. Mühe
yYW10	WCG4a MATa *atg11*Δ::HIS3	Y. Mühe

Yeast strains for mating type determination

Tab. 3 *S. cerevisiae* strains for mating type determination

Strain	Genotype	Source
YR312	Mata *his1-123* test strain for mating type determination	H. Rudolph, Stuttgart
YR320	Matα *his1-123* test strain for mating type determination	H. Rudolph, Stuttgart

3.1.2 *Escherichia coli* strains

Tab. 4 *E. coli* strain DH5α

Strain	Genotype	Source
DH5α	F' (Φ *80* (*ΔlacZ*) *M15*) *Δ* (*lacZYA-argF*) *U169 recA1 endA1 hsdR17* r_k- m_k + *supE44 thi-1 gyrA relA*	Hanahan *et al.*, *1983*

3.1.3 Plasmids

Tab. 5 Plasmids used in this study

Name	Genotype	Source
GFP-Atg8	pRS316 CEN6 URA3 GFP-*ATG8*	Suzuki *et al.*, 2001
GFP-Atg8-cherry	pRS316 CEN6 URA3 GFP-Atg8-cherry	This study
GFP-Atg9	CEN6 URA3 MET25 GFP-Atg9	T. Lang
Nab 2 NLS-2m Cherry	pYX242 2µ LEU2 TPI Nab2NLS-2m cherry	B. Timney and M. Rout at the Rockefeller University
pGFP-Atg8-FG	pRS316 CEN6 URA3 GFP-Atg8-FG	Suzuki *et al.*, 2001
pJH1	pRS313 CEN6 HIS3 Ape1-RFP	U. Epple
POM42	POM40 URA3 yEGFP	Euroscarf
pFA6-natNT2	natNT2	Euroscarf; Janke et al., 2004
pRS315	pRS315 CEN6 LEU2 empty vector	K. Meiling-Wesse
pRS315-APE1-RFP	pRS315 CEN6 LEU2 Ape1-RFP	R. Krick
pRS315-mRFP-2xFYVE	pRS315 CEN6 LEU2 TEF mRFP-2xFYVE	S. Henke
pRS316-PGK-GFP	pRS316 CEN6 URA3 PGK-GFP	P. Schlotterhose; Y. Mühe
pRS416-GFP-OSH1	pRS416 CEN6 URA3 GFP-Osh1	Lowen et al. 2003
pSH65	CRE-recombinase with GAL-promoter phleomycin resistance	Euroscarf
pUG23_Nvj1	pUG23 CEN6 HIS3 MET25 Nvj1	This study
pUG23_Nvj1_GFP	pUG23 CEN6 HIS2	This study

Name	Genotype	Source
pUG35_Nvj1	MET25 Nvj1-GFP pUG35 CEN6 URA3 MET25 Nvj1	This study
pUG35_Nvj1_GFP	pUG35 CEN6 URA3 MET25 Nvj1-GFP	This study
UbK29R	YEP96 TRP1 Cup1 ubiquitin (K29R)	Horak J.
UbK48R	YEP96 TRP1 Cup1 ubiquitin (K48R)	Horak J.
UbK63R	YEP96 TRP1 Cup1 ubiquitin (K63R)	Horak J.
Ub-noLys	YEP96 TRP1 Cup1 ubiquitin (no lysines)	Horak J.
YEp96	2µ TRP1 Cup1	Horak J.

3.1.4 Oligonucleotides

Tab. 6 Oligonucleotides used in this study

Name	Sequence 5`-3`
Vps4Δ::NAT	
Primer 1 vps4 ko NAT	GAAGACAAAA ATAAAGCAGC ATAGAGTGCC TATAGTAGAT GGGGTACAAA TG*CGTACGCTG CAGGTCGAC*
Primer 2 vps4 ko NAT	CATGTACACA AGAAATCTAC ATTAGCACGT TAATCAATTG ACTAGTTACC *ATCGATGAAT TCGAGCTCG*
Atg4Δ::NAT	
Primer 1 Atg4 ko NAT	GTTAGTAGAT GAAGAATGGA CGACTTCTTA TCACGTATAG GAGTGATATA CATG*CGTACG CTGCAGGTCG AC*
Primer 2 Atg4 ko NAT	GAATATATTA AAACAAGTAT ATATGCTTATG AACTAGTGAA TTCCTTACAC TA *ATCGATG AATTCGAGCT CG*
Atg27Δ::HIS	
Primer 1 Atg27 ko HIS	TCTTCAATCG ATGCGATAGA TAAAGGTAAG GAAAGCTTTC ACGATGCGGA TCCCCGGGTT AATTAA
Primer 2 Atg27 ko HIS	GCACTGCTGT TGCAAAAATA TCGAATTGTA AGCCAGTAAA CTTATTTAGA ATTCGAGCTC GTTTAAAC

Name	Sequence 5`-3`
Chromosomal GFP-Atg8	
cGFP-Atg8 1f	TAATTGTAAA GTTGAGAAAA TCATAATAAA AATAATTACT AGAGACATGT GCAGGTCGAC AACCCTTAAT
cGFP-Atg8 2r (linker)	CGCCTTCCTT TTTTCAAATG GATATTCAGA CTTAAATGTA GACTTGCGGC CGCATAGGCC ACT
Plasmid GFP-Atg8-cherry	
GFP-Atg8-cherry 1f	CGGGTTTTTG TATGTCACTT ACTCAGGAGA AAATACATTT GGCAGGATGG TGAGCAAGGG CGAGGAGG
GFP-Atg8-cherry 2r	GCTCGGAATT AACCCTCACT AAAGGGAACA AAAGCTGGGT ACCGGGCCTA CTTGTACAGC TCGTCCATGC
Sequence Primer Atg8	
Atg8 seq 0f	GGAGGCCGGT TATTTTCGG
Atg8 seq 1f	GAAGGCGGAG TCGGAGAG
Atg8 seq 1r	CTCTCCGACT CCGCCTTC
Atg8 seq 2f	GGACGGGTTT TTGTATGTCA C
Atg8 seq 2r	GTGACATACA AAAACCCGTC C
Sequence Primer Atg9	
Atg9 seq 1f	GATGATTCTG TGCCCAAAGT C
Atg9 seq 1r	GACTTTGGGC ACAGAATCAT C
Atg9 seq 2f	CTGAATTTAT CCTTGCCTAT TCC
Atg9 seq 2r	GGAATAGGCA AGGATAAATT CAG
Atg9 seq 3f	GCGATTCATT TCTCAACAAT AAG
Atg9 seq 3r	CTTATTGTTG AGAAATGAAT CGC
Atg9 seq 4r	CGGTTATTCT GTAAGATATG CC
Atg9 seq 5f	CCTTTGGATG TTTTATTTCT TCG
Atg9 seq 6f	GCAAGTATGC TATGTTTAAC ATG
Sequence Primer RFP	
RFP seq1r	CGTGGCCGTT CACGGAGC

3.1.5 Media

All media were prepared with deionised water (ddH$_2$O) and autoclaved 20 min at 121°C and 2 bar. To obtain solid media, 2% Bacto-Agar was added. The pH of the medium was adjusted with either NaOH or HCl. All percent values in this chapter are weight per volume (w/v).

3.1.5.1 YPD-medium, pH 5.5

YPD is a rich medium for yeast cultures containing:

1%   Bacto® Yeast Extract

2%   Bacto® Pepton

2%   D-glucose

3.1.5.2 CM-medium, pH 5.6

CM-medium is a synthetic medium for yeast cultures consisting of:

0.67%	Yeast Nitrogen Base w/o amino acids		
2%	D-glucose		
0.0117%	L-alanine	0.0117%	L-methionine*
0.0117%	L-arginine	0.0117%	L-phenylalanine
0.0117%	L-asparagine	0.0117%	L-proline
0.0117%	L-aspartic acid	0.0117%	L-serine
0.0117%	L-cysteine	0.0117%	L-threonine
0.0117%	L-glutamine	0.0117%	L-tyrosine
0.0117%	L-glutamic acid	0.0117%	L-valine
0.0117%	L-glycine	0.0117%	myo-inositol
0.0117%	L-isoleucine	0.00117%	p-aminobenzoic acid

Depending on selection conditions the following supplements were added:

0.3 mM	L-histidine	0.4 mM	L-tryptophan
1.7 mM	L-leucine	0.3 mM	adenine
1 mM	L-lysine	0.2 mM	uracil**

* For overexpression experiments using a MET25 promoter L-methionine was excluded from the drop out mix.
** Uracil was resuspended in 0.5% sodium hydrogen carbonate solution.

3.1.5.3 SD(-N)-medium

Nitrogen free SD(-N)-medium was used as starvation medium for yeast cells.

0.67%   Yeast Nitrogen Base w/o amino acid and w/o ammonium sulfate

2%   D-glucose

3.1.5.4 1% potassium acetate

1% potassium acetate medium was used to induce sporulation and tetrade formation of yeast cells and for carbon starvation.

1%	potassium acetate

3.1.5.5 MV-medium, pH 5.5

MV-medium was used as a minimal medium to determine the mating type of a haploid yeast strain.

0.67%	Yeast Nitrogen Base w/o amino acids
2%	*D*-glucose

3.1.5.6 LB-medium, pH 7.5

LB-medium was used as standard growth medium for *E. coli* cultures.

1%	Bacto® Trypton
0.5%	Bacto® Yeast extract
0.5%	sodium chloride

For plasmid selection 75 µg / ml ampicillin was added.

3.1.5.7 SOC-medium, pH 7.5

SOC-medium was used as a regeneration medium for electroporated *E. coli* cells.

2%	Bacto® Trypton		
0.5%	Bacto® Yeast extract		
0.4%	D-glucose		
10 mM	sodium chloride	10 mM	magnesium sulfate
10 mM	magnesium chloride	2.5 mM	potassium chloride

3.1.6 Antibodies

Tab. 7 Antibodies used in this study

Name of antibody	Dilution	Source
anti-mouse-HRPO-conjugate	1 : 10000*	Dianova, Hamburg
anti-rabbit-HRPO-conjugate	1 : 5000*	Medac, Hamburg
mouse-anti-GFP	1 : 10000*	Roche, Mannheim
mouse-anti-PGK	1 : 10000 in TBST	Molecular Probes, Leiden, NL
rabbit-anti-Ape1p	1 : 3000*	Eurogentech, Belgium

* in TBST (20 mM Tris/HCl pH 7.6; 137 mM sodium chloride; 0.1% Tween 20 (w/v)) containing 1% skim milk powder (w/v)

3.1.7 Commercial available Kits

Tab. 8 Commercial available Kits used in this study

Name of product	Source
ECL Plus^{TM} Western Blotting Detection Reagents	Amersham Biosciences, GB
Gene Images Random-Prime Labeling Module-Kit	GE Healthcare, Munich
Gene Images CPD-Star Detection Module-Kit	GE Healthcare, Munich
Rodeo^{TM}ECL Western Blotting Detection Kit	USB, Staufen
QIAquick Gel Extraction Kit	Qiagen, Hilden
QIAquick PCR Purification Kit	Qiagen, Hilden
Wizard PlusSV Miniprep Kit	Promega, Mannheim

3.1.8 Chemicals and consumables

Tab. 9 Chemicals and consumables used in this study

Name of product	Source
Acetic acid	Riedel-De Haën, Seelze
Acetone	Roth, Karlsruhe
Adenine	Sigma, Deisenhofen
Agarose NEEO	Roth, Karlsruhe
L-alanine	Sigma, Deisenhofen
Ammonium acetate	Roth, Karlsruhe

Name of product	Source
Ammonium persulfate	Merck, Darmstadt
Ampicillin	Boehringer Mannheim, Mannheim
Antipain	Sigma-Aldrich, Deisenhofen
Aprotinin	Merck, Darmstadt
L-arginine	Sigma, Deisenhofen
L-asparagine	Sigma, Deisenhofen
L-aspartic acid	Sigma, Deisenhofen
Bacto®- Agar	Becton Dickinson, Heidelberg
Bacto®- Peptone	Becton Dickinson, Heidelberg
Bacto®- Tryptone	Becton Dickinson, Heidelberg
Bacto®- Yeast Extract	Becton Dickinson, Heidelberg
Benzamidin	Merck, Darmstadt
Bromphenolblue	Riedel-De Haën, Seelze
Chloroform	Roth, Karlsruhe
Chymostatin	Merck, Darmstadt
CMAC (7-amino-4-chloromethylcoumarin)	Invitrogen, Karlsruhe
CompleteTM protease inhibitor	Roche, Mannheim
Copper sulfate	Roth, Karlsruhe
L-cysteine	Sigma, Deisenhofen
DAPI (4',6-diamidino-2-phenylindole)	Sigma, Deisenhofen
Deoxyadenosin-triphosphate (dATP)	NEB, Frankfurt
Deoxycytidin-triphosphate (dCTP)	NEB, Frankfurt
Deoxyguanosin-triphosphate (dGTP)	NEB, Frankfurt
Deoxythymidin-triphosphate (dTTP)	NEB, Frankfurt
1,4-Dithiothreitol (DTT)	Roth, Karlsruhe
D-galactose	Roth, Karlsruhe
D-glucose	Roth, Karlsruhe
L-glutamine	Sigma, Deisenhofen
L-glutamic acid	Sigma, Deisenhofen
L-glycine	Sigma, Deisenhofen
DMSO (dimethyl sulfoxide)	Merck, Darmstadt
DNA-marker (1kb DNA-letter)	NEB, Frankfurt
EDTA (ethylenediaminetetraacetic acid)	Sigma, Deisenhofen
Ethanol	Roth, Karlsruhe
Ethidiumbromid	Sigma, Deisenhofen
Filterpaper GB 002 und GB 003	Heinemann, Göttingen
FM4-64	Invitrogen, Karlsruhe
Formaldehyde, 37%	Sigma, Deisenhofen
Genticindisulfate (G418; kanamycin)	Roth, Karlsruhe
Glass beads	Schütt, Göttingen
Glycerol	Riedel-De Haën, Seelze
Herring-sperm-DNA	Promega, Madison, USA
L-histidine	Sigma, Deisenhofen
Hoechst 33342	Molecular Probes, Freiburg
Hybond-*N* +	Amersham Biosciences, GB
Hybond-P	Amersham Biosciences, GB
Immersion oil "Immersol" 518F	Zeiss, Göttingen
Isobutanol	Sigma, Deisenhofen

Name of product	Source
L-isoleucine	Sigma, Deisenhofen
Isopropyl alcohol	Sigma, Deisenhofen
Leupeptin	Merck, Darmstadt
Liquidblock	GE Healthcare, Munich
L-leucine	Sigma, Deisenhofen
Lithium acetate	Sigma, Deisenhofen
L-lysine	Sigma, Deisenhofen
Magnesium chloride	Roth, Karlsruhe
Magnesium sulfate	Roth, Karlsruhe
2-mercaptoethanol (β-ME)	Roth, Karlsruhe
Methanol	Roth, Karlsruhe
L-methionine	Sigma, Deisenhofen
MOPS (3-(N-Morpholino)-2-hydroxypropansulfonsäure)	
	Roth, Karlsruhe
Myo-inositol	Roth, Karlsruhe
Nourseotricine (clonNAT)	Werner BioAgents, Jena
Nonidet P40	Roche, Mannheim
PEG (polyethylene glycol)	Sigma, Deisenhofen
Pepstatin A	Merck, Darmstadt
Phenol, TE-saturated (Roti®-Phenol)	Roth, Karlsruhe
L-phenylalanine	Sigma, Deisenhofen
PMSF (phenylmethylsulphonyl fluoride)	Merck, Darmstadt
Poly-*L*-lysine	Sigma, Deisenhofen
Potassium acetate	Merck, Darmstadt
Potassium chloride	Merck, Darmstadt
Potassium dihydrogen phosphate	Merck, Darmstadt
Potassium hydrogen phosphate	Roth, Karlsruhe
Precision Plus Protein All Blue Standards	Biorad, Munich
L-proline	Sigma, Deisenhofen
Protogel, 30% acrylamide: 0,8% bis-acrylamide (37,5 : 1)	
	Biozym, Hessisch Oldendorf
Bovine serum albumin (BSA)	Sigma, Deisenhofen
RNAse A	Applichem, Darmstadt
Hydrochloric acid 37%	Riedel-De Haën, Seelze
L-serine	Sigma, Deisenhofen
Sequencing buffer	Applied Biosystems, Darmstadt
Skim milk powder	Granovita, Lüneburg
Sodium acetate	Merck, Darmstadt
Sodium azide	Riedel-De Haën, Seelze
Sodium chloride	Roth, Karlsruhe
Sodium citrate	Sigma, Deisenhofen
Sodium dihydrogen phosphate	Roth, Karlsruhe
Sodium dodecyl sulfate (SDS)	Sigma, Deisenhofen
Sodium hydrogen phosphate	Roth, Karlsruhe
Sodium hydroxide	Merck, Darmstadt
D-sorbitol	Sigma, Deisenhofen
D-sucrose	Roth, Karlsruhe
Sterile filter: 0,2 µm pores	Sartorius, Göttingen

Name of product	Source
125 and 500 ml vacuum filtration	Schleicher & Schuell, Dassel
TEMED (1,2-Bis(dimethylamino)ethane)	Merck, Darmstadt
L-threonine	Sigma, Deisenhofen
Trichloroacetic acid (TCA)	Roth, Karlsruhe
Tris (tris(hydroxymethyl)aminomethane)	Roth, Karlsruhe
TritonX-100	Roth, Karlsruhe
L-tryptophan	Sigma, Deisenhofen
Tween 20	Sigma, Deisenhofen
L-tyrosine	Sigma, Deisenhofen
Uracil	Sigma, Deisenhofen
L-valine	Sigma, Deisenhofen
Yeast nitrogen base	Becton Dickinson, Heidelberg
Difco Yeast nitrogen base w/o amino acids	Becton Dickinson, Heidelberg
Difco Yeast nitrogen base w/o amino acids and ammonium	Becton Dickinson, Heidelberg
Zymolyase T20	Seikagaku, Japan
Zymolyase T100	Seikagaku, Japan

3.1.9 Devices

Tab. 10 Devices used in this study

Name of product	Source
Analysis scale	Sartorius, Göttingen
Autoclav: TECNOCLAV 50	Tecnomara-Fedegari, Zürich, CH
Autoclav: Tuttnauer 3870 EL	Systec, Wettenberg
Axioscope2 mot plus microscope	Zeiss, Göttingen
Bunsen burner flammy S	Schütt, Göttingen
Centrifuge 5417C / 5415R	Eppendorf, Hamburg
Centrifuge J2-MC	Beckmann, Krefeld
DNA-gel electrophoresis apparatuses	Biorad, Munich
Electrophoresis chamber for SDS-PAGE	Biorad, Munich
Elektrophoresis Power Supply Consort E831	Topac, USA
Electrophoresis system Mini PROTEAN 3	Biorag, Munich
Elektroporator 2510	Eppendorf, Hamburg
Hood	BDK Luft- und Reinraumtechnik, Sonnenbrühl-Genkingen
Hybridisation oven	Schütt, Göttingen
Incubators	Hereaus, Hanau
Inkubator 4200	Innova, USA
Labshaker for diverse culture sizes	A. Kühner, Birsfelden, Schweiz
LAS-3000 Intelligent Dark Box	Fuji/ Raytest, Benelux
Leica TCS SP2 AOBS confocal LSM	Leica, Wetzlar
Magnetic stirrer MR 3001	Heidolph, Kelheim

Name of product	Source
Micromanipulator	Zeiss, Göttingen
Microprocessor pH Meter 537	WTW, Weilheim
Microwave R-939	Sharp, Hamburg
Mini Trans-Blot Cell	Biorad, Munich
Multivortex IKA VIBRAX VXR basic	IKA, Staufen
Over head shaker *REAX2*	Heidolph, Kelheim
Photometer	Eppendorf, Hamburg
PCR Mastercycler gradient	Eppendorf, Hamburg
Photostation for agarose gels	Canon-Kamera
PowerPac Basic Power Supply	Biorad, Munich
PowerPac HC Power Supply	Biorad, Munich
Rotor JA 10	Beckmann, Krefeld
Rotor JA 20	Beckmann, Krefeld
Rotor TLA-100.3	Beckmann, Krefeld
Table centrifuge 5804R	Eppendorf, Hamburg
Thermomixer comfort	Eppendorf, Hamburg
Trans-Blot Cell	Biorad, Munich
Transilluminator TI 1	Whatman Biometra, Göttingen
Ultracentrifuge TL-100 and L8-M	Beckman, Krefeld
Vacuum pump	Vacuubrand, Wertheim
Vortex Genie2	Scientific Industries, USA
Water bath SWB25	Thermo Electron, Karlsruhe

3.2 Methods

3.2.1 Cultivation of yeast cells

3.2.1.1 Growth of yeast cultures

Yeast liquid cultures were inoculated with cells from an agar plate using a sterile toothpick or from a pre-culture with a defined dilution. The cells were incubated overnight (14 - 16 h) on a shaker with 220 rpm at 30°C (if not pointed out otherwise).

3.2.1.2 Short-term yeast storing

To prepare short-term yeast stocks, yeast strains on agar plates were duplicated every 4 - 6 weeks, incubated for 1 - 2 days at 30°C and stored at 4°C.

3.2.1.3 Long-term yeast storing

Long-term yeast stocks were prepared from fresh agar plates or liquid in 15% (v/v) glycerol solution and stored at -80°C.

3.2.1.4 Cell density determinataion

The cell density was measured using the optical density at 600 nm (OD_{600}) in a dilution of 1 : 20 (using empty medium as reference). 1 OD_{600} of growing yeast cells correspond to 3×10^7 cells / ml.

3.2.1.5 Yeast mating type determination

To determine the mating type of a *S. cerevisiae* strain two tester strains YR312 (Mat a) and YR320 (Mat α) were streaked in two separate lines on a MV-medium agar plate. Both strains have the rare *His1* allele, while the other markers are wild type. To test a strain for its mating type it was streaked through each of the tester strain lines. The plates were incubated for 2 days at 30°C. The tested strains will mate only with the tester strain of contrariwise mating type, resulting in a diploid strain that growth on MV-medium.

3.2.2 Isolation of yeast DNA

3.2.2.1 Isolation of chromosomal DNA

To isolate chromosomal yeast DNA 1.5 ml of an overnight culture was harvested (RT, 13000 rpm, 1 min), washed with 500 µl ddH_2O and resuspended in 200 µl breaking buffer (10 mM Tris/HCl pH 8.0; 100 mM sodium chloride; 1 mM EDTA; 1% (w/v) SDS; 2% (v/v) TritonX-100). 200 µl glass beads (0.4 – 0.5 mm; neutralised) and 200 µl phenol/chloroform solution (50% (v/v) phenol; 50% (v/v) chloroform) were added and the reaction was mixed harsh four times for 1 min interrupted by 1 min on ice. Before centrifugation (RT, 13000 rpm, 5 min) 200 µl ddH_2O were added. 200 µl of the upper fraction were transferred to a new reaction cup and the DNA was precipitated with 1 ml of ethanol (-20°C, 100%) for 10 min at -20°C. After

centrifugation (RT, 13000 rpm, 10 min) the sediment was resuspended in 400 µl ddH$_2$O containing 3 µl RNAse A (10 mg / ml). The solution was incubated at 37°C for 5 min and again precipitated for 10 min at -20°C using 10 µl 5 M ammonium acetate and 1 ml of ethanol (-20°C, 100%). The DNA was sedimented (RT, 13000 rpm, 10 min), the supernatant quantitatively removed and the sediment dried for 5 min at 37°C. The DNA sediment was resuspended in 30 µl ddH$_2$0 and stored at -20°C.

3.2.2.2 Isolation of plasmid DNA (plasmid rescue)

To isolate plasmid DNA, 2 ml yeast overnight culture were harvested (RT, 1 min, 13000 rpm) and resuspended in breaking buffer (10 mM Tris/HCl pH 8.0; 100 mM sodium chloride; 1 mM EDTA; 1% (w/v) SDS; 2% (v/v) TritonX-100). 200 µl Phenol and 200 µl glass beads (0.4 – 0.5 mm; neutralised) were added and the solution was incubated on a shaker for 10 min at 4°C. After centrifugation (RT, 13000 rpm, 10 min) 200 µl of the upper fraction were transferred to a new reaction cup. The DNA was precipitated using 1/10 volume 3 M sodium acetate solution and 2.5 times volume ice-cold ethanol (100%). The DNA sediment was washed with 70% ethanol, dried and resuspended in 30 µl ddH$_2$O. This solution contained chromosomal DNA and plasmid DNA. DNA transformation in *E. coli* excluded chromosomal DNA resulting in enrichment of pure plasmid DNA (see chapter 3.2.6 Transformation of *E. coli* cells).

3.2.3 Transformation of yeast cells

3.2.3.1 High efficient transformation of yeast cells

A 50 ml culture was prepared by dilution 1 : 10 from a log-phase pre-culture. Cells were grown to an OD$_{600}$ of 0.5 – 0.8, harvested (RT, 2000 rpm, 5 min), washed two times with 10 ml ddH$_2$O and once with 2.5 ml LiOAc-sorbitol-buffer (10 mM Tris/acetate pH 8.0; 100 mM lithiumacatate; 1 mM EDTA; 1 M D-sorbitol). The cells were resuspended in 100 µl LiOAc-sorbitol-buffer and incubated for 15 min at 30°C to make them competent. The cell suspension was separated in 50 µl aliquots and mixed with 300 µl PEG in Li-TE-buffer (10 mM Tris/acetate pH 8.0; 100 mM lithium acetate; 1 mM EDTA; 40% PEG 3350). 5 µl herring-sperm DNA (10 mg / ml) and 1 - 5 µl of the DNA were added. The samples were first incubated for 30 min at 30°C

and shifted for 15 min at 42°C, followed by a regeneration in 2 ml YPD-medium for 1 - 4 h at 30°C at 220 rpm. The cells were sedimented (RT, 2000 rpm, 3 min), resuspended in water and spread on selection medium.

3.2.3.2 "Quick and dirty" transformation of plasmid DNA in yeast

For fast transformation of plasmid DNA in yeast, cells from an agar plate were resuspended in 300 µl PEG in Li-TE-buffer (100 mM lithium acetate; 10 mM Tris; 1 mM EDTA, 40% (v/v) PEG 3350; pH 8.0 with acetic acid). 5 µl herring-sperm DNA (10 mg / ml) and 1 - 5 µl DNA were added and the samples were gently mixed and incubated as described in 3.2.3.1 High efficient transformation of yeast cells.

3.2.4 *E. coli* cell culture

3.2.4.1 Growth of *E. coli* cultures

E. coli liquid cultures were inoculated with cells from an agar plate or from a long term culture. Liquid cultures were incubated overnight at 220 rpm, 37°C and then harvested (for example for plasmid isolations).

3.2.4.2 *E. coli* long term storing

To prepare a long term stock 500 µl *E. coli* overnight culture were mixed with 500 µl 60% (v/v) glycerol and stored at -80°C.

3.2.5 Preparation of electro-competent *E. coli* cells

Competent cells can take up DNA from the outside of the cell. To produce these competent cells a main-culture of 600 ml LB-medium was inoculated 1 : 100 from an overnight pre-culture of *E. coli* strain DH5α. The cells were incubated at 37°C to an OD_{600} of 0.6 – 0.7, chilled on ice for 10 min and harvested (4°C, 6500 rpm, 8 min). Three washing steps followed: The first with 1 l ice-cold ddH_2O, the second with 0.5 l ice-cold ddH_2O and the third with 20 ml 4°C cold 10% (v/v) glycerol (4°C, 6500 rpm,

8 min). Finally the cells were resuspended in 2 ml cold 10% (v/v) glycerol, divided in 40 µl aliquots and stored at -80°C.

3.2.6 Transformation of *E. coli* cells

In this study electroporation was used to transform *E. coli* cells. Electroporation is used to make the cell membrane more permeable to DNA by an electric impulse. Competent *E. coli* cells were thawn on ice and 1 - 2 µl of the transforming DNA was added. The sample was transferred to a pre-chilled electroporation cell and electroporated at 2500 V. 900 µl SOC-medium were immediately added to the cells and incubated for 1 h at 37°C, 220 rpm. 100 - 500 µl of these cells were spread on LB-plates containing ampicillin and incubated overnight at 37°C.

3.2.7 Plasmid isolation from *E. coli* cells

3.2.7.1 Plasmid isolation from *E. coli* cells by alkaline lysis

To isolate plasmids from *E. coi* cells, 1.5 ml of an overnight culture was harvested (RT, 13000 rpm, 1 min) and the cells were resuspended in 100 µl solution 1 (25 mM Tris/HCl pH 8.0; 50 mM D-glucose; 10 mM EDTA). After adding 200 µl of solution 2 (fresh mixed: 200 mM sodium hydroxide; 1% SDS (w/v)) and gently mixing, 150 µl of solution 3 (3 M potassium acetate; 2 M acetic acid) were added and mixed again. After centrifugation (RT, 13000 rpm, 5 min) the supernatant was transferred to a new reaction cup and the DNA was precipitated for 2 min with 900 µl ethanol (100%). The sample was centrifuged (RT, 13000 rpm, 5 min) and the DNA sediment was air dried. The plasmid DNA was resuspended in 50 µl ddH$_2$O incubated with 0.5 µl RNAse A (10 mg / ml) for 30 min at room temperature. The DNA was stored at -20°C.

3.2.7.2 Plasmid isolation from *E. coli* cells by Wizard Plus SV Kit

To isolate small amounts of clean DNA the Wizard Plus SV Kit from Promega was used as described in the manufacturer's manual.

3.2.7.3 Plasmid isolation fom *E. coli* cells by Quiagen Maxi Kit

To isolate huge amounts of clean DNA the Qiagen Plasmid Maxi Kit from Qiagen was used as described in the manufacturer's manual. The GFP-Osh1 plasmid was isolated using this kit.

3.2.8 Restriction analysis of DNA

DNA was digested with specific restriction enzymes to analyse and prepare DNA. For a 15 µl digestion 1 - 5 µl DNA, 1.5 µl buffer (10 x concentrated), often 0.15 µl BSA (100 x concentrated) and 2 - 10 U enzyme was used. The reaction was incubated for 1 - 2 hours at optimal enzyme temperature. All reactions were done following the manufacturers advice from NEB. 9 µl of the reaction were mixed with 1 µl of DNA sample buffer (1M Tris/HCl H 8.0; 50% (v/v) glycerol; 0.1% (w/v) bromphenolblue). The digest was tested using DNA agarose gel electrophoreses. For preparative digestions the standard reaction was scaled up.

3.2.9 DNA agarose gel electrophoreses

DNA fragments can be separated by size in an electric field using agarose gels. Dependent on the expected size of the fragments agarose gels between 0.8 and 1.5% (w/v) agarose with 1 µg / ml ethidiumbromide in TAE buffer (40mM Tris/acetate pH 8.1; 2 mM EDTA; 0.114% acetic acid) were taken and used to separate DNA in an electrophoresis chamber in TAE buffer. The DNA samples were prepared with DNA sample buffer (1M Tris/HCl H 8.0; 50% (v/v) glycerol; 0.1% (w/v) bromphenolblue) and separated for 25 min at 120 V. Incorporation of ethidiumbromide allowed the detection of the DNA under UV-light (λ = 254 nm).

3.2.10 Gel extraction of DNA (Gel Extraction Kit)

To purify DNA fragments from agarose gels the QIAEX II Gel Extraction Kit from Qiagen was used as described in the manufacturer's manual.

3.2.11 Sizing of DNA fragments

To determine the size of linearized DNA fragments the Standard TriDye 1 kb DNA Ladder (NEB, Frankfurt) was used.

Tab. 11 Standard TriDye 1kb DNA Ladder

Fragment	1	2	3	4	5	6	7	8	9	10
Size (kb)	10	8	6	5	4	3	2	1.5	1	0.5

3.2.12 Ligation of DNA fragments

To ligate DNA fragments 2 - 6 µl insert DNA (prepared with restriction enzymes), 0.5 - 3 µl vector DNA (prepared with corresponding restriction enzymes), 2.5 U T4-DNA-ligase and 1 x ligation buffer (10 x concentrated) were filled to 10 µl with ddH$_2$O and incubated overnight at 16°C. The enzyme ligated the overhanging DNA sequences or the blunt end fragments. Afterwards 1 - 2 µl of the sample were transformed into *E. coli* cells. Only circular plasmids enabled the *E. coli* cells to grow on selection plates.

3.2.13 Polymerase chain reaction (PCR)

The polymerase chain reaction allows the amplification of a DNA molecule using a DNA polymerase.

A 100 µl PCR reaction contained 1 x PCR buffer (10 x concentrated), 100 pmol per oligonucleotide, 1 µl template DNA, 1 µl dNTP mix (25 mM each dNTP), up to 2 µl DMSO (for chromosomal DNA as template) and up to 5 U DNA polymerase. For small fragments Taq DNA polymerase (NEB) was used. To amplify longer DNA Fragments the proof reading polymerase Fideli Taq (USB) was used. This enzyme required special conditions (see manufacturers advice). Up to 30 cycles of DNA denaturation, oligonucleotide annealing and DNA synthesis followed. The program was specially designed for each experiment, depending on the oligonucleotides and the product size. The synthesized product could be analysed in an agarose gel electrophoresis.

3.2.14 DNA sequencing

A sequencing reaction consisted of 1 µl template DNA (preferably plasmid DNA from a Wizard Plus SV Kit purification), 1 µl sequencing mix (polymerase; dNTP´s with fluorescent dyes; 30 mM magnesium chloride and buffer substances), 1 µl oligonucleotide (1 : 100 diluted; compared to usual PCR), 1.5 µl sequencing buffer and 6 µl ddH$_2$O. The PCR program consisted of 25 cycles with a 10 s denaturation step at 95°C, an annealing step for 5 s at 50°C and an elongation step for 4 min at 60°C. The PCR product was precipitated by adding 1 µl 3 M sodium acetate (pH 5.2), 1 µl 125 mM EDTA and 50 µl ethanol (100%, RT). After centrifugation (RT, 13000 rpm, 10 min) the sediment was washed with 70 % ethanol and air-dried. 15 µl formamide were added to stabilize the DNA. The reactions were analysed by the developmental biology of the Georg-August-Universität Göttingen.

3.2.15 Gene deletion using homologue recombination

The deletion of genes as described in Longtine et al. (1998) (Longtine, 1998) was used for the deletion of *atg4*, *atg27* and *vps4* in different background strains. A DNA fragment was amplified using the primers listed in chapter 3.1.4 Oligonucleotides. The primers had a 20 bp homologue region to the template (either a NAT cassette or a HIS3 cassette) and a 45 bp homologue region to the flanking regions of the gene origin. This PCR product was used in a high efficient transformation reaction as described in chapter 3.2.3.1. The yeast cells with the homologues integrated NAT or HIS3 cassette could be selected on medium containing nourseotricine (clonNAT) or lacking histidine.

3.2.16 Generating a CDC48.3 strain in WCG background

3.2.16.1 Crossing of haploid yeast strains

To obtain diploid yeast cells two strains with corresponding mating type were mixed on a agar plate and incubated for 6 h at 30°C.

Tab. 12 Strains for the generation of CDC48.3 in WCG background

Strain	Genotype	Source
cdc48-3	MATa pep4Δ::URA3 cdc48-3 temperature sensitive at 36°C	F. Madeo
WCG4	WCG4a MATα his3-11,15 leu2-3,112 ura3	W. Heinemeyer, Stuttgart

Then the cells were selected for diploids at 36.5°C on CM -HIS selection plates for 2 days.

3.2.16.2 Sporulation

The diploid cells were shifted to fresh GNA agar plates (100 ml contain: 5 g D-glucose; 3 g Difco nutrient broth; 1 g Difco yeast extract and 2% (w/v) agarose) for one day. Then the cells were transferred in 2 ml supplemented liquid sporulation medium (200 ml contain: 20 ml 10% (w /v) potassium acetate stock; 2 ml 0.5% (w/v) zinc acetate stock; 2 ml uracil solution (0,2 mM in 0.5% sodium hydrogen carbonate solution); 1 ml L-histidine solution (0.3 mM); 3.3 ml L-leucine solution (1,7 mM)) for 5 days at 25°C.

3.2.16.3 Random spores

1×10^8 cells and asci of a sporulated culture were mixed with 180 µl ddH$_2$O in a polypropylen tube. 20 µl of 5 mg / ml Zymolyase 20T in ZL-buffer (0.1 M sodium phosphate pH 6.5; 1.2 M sorbitol; 40% glycerol (w/v)) were added and the reaction was incubated for 30 min at 30°C while shaking. The cells were harvested (13000 rpm, 30 sec), washed once with water and resuspended in 100 µl ddH$_2$O. Afterwards they were gently mixed for 2 min and the supernatant was discarded. The

reaction was washed two times with ddH$_2$O and discarded again. 1 ml of sterile 0.01% (v/v) NP-40 in ddH$_2$O was added and the mixture was treated for 2 min with ultrasonic. The solution was diluted (1 : 10 - 1 : 10000) and spread on YPD plates.

3.2.17 Chromosomal N-terminal fusion of GFP-Atg8 using the cre recombinase system

A PCR product for homologue recombination of GFP between Atg8 and its promoter was constructed (Fig. 13 upper part and text). As template the plasmid POM42 and as primers the primers cGFP-Atg8 1f and cGFP-Atg8 2r were used. After homologue recombination (see 3.2.15 Gene deletion using homologue recombination) the URA selection cassette was recombined out of the chromosome by the induction of a cre recombinase (using the Plasmid pSH65) as describen in Gauss R., Yeast 2005 (Gauss, 2005).
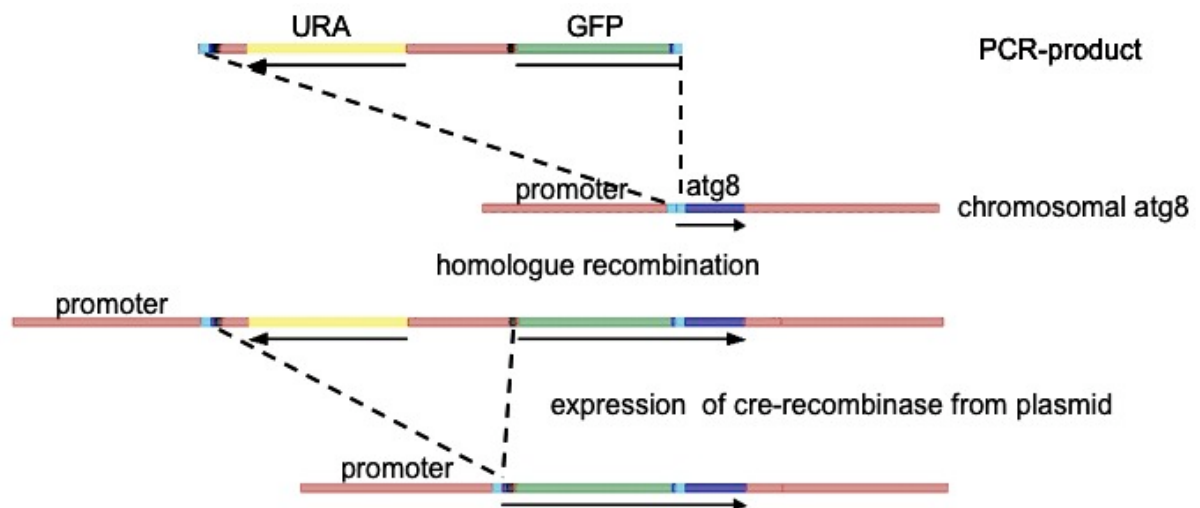
Fig. 13 Construction of the chromosomal n-terminal fusion protein GFP-Atg8
The construction took place in two steps. In the first step the homologue regions in light blue are required for recombination. They lie directly between the promoter region and *atg8*. In the second step a cre recombinase catalyses a homologue recombination between the two lox sites (in black). The arrows indicate open reading frames.

All steps were followed by PCR.

3.2.18 Southern blot

Chromosomal DNA fragments were digested with restriction enzymes and separated by agarose gel electrophoresis. Then the DNA was transferred to a PVDF membrane and analysed with a labled single strand probe.

In a first step a specific DNA hybridisation probe was produced using the manufacturers advice (Gene Images^{TM} Random-Prime Labeling Module-Kit). 20 µg chromosomal DNA was digested overnight with 10 U of a restriction enzyme in a total volume of 50 µl (chapter 3.2.8 Restriction digest). The fragments were separated in a 0.8% agarose gel for 1,5 h at 90 V. Afterwards the gel was washed two times for 8 min in acid-nicking-buffer (250 mM hydrochloric acid), once for 15 min in denaturing buffer (1.5 M sodium chloride; 500 mM sodium hydroxide) and for 1h in neutralisation buffer (500 mM Tris/HCl pH 7.0; 3 M sodium chloride). Then the DNA was transferred to a Hybond N+-nylon-membrane using a diffusion blot overnight with 6 x SSC buffer (90 mM sodium citrate; 900 mM sodium chloride; pH 7.0) (Fig. 14). After the transfer the DNA was cross-linked to the membrane using UV light (5 min on an UV table). The membrane could be stored at 4°C or used for hybridisation.
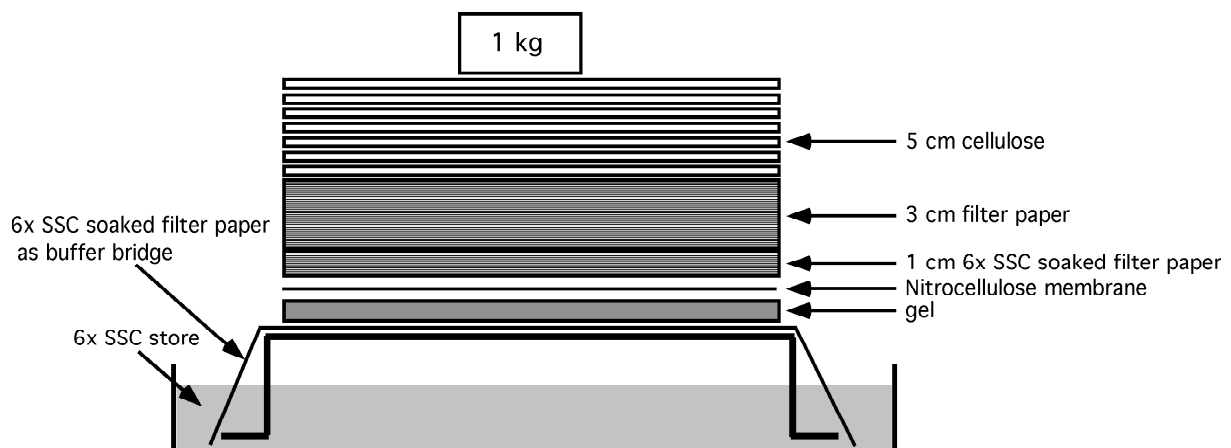
Fig. 14 Diffusion blot

The membrane was washed in hybridisation buffer (0.75 M sodium chloride; 75 mM sodium citrate; 0.1% (w/v) SDS; 5% (w/v) dextransulfate; 5% liquid block (from GE Healthcare)) which was preheated at 60°C for 3 - 5 h in a hybridisation oven at 60°C. The DNA hybridisation probe was added, after boiling for 5 min and chilling on ice for 5 min, to the membrane and incubated overnight. The probe could be reused several times.

After hybridisation the membrane was washed for 15 min with wash buffer 1 (150 mM sodium chloride, 15 mM sodium citrate, 0.1% (w/v) SDS) at 60°C and further washed for 15 min with wash buffer 2 (75 mM sodium chloride, 7.5 mM sodium citrate, 0.1% (w/v) SDS) at 60°C. The subsequent washing steps were performed with diluent buffer (300 mM sodium chloride, 100 mM Tris/HCl, pH 9.5) for 5 min, with 10% liquid block for 60 min and with diluent buffer for 5 min at room temperature. The AP-conjugate was diluted 1 : 5000 in diluent buffer with 0.5% (w/v) BSA and incubated with the membrane for 1h (shaking, RT). After three washing steps with diluent buffer for 15 min, the DNA was detected using the Gene Images CDP-Star Detection Reagent from Amersham (see manufacturers advice).

3.2.19 Alkaline lysis of yeast cells

For alkaline lysis 2 OD_{600} of logarithmic, stationary or starved yeast cells were used. The cells were transferred to a reaction cup and sedimented at 3000 rpm for 5 min. The sediment was resuspended in 1 ml of cold ddH_20 and mixed with 150 µl cold lysis-solution (fresh prepared: 1.85 M sodium hydroxide; 7.5% (v/v) ß-mercaptoethanol). The reaction was mixed every 2 min and kept on ice. After 10 min of incubation 150 µl 50% trichloroacetic acid (w/v) were added and the reaction was incubated on ice for 10 min. The precipitated proteins were sedimented (4°C, 13000 rpm, 10 min), washed twice with acetone and dried for 5 min at 37°C. The sediment was resuspended in 100 µl 2 x Lämmli-buffer (116mM Tris/HCl pH 6.8; 12% (w/v) glycerol; 3.42% SDS (w/v); a tip bromphenolblue; 1% ß-mercaptoethanol) by harsh vortexing for 30 min at 30°C. Before loading the probe on a polyacrylamide gel the cell debris was centrifuged to the bottom of the cup (RT, 13000 rpm, 5 min).

3.2.20 SDS-Polyacrylamid-Gel-Electrophoreses (PAGE)

The discontinuous SDS-PAGE was used as described in Laemmli et al. (Laemmli, 1970) in a Mini-Protean III electrophoreses chamber from Biorad following the manufacturer advice. To separate the samples 8 - 12% acrylamide separating gels and 5% acrylamide collecting gels were used.

Tab. 13 Composition of SDS Polyacrylamid gels

	10%separating gel	5% collecting gel
ddH$_2$0	1.9 ml	3.0 ml
1.5M Tris, pH 8.8	1.25 ml	-
0.5M Tris PH 6.8	-	1.25 ml
Protogel	1.8 ml	0.7 ml
10% (w /v) SDS	50 µl	50 µl
10% (w /v) APS	50 µl	50 µl
TEMED	2.5 µl	5 µl

As molecular maker the "Precision Plus Protein All Blue Standards" marker from Biorad was used, consisting of the following molecular weights: 250 kDa, 150 kDa, 100 kDa, 75 kDa, 50 kDa, 37.5 kDa, 25 kDa, 15 kDa, 10 kDa. After loading the gel (10µl / probe) and filling the gel chamber with SDS-running buffer (200 mM glycerol, 25 mM Tris, 0.1% SDS) the gel run was started with 100 V. When the samples enter the collecting gel the voltage was raised to 150 V. The gel run was stopped after the bromphenolblue band reached the end of the gel, the collecting gel was cut off and the rest of the gel was used for western blot analysis.

3.2.21 Western blot analysis using a trans blot cell

As standard for western blot analysis a Mini Trans-Blot Cell from Biorad was used to blot 2 Gels on PVDF membranes. In bigger approaches up to 8 gels could be blotted at the same time in a Trans blot cell from Biorad. The transfer assembly was built up in a gel holder cassette as follows:
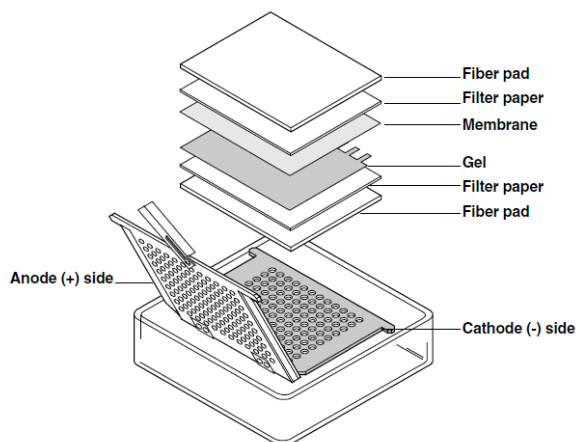
Fig. 15 Cartoon of a gel holder cassette
Two peaces of filter papers (GB 002) were aequilibrated in blotting buffer. The PVDF membrane was activated in methanole (100%) before usage. (picture taken from the Biorad manual)

This packed gel holder cassette was inserted into the buffer tank, which was filled with cold blotting buffer (192 mM glycerol; 25 mM Tris; 20% methanole; 4°C cold). The transfer time was at least 4 hours or overnight at 90 mA per gel. After the blotting process the PVDF-membrane was blocked in TBST (20 mM Tris/HCl pH7.6; 137 mM sodium chloride; 0.1% Tween 20 (w/v)) containing 10% (w/v) skim milk powder, to block up all unspecific binding sites on the membrane, for 1 h at room temperature or overnight at 4°C. The immunoblot was washed three times with 25 ml TBST for 5 min. In the next step the blot was incubated with the primary (first) antibody in TBST at room temperature for at least one hour or overnight at 4°C. The immunoblot was washed three times with 25 ml TSBT for 5 min and then incubated with the second antibody (in TBST with 1% skim milk powder (w/v)) for 1 h. After six 5 min washing steps with TBST, the blot was developed with ECL^{TM} Plus (Amersham) following the manufacturer´s advice.

Afterwards the immunoblot was analysed using a LAS-3000 (Fujifilm). Quantitative statistics from blots were done using the AIDA Software, Version 4.06.116 (Raytest, 2005).

3.2.22 Stripping of once immunodetected membranes

To remove an antibody from an already used immunoblot the membrane was air-dried for 5 min. As first step the blot was washed with methanol and three times with TBST-buffer. Then the attached antibodies were denatured and washed of the membrane by a 10 min incubation with 10% acetic acid (v/v). The acetic acid was removed by washing five times using 25 ml TBST for 5 min. The method continued as described in chapter 3.2.21 with blocking in TBST containing 10% (w/v) skim milk powder.

3.2.23 Subcellular fractionation

For subcellular fractionation 60 OD_{600} of 4h SD(-N) starved cells (OD_{600} of 6) were harvested (2000 rpm, 5min) and incubated for 15 min in 30 ml DTT-buffer (10 mM Tris sulfate pH 9.4; 10 mM DTT). The cells were sedimented (RT ,2000 rpm, 5min), the supernatant discarded and the cells resuspended in 6 ml SP-buffer (1 M sorbitol;

20 mM PIPES pH 6.8). 120 µl of freshly solved Zymolyase T20 (10 mg / ml) in SP-buffer were added and the reaction was incubated in a water bath at 30°C and 20 rpm for 25 min. The spheroplasts were sedimented (RT, 3000 g, 15 min) and resuspended with a glass stick in 6 ml SP-buffer. After a second centrifugation (RT, 3000 g, 3 min) the speroplasts were hypotonically lysed in lysis buffer (0.2 M sorbitol; 20 mM PIPES pH 6.8; 5 mM $MgCl_2$; 1x Complete protease inhibitor (Roche); 1 mM PMSF and 1 x protease inhibitor mix (1000 x concentrated stock 1 mg Antipain, 1 mg Aprotinin, 1 mg Benzamidin, 1 mg Pepstatin A, 1 mg Leupeptin, 1 mg Chymostatin in 1 ml DMSO)). Lysates were generated by centrifugation at 500 g for 10 min. Low-speed pellet P13 (13000 g pellet), high-speed pellet P100 (100000 g pellet) and high speed supernatants S100 (100000 g sup) were generated as described by Kirisako et al. (Kirisako, 2000). The sediments were resuspended in a corresponding volume of 2 x Laemmli buffer and processed for immunoblots.

3.2.24 Sucrose gradient

For a sucrose gradient 600 OD_{600} of 4 h SD(-N) starved cells (OD_{600} of 6) were harvested (500 g, 5 min, 4°C). Cells were washed with 30 ml ice-cold 10 mM sodium azide and centrifuged again (500 g, 5 min, 4°C). The sediment was resuspended in 10 ml spheroplasting (SP) buffer (50 mM potassium dihydrogen phosphate pH 7.5; 10 mM sodium azide; 40 mM ß-mercaptoethanol) containing 3 mg Zymolyase T100 and incubated for 30 - 45 min at 30°C. All following steps were done at 4°C. The spheroplasts were centrifuged (500 g, 10 min, 4°C) and the sediment was resuspended with a glass stick in 10 ml SP-buffer. After a centrifugation (500 g, 10 min, 4°C) the sediment was resuspended in lysis buffer (0.8 M sorbitol; 10 mM MOPS pH 7.2; 1 mM EDTA; PMSF and 1x protease inhibitor mix (1000x concentrated stock 1 mg Antipain, 1 mg Aprotinin, 1 mg Benzamidin, 1 mg Pepstatin A, 1 mg Leupeptin, 1 mg Chymostatin in 1 ml DMSO)) and homogenized with 40 beats of a douncer. After preclearing (5000 rpm, 10 min, 4°C) the supernatant was applied on the top of a sucrose gradient (per step 1 ml of 18, 22, 26, 30, 34, 38, 42, 46, 50, 54% sucrose (w/v)). After 3 h of ultracentrifugation (Beckman ultracentrifuge, SW41 rotor, 34000 rpm) 18 fractions each 610 µl were collected and precipitated with trichloroacetic acid. The sediments were washed two times with acetone and resuspended in 75 µl of 2 x Lämmli-buffer (116 mM Tris/HCl pH 6.8; 12% (w/v)

glycerol; 3.42% SDS (w/v); a tip bromphenolblue; 1% ß-mercaptoethanol) and processed for immunoblots.

3.2.25 Measuring the breakdown of GFP fused proteins

3.2.25.1 Measurement of the breakdown of GFP-Osh1p

All deletion strains were transformed with pRS416-GFP-Osh1. These transformed cells were used for a pre-culture in selective medium (usually CM -URA) overnight at 30°C at 220 rpm agitation. After 26 h of incubation the pre-culture was diluted 1 : 100 as main-culture in the same selective medium and grown overnight at 30°C at 220 rpm. The next morning the cells were harvested at an OD_{600} of 5 - 9. 20 OD_{600} cells were washed with SD(-N) starvation medium, resuspended in 2ml SD(-N)-medium and incubated at 30°C at 220 rpm. 200 µl samples (2 OD_{600} cells) were taken at the given time points (usually 0, 2, 4, 6 and 8h) and alkaline lysed (see chapter 3.2.19 Alkaline lysis of yeast cells). These samples were applied on 10% acrylamide gels containing 6 M urea, analysed with western blots using a trans blot cell (see chapter 3.2.21) and detected with ECL^{TM} Plus (Amersham). After rapamycine-induced starvation the same washing steps were done with fresh CM-medium containing rapamycine (0.2 µg / ml end concentration from a stock solution 1 mg / ml rapamycine in DMSO). When using potassium acetate as starvation medium the cells were washed with 1% potassium acetate (w/v) or 1% potassium acetate (w/v) and 2% glucose.

3.2.25.2 Measurement of the breakdown of GFP-Osh1p or GFP-Atg8 in temperature sensitive strains

To measure the breakdown of GFP-Osh1 or GFP-Atg8 in temperature sensitive strains, the cells were transformed with the pRS416-GFP-Osh1 or GFP-Atg8 plasmid. Transformed cells were taken from agar plates, inoculated as a pre-culture in liquid selection medium (usually CM -URA) and grown overnight at 23°C (permissive temperature) at 220 rpm. Once the cells reached a stationary culture (OD_{600} = 6 - 10), a 20 ml main-culture was started with a dilution of about 1 : 80 which was incubated overnight at 23°C at 220 rpm. The next morning the OD_{600} of the

cultures usually were between 4 and 8. 50 OD_{600} cells were taken, washed two times with 10 ml SD(-N)-medium and then resuspended again in 10 ml SD(-N)-medium. The sample was then divided in two equal parts. One was transferred to a water bath at 23°C (permissive temperature), 110 rpm and the other to a water bath at 34°C, 36°C or 38°C (restrictive temperature), 110 rpm. 400 µl samples (2 OD_{600} cells) were taken at the given time points (0, 1, 2, 3 and 4h) and alkaline lysed (see chapter 3.2.19 Alkaline lysis of yeast cells). These samples were applied on 10% acrylamide Geld containing 6 M urea, analysed with western blots using a trans blot cell (see chapter 3.2.21) and detected with ECL^{TM} Plus (Amersham).

3.2.26 Microscopy

3.2.26.1 Fluorescence microscopy

Most of the fluorescence microscopy was done using a Zeiss Axioskope 2. The pictures were taken with a digital camera (AxioCam MRm) and the AxioVision software (release 4.5, Zeiss). The images were converted and processed with Adobe Photoshop CS3 or Canvas X. Fluorescent pictures were taken with corresponding filter sets: GFP, RFP / Cy3 and DAPI.

5 µl of yeast cells were taken at the indicated time points, dropped on a glass slide and covered with a cover slip.

3.2.26.2 Laser scanning microscopy

To visualize two fluorescent dyes simultaneously a Leica TCS SP2 AOBS confocal laser scanning microscope was used.

3.2.26.3 Endosome and vacuole staining using the dye FM4-64

Yeast cells were grown overnight to an OD_{600} of 0.5 – 6.0. 20 OD_{600} cells were sedimented (RT, 5 min, 2000 rpm) and resuspended in 1 ml YPD-medium containing 2 µl of a FM4-64 solution (1 mg FM4-64 in 100 µl DMSO). The cells were incubated 30 min at 30°C at 220 rpm shaking then transferred to fresh YPD-medium and

directly visualized in the microscope or shifted to starvation medium (SD-(N)) for up to 4 hours. For the visualisation a Cy-3 filter set was used.

3.2.26.4 Vacuole staining of Cell tracker blue (CMAC)

To visualize the vacuole the Cell tracker blue (CMAC) was used. 20 OD_{600} of yeast cells were harvested and resuspended in 1 ml YPD. 2 µl of a 10 mM Cell tracker blue CMAC solution (Invitrogen) were added and the cells were incubated for 30 min at 30°C at 220rpm. The cells were then starved for up to 4 hours and analysed with a DAPI blue filter set.

4. Results

4.1 Where are the autophagic membranes coming from?

Double membrane layered vesicles are formed out of the pre-autophagosomal structure (PAS). Where these membranes come from has been addressed for a long time but not answered yet. Different cell components have been discussed as potential membrane sources (Reggiori, 2004) (Reggiori, 2005) (Young, 2006) (Obara, 2008a). Probably more than one membrane source is required: one for the constitutive Cvt-pathway and an additional one under nutrient limitation for the larger autophagosomes.

Only two transmembrane proteins are known to locate at the PAS. These proteins are Atg27 that has been described to locate at the PAS, the mitochondria and the Golgi complex (Yen, 2007) and Atg9 that has been proposed to cycle between the PAS and mitochondria (Reggiori, 2005) dependent on Atg27. This cycling of Atg9 could deliver lipids to the PAS and thus facilitate the formation of Cvt vesicles and autophagosomes. In *atg1Δ atg27Δ* double deletion cells the localization of Atg9 to its peripheral pool, which corresponds in part to mitochondria, is increased (Yen, 2007).

4.1.1 Analysis of the peripheral Atg9 pool

To enrich the peripheral pool of Atg9 several knockout strains in the WCG4a background were generated as described in chapter 3.2.15. All knockout strains were analyzed using southern blot analysis as described in 3.2.18 (data not shown).
The resident vacuolar hydrolases, aminopeptidase I (Ape1) is synthesized as pro form (pApe1) in the cytosol and transported either constitutively via the Cvt pathway or via the starvation induced macroautophagy pathway to the vacuole. The protein is matured (mApe1) by proteinase A (*pep4*), which can be monitored by western blot.
As additional control of the correct knockout strains were harvested at stationary phase and after 4 h starvation in SD(-N)-medium, alkaline lysed and prepared for immunoblots (Fig. 16 (A.)). A rabbit polyclonal Ape1 antibody was used for detection.

One aim of this study was to review the actual localization of Atg9, since

mitochondria seem unlikely as a membrane source for the PAS.

Atg9Δ, atg1Δ, atg1Δ atg27Δ and *atg4Δ atg27Δ* cells were transformed with GFP-Atg9 and the PAS marker Ape1-RFP (Fig. 16 (B.)).
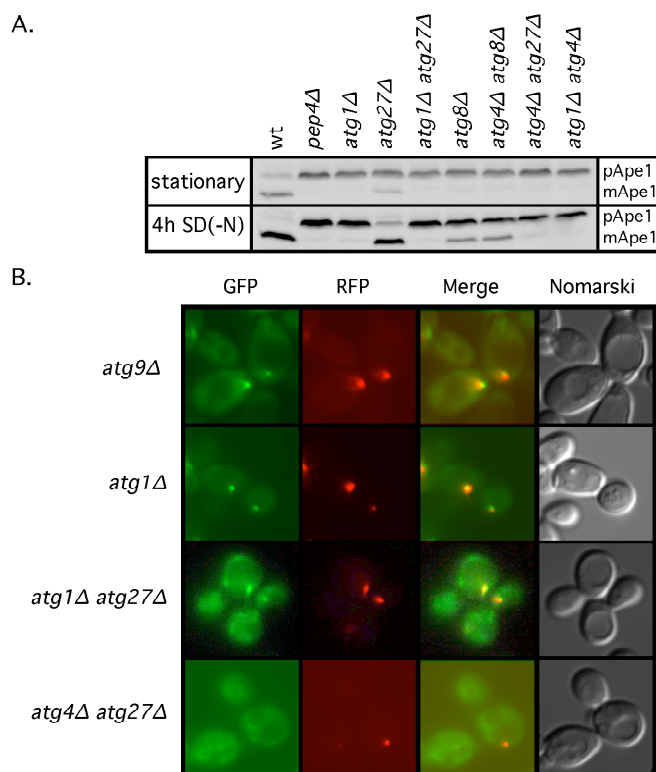
Fig. 16 Verification of the autophagic phenotype of the atg27Δ, atg4 atg27Δ and atg1Δatg27Δ strains using Ape1 (A.) or GFP-Atg9 (B.) as a marker.
All strains in WCG background. **(A.)** Western blot of stationary and 4 hours SD(-N) starved alkaline lysed yeast cells. The full length (pApe1) and the matured form (mApe1) were detected using a polyclonal rabbit Ape1 antibody. **(B.)** Microscopy of stationary grown yeast cells carrying methionine inducible GFP-Atg9 (URA) and Ape1-RFP (LEU); medium: CM -URA -LEU +0,3mM MET.

In wild type cells Ape1 was matured. The vacuolar proteinase A is required for the maturation of Ape1 in the vacuole and Atg1 for the formation of its transport vesicles, independent on the growth conditions.

Atg27Δ cells showed only a small amount of mature Ape1 at stationary phase, but complete maturation after starvation. In *atg8Δ* cells the pro form accumulated but after 4 h starvation 20% of Ape1 was matured (Fig. 16 (A.)).

The plasmid expressed GFP-Atg9 complemented the *atg9Δ* phenotype (after 4 h starvation the Ape1 signal was vacuolar; data not shown). In *atg1Δ* cells GFP-Atg9 accumulated at the PAS. The *atg1Δ atg27Δ* strain showed a GFP-Atg9 co-localization with the PAS marker Ape1 but had additional peripheral dots. This additional pool only existed in some cells and was not stable in further experiments. The *atg4Δ atg27Δ* strain lost the clear peripheral GFP-Atg9 pool (Fig. 16 (B.)).

4.1.2 Identifying a peripheral Atg8 pool

Problems with the stability of the peripheral GFP-Atg9 pool and the finding that the Atg8 protease Atg4 plays a role in the Atg9 cycling, led to the analysis of Atg8. Yeast cells were transformed with GFP-Atg8 and Ape1-RFP and analyzed after 4 h starvation in SD(-N)-medium (Fig. 17).
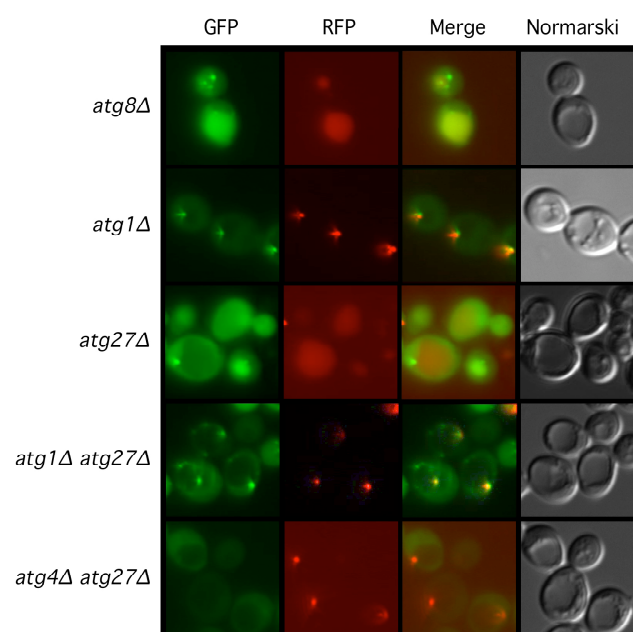
Fig. 17 Identifying a peripheral pool of Atg8 in *atg1Δ atg27Δ* cells
All strains in WCG background. Microscopic analysis of the localization of GFP-Atg8 in different knockout strains. Stationary grown yeast cells carrying GFP-Atg8 and Ape1-RFP were starved in SD(-N) for 4 h before visualization.

The plasmid expressed GFP-Atg8 complemented the *atg8Δ* phenotype. As control, the *atg1Δ* strain was used that restricted Atg8 to the PAS shown by its colocalization with the PAS marker Ape1-RFP. In the *atg1Δ atg27Δ* strain GFP-Atg8 partially colocalized with the PAS and showed an additional peripheral pool. In contrast GFP-Atg8 gave a diffuse and often vacuolar signal in *atg27Δ* cells. *Atg4Δ atg27Δ* cells only showed a diffuse cytosolic signal.

4.1.3 Lipidation of Atg8 is essential for its peripheral pool

To analyze the lipidation state of Atg8 at its peripheral pool and the requirement of the modification machinery for this localization, two different GFP-Atg8 plasmids were used. A full length GFP-Atg8 and an additional GFP-Atg8*, lacking the C-terminal arginine. This arginine is *in vivo* cleaved of by Atg4 before it is coupled to phosphatidylethanolamine (PE) in an ubiquitin like reaction with E1 / Atg3 and E2 / Atg7 (chapter 2.5.6.1). The maturation of Ape1p was tested under stationary and starvation conditions (Fig. 18 (A.)).

The localization of GFP-Atg8 and GFP-Atg8* in *atg4Δ atg8Δ* cells was examined. Cells were cotransformed with GFP-Atg8 or GFP-Atg8* and Ape1-RFP (Fig. 18 (B.) upper part) or stained using FM4-64 as described in chapter 3.2.26.4 (Fig. 18 (B.) lower part). Cells were imaged after 4 h starvation in SD(-N)-medium.
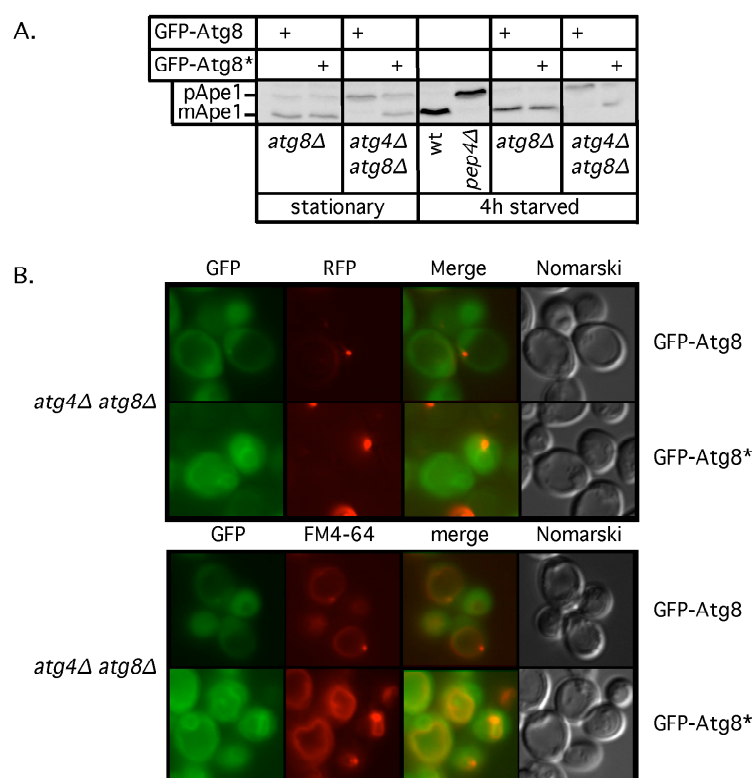
Fig. 18 Analysis of GFP-Atg8 and a GFP-Atg8 mutant lacking the C-terminal arginine (GFP-Atg8*)
All strains in WCG background. **(A.)** Complementation study of GFP-Atg8 and GFP-Atg8* using a polyclonal rabbit Ape1 antibody. **(B.)** Microscopic analysis of the localization of GFP-Atg8 and GFP-Atg8* in the *atg4Δ atg8Δ* strain using the PAS marker Ape1-RFP (upper part) and the endosomal / vacuolar membrane marker FM4-64 (lower part). Cells were starved 4 h in SD(-N)-medium.

Both GFP-Atg8 constructs rescued the Ape1 maturation phenotype of *atg8Δ* cells but in *atg4Δ atg8Δ* cells only the GFP-Atg8* construct complemented the knockout phenotype (Fig. 18 (A.)).

The plasmid carrying wild type GFP-Atg8 had a weak GFP signal but colocalized with the PAS maker Ape1-RFP. The mutant GFP-Atg8* accumulated at a ring around the vacuole. This ring signal colocalized with FM4-64, an endosomal / vacuolar membrane marker (Fig. 18 (B.)).

A plasmid expressing a GFP-Atg8-cherry protein was constructed by insertion of the cherry sequence into the GFP-Atg8 plasmid. The cherry sequence was amplified in a PCR reaction using a plasmid containing NLS-mcherry as template and the primers GFP-Atg8-cherry 1f / GFP-Atg8-cherry 2r (chapter 3.2.13). The resulting PCR product was cotransformed with the linearized GFP-Atg8 plasmid into *atg8Δ* yeast cells for homologous recombination. The plasmid was rescued and sequenced.

Atg8 is coupled by its C-terminus to the inside and outside of autophagosomal membranes and its internal part reaches the vacuole. Because of the stability of GFP in the vacuole, the degradation of GFP-Atg8 can be visualised by immunoblots. The GFP-Atg8-cherry plasmid was constructed to differentiate between uncoupled (GFP and cherry signal colocalizing) and PE-coupled Atg8 (cherry is cleaved of Atg8; no colocalization of GFP and cherry).

The GFP-Atg8-cherry plasmid was transformed in wt, *atg8Δ*, *atg1Δ*, *atg1Δ atg27Δ* and *atg1Δ atg4Δ atg27Δ* cells. The cells were starved, alkaline lysed at the indicated time points and prepared for immunoblots. The membranes were probed with monoclonal GFP antibody (Fig. 19 (A.)). The same cells were analysed in a microscope after 4 h starvation in SD(-N)-medium using a Cy3 and a GFP filter set (Fig. 19 (B.)).
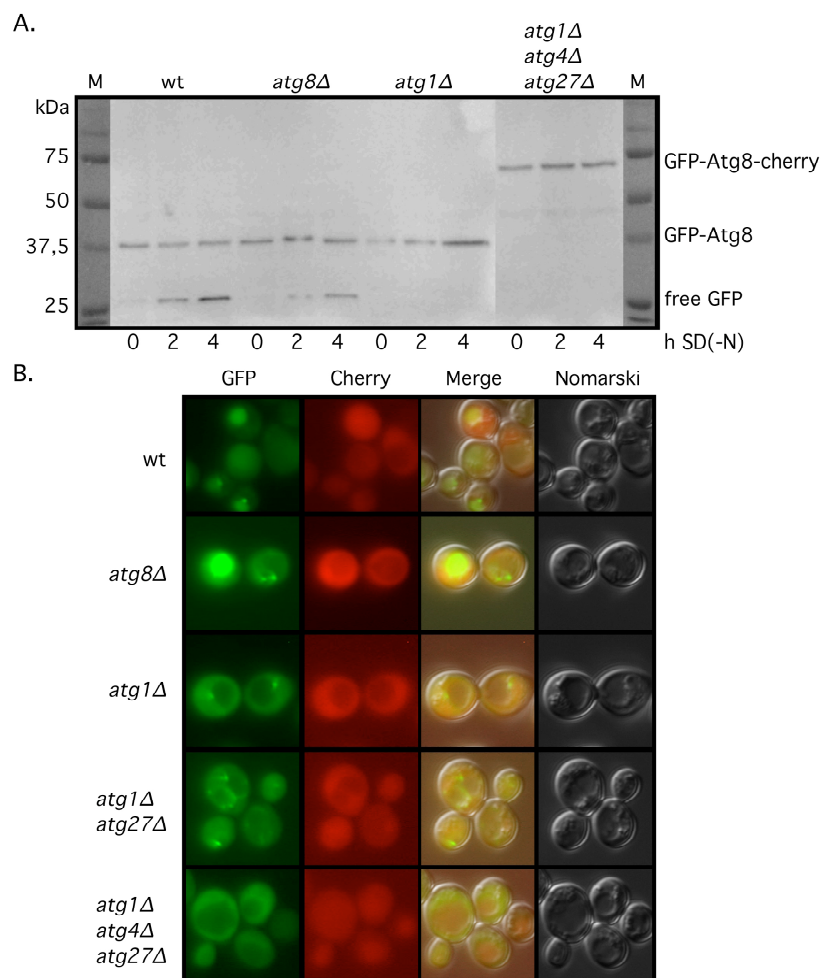
Fig. 19 Lipidation of Atg8 is essential for the peripheral pool
All strains in WCG background. **(A.)** Western blot of stationary (0 h) and SD(-N) starved (2 - 4 h) alkaline lysed yeast cells. The plasmid GFP-Atg8-cherry was detected using a mouse monoclonal GFP Antibody. Size of proteins: GFP = 240 aa = 26 kDa; GFP-Atg8 = 365 aa = 40 kDa; GFP-Atg8-cherry = 594 aa = 65 kDa; **(B.)** Microscopy of stationary yeast cells starved for 4 h in SD(-N) also carrying the GFP-Atg8-cherry plasmid.

The GFP-Atg8-cherry plasmid showed free GFP, thus the plasmid complemented the *atg8Δ* phenotype in western blot analysis. Microscopy provided this by GFP accumulating in the vacuole in those cells. The construct only showed a diffuse microscopic cherry signal in all strains. In *atg1Δ atg27Δ* cells a peripheral GFP pool was visible. The peripheral pool vanished in the *atg1Δ atg4Δ atg27Δ* cells, where cherry was not cleaved of by Atg4 and was full length. Antibodies against the cherry protein were not specific and showed only cross reactions with high molecule weight in immunoblots (data not shown).

4.1.4 The peripheral pool of Atg8 localizes to a PI3P containing ring around the vacuole

The *atg8Δ, atg1Δ* and *atg1Δ atg27Δ* strains were transformed with the pGFP-Atg8 plasmid. The cells were stained with the endosomal / vacuolar membrane marker FM4-64 as described in chapter 3.2.26.3 (Fig. 20 (A.)).

In Fig. 20 (B.) the cells were cotransformed with GFP-Atg8 and a plasmid expressing a RFP-FYVE fusion protein. The FYVE domain binds to PI3P (Stenmark, 2002). The vacuole was additionally visualized using the vacuolar marker Cell tracker blue CMAC as described in chapter 3.2.26.4.
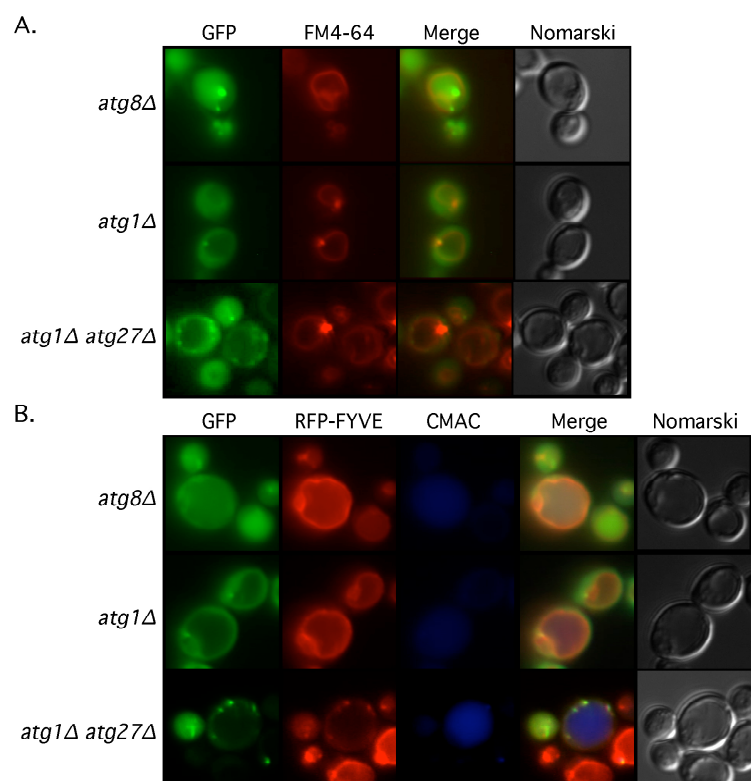
Fig. 20 The peripheral pool of Atg8 localizes to a PI3P containing ring around the vacuole
All strains in WCG background. **(A.)** Microscopic analysis of the localization of GFP-Atg8 in different knockout strains after 4 h starvation in SD(-N)-medium using the endosomal / vacuolar membrane marker FM4-64 and **(B.)** a combination of the RFP-tagged PI3P binding domain FYVE and the vacuolar marker Cell tracker blue CMAC.

The GFP-Atg8 plasmid complemented the *atg8Δ* phenotype. As a control the *atg1Δ* strain was used that restricted Atg8 to the PAS. In the *atg1Δ atg27Δ* strain GFP-Atg8 partially colocalized with the PAS and showed an additional peripheral pool that colocalized with FM4-64 (Fig. 20 (A.)) and RFP-FYVE (Fig. 20 (B.)).

4.1.5 The peripheral pool of Atg8 localizes to endosomes

Vps4 is an AAA[+] ATPase (Babst, 1997). It plays a critical role in the MVB sorting pathway by catalyzing the dissociation of all three ESCRT complexes from the endosome (Katzmann, 2001). Inactivation of Vps4 results in the accumulation of the ESCRT machinery on the endosomal surface leading to enlarged endosomal structures (Hurley and Emr, 2006).

In the WCG4a *atg1Δ atg27Δ* strain the *vps4* gene was deleted. A PCR reaction using the primers (Primer 1 vps4 ko NAT and Primer 2 vps4 ko NAT) and the pFA6-natNT2 plasmid as template was performed. The resulting deletion cassette was used for homologues recombination in the WCG4a *atg1Δ atg27Δ* strain (chapter 3.2.15). The cells were grown on nourseotricin (clonNAT) and tested for correct integration using southern blot (chapter 3.2.18) (data not shown).

The *atg1Δ atg27Δ* strain was used as a control for the normal size of the peripheral GFP-Atg8 dots. Together with *atg1Δ atg27Δ vps4Δ* cells they were cotransformed with GFP-Atg8 and Ape1-RFP and imaged (Fig. 21 (A.)).

Snf7 is one of two major components of ESCRT-III that localizes to endosomal membranes (Hurley and Emr, 2006) and can therefore be used as an endosomal marker.

Two strains *atg1Δ atg27Δ* (WCG4a MATα *atg1Δ*::KAN *atg27Δ*::HIS3) and Snf7-RFP (S288C MATa Snf7-RFP::KAN), carrying a pRS315 (LEU) plasmid, were crossed. The diploid cells were selected on CM –HIS -LEU and transferred to 1% potassium acetate for 5 days. The sporulated cells were used for random spores treatment as described in chapter 3.2.16.3 and then selected on CM –HIS –LEU +KAN to receive a haploid *atg1Δ atg27Δ* Snf7-RFP strain. The cells were tested by western blot analysis for maturation of Ape1 after 4 h SD(-N) starvation and their RFP signal in microscopy (data not shown).

Atg1Δ atg27Δ and *atg1Δ atg27Δ* SNF7-RFP cells were transformed with GFP-Atg8 and imaged after 4 h starvation in SD(-N) (Fig. 21 (B.))

A.

B.
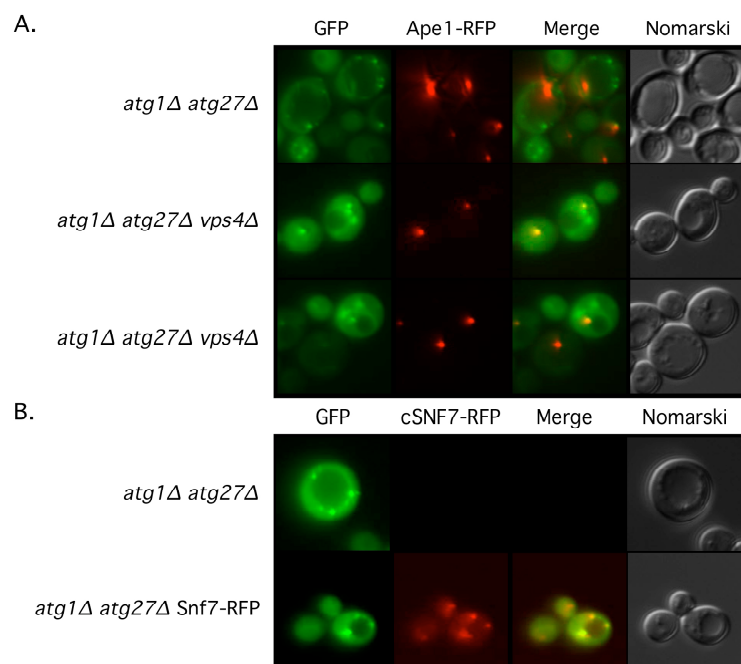
Fig. 21 Accumulation of the peripheral Atg8 pool in *vps4Δ* cells and colocalization with the endosomal protein SNF7.
(A.) Microscopic analysis of the localization of GFP-Atg8 in different knockout strains using the PAS marker Ape1-RFP. The upper row of pictures shows *atg1Δ atg27Δ* cells, the lower two rows of pictures show *atg1Δ atg27Δ vps4Δ* cells. **(B.)** Microscopic analysis of GFP-Atg8 in an *atg1Δ atg27Δ* chromosomally Snf7-RFP tagged strain.

The *atg1Δ atg27Δ vps4Δ* strain showed a clear accumulation of GFP-Atg8 at the peripheral dots compared to the *atg1Δ atg27Δ* strain (Fig. 21 (A.)).

The chromosomal integrated Snf7-RFP colocalized with the GFP-Atg8 in the *atg1Δ atg27Δ* yeast (Fig. 21 (B.)).

4.1.6. Quantification of the Atg8 peripheral pool in different deletion strains

GFP-Atg8 was transformed into *atg1Δ*, *atg1Δ atg27Δ* double mutant and *atg1Δ atg27Δ vps4Δ* triple mutant cells.

At least three independent experiments were quantified. Cells with clear GFP-Atg8 dots were sorted into one of the following categories: one GFP-dot; two GFP-dots; more than two GFP-dots.

contigent of yeast cells with GFP-dots
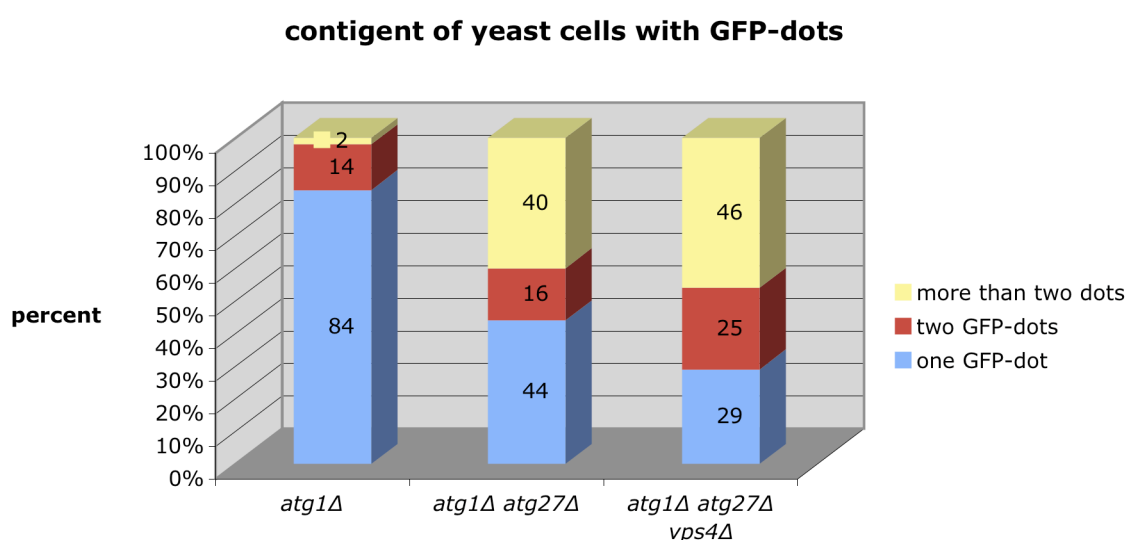
Fig. 22 Quantification of the Atg8 peripheral pool in different deletion strains
Data from at least three independent experiments (*atg1Δ* n=193; *atg1Δ atg27Δ* n=314; *atg1Δ atg27Δ vps4Δ* n=145)

84% of *atg1Δ* cells had one GFP-Atg8 dot. Only 2% showed more than two dots. But 40% of *atg1Δ atg27Δ* cells and even 46% of *atg1Δ atg27Δ vps4Δ* cells had more than two GFP-Atg8 dots. The amount of cells with more than one GFP-dot increased in cells lacking Atg1 Atg27 and additionally Vps4.

4.1.7 Characterization of the Atg8 peripheral pool

Kirisako et al. showed a shift in the distribution of GFP-Atg8* compared to wildtype GFP-Atg8 from P100 to P13 in *atg4Δ atg8Δ* cells in a subcellular fractionation experiment (Fig. 23 (A.)) (Kirisako, 2000). This shift represented the different localizations of wild type and mutant GFP-Atg8* in microscopy (Fig. 18 (B.)). The fractionation experiment was extended to analyze the peripheral pool in *atg1Δ*

atg27Δ cells compared to *atg1Δ* cells (Fig. 23 (A.)). GFP-Atg8 was transformed in *atg1Δ, atg1Δ atg27Δ* and *atg4Δ atg8Δ* cells. As a control for experimental procedure *atg4Δ atg8Δ* cells were also transformed with GFP-Atg8*. In Fig. 23 (A.) stationary cells were harvested, converted to spheroplasts and hypotonically lysed. Lysates were cleared by centrifugation at 500 g for 10 min. Low-speed pellet P13 (13000 g pellet), high-speed pellet P100 (100000 g pellet) and high-speed supernatant S100 (100000 g sup.) were generated as described by Kirisako et al. (Kirisako, 2000). The pellets were dissolved in corresponding volume of Laemmli buffer and processed for immunoblots (chapter 3.2.23).

In Fig. 23 (B.) SD(-N) starved cells were harvested. Cells were converted to spheroplasts, solubilized in lysisbuffer and homogenized with 40 beats of a douncer. After preclearing, supernatant was applied on the top of a sucrose gradient (18%-54% sucrose). After 3 h of ultracentrifugation 18 fractions were collected and precipitated. The pellets were dissolved in Laemmli buffer and processed for immunoblots (chapter 3.2.24).
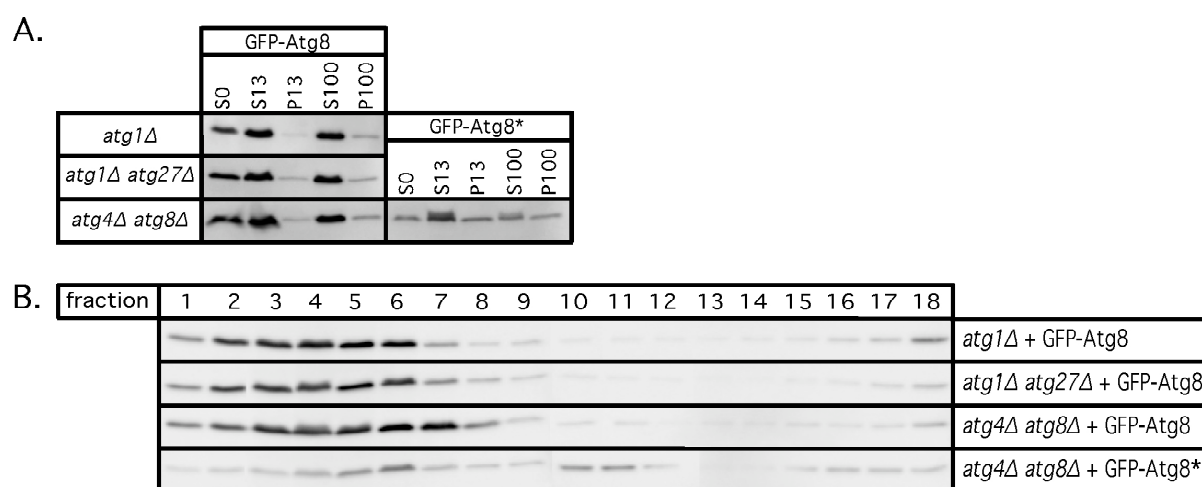
Fig. 23 Characterization of the Atg8 peripheral pool.
All strains in WCG background. Cells expressing GFP-Atg8 from a plasmid were treated as described in chapter 3.2.23 **(A.)** Subcellular fractionation and 3.2.24 **(B.)** Sucrose gradient analyzed by western blot using a monoclonal GFP mouse antibody.

In the subcellular fractionation experiment (Fig. 23 (A.)), no shift of plasmid expressed wild type GFP-Atg8 could be detected in the distribution pattern of *atg1Δ* compared to the double deletion *atg1Δ atg27Δ*.

In the sucrose gradient (Fig. 23 (B.)) also no shift in the distribution of Atg8 in *atg1Δ atg27Δ* cells compared to *atg1Δ* could be detected. The quality of the sucrose

gradient was tested using the endosomal marker Pep12 that was mainly located in fraction 5 and 6 in all four gradients (data not shown).

In the subcellular fractionation as well as the sucrose gradient, a shift could be seen in *atg4Δ atg8Δ* cells expressing GFP-Atg8 and GFP-Atg8* used as a control for the successful experiment.

4.1.8 Chromosomal integration of GFP-Atg8

GFP-Atg8 was chromosomally integrated behind the endogenous Atg8 promoter using a Cre-Lox recombination strategy (chapter 3.2.17). The integration was done in WCG4a wt, *atg1Δ* and *atg1Δ atg27Δ* cells and verified by PCR (data not shown). All three strains were grown to stationary phase and shifted to SD(-N)-medium for 4 h before imaging.
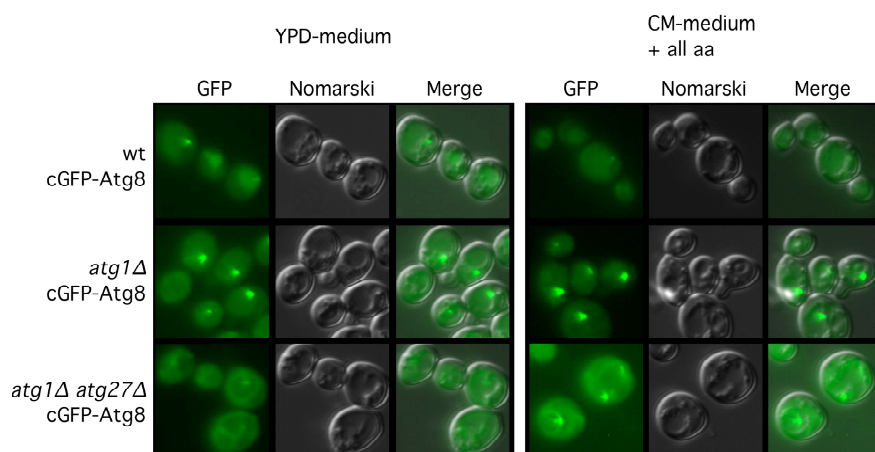
Fig. 24 Chromosomal integrated cGFP-Atg8
YPD-medium (left) and CM-medium containing all amino acids (right) were used as growth medium. At stationary phase (OD_{600} = 6) cells were starved for 4 h in SD(-N) and photos were taken.

GFP-Atg8 accumulated in the vacuole of wild type cells. Some cells showed one GFP-Atg8 dot. The majority of *atg1Δ* cells the GFP signal was restricted to a single dot. *Atg1Δ atg27Δ* cells often showed membranous GFP structures but rarely dots.

4.1.9 Comparison of plasmid GFP-Atg8 and chromosomal GFP-Atg8
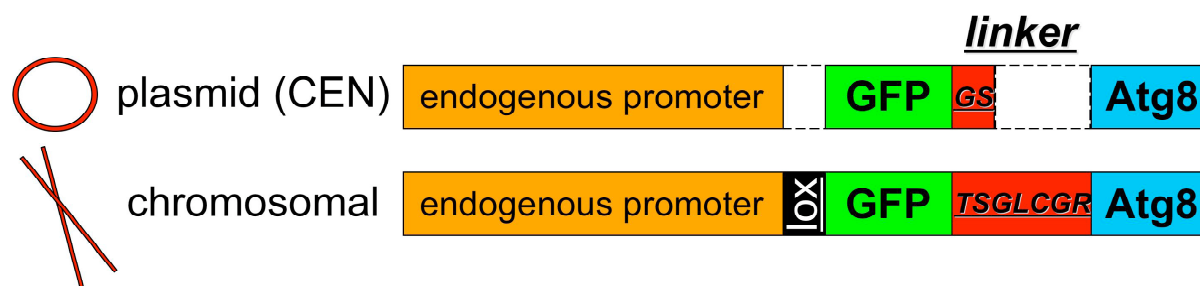
Fig. 25 Comparison of plasmid and chromosomal GFP-Atg8
The proportions in this figure are not correct. The letters between GFP and Atg8 represent amino acids in single letter code. The lox site derives from the cre recombination (chapter 3.2.17), it is 69 bp long and leads to 23 additional amino acids in front of GFP.

The two GFP-Atg8 differ in three points: the expression level, the remaining lox site between promoter and GFP and the linker connecting the GFP with Atg8.

4.2 Piecemeal microautophagy of the nucleus (PMN / micronucleophagy)

In the yeast *S. cerevisiae* autophagy selective degradation of nearly all compartments by autophagy has been described. Even the nucleus is degraded in a microphagic process, which has been called piecemeal microautophagy of the nucleus (PMN), and is induced by nitrogen starvation (Roberts, 2003). PMN occurs at contact sites between the nucleus and the vacuole, the so called vacuolar junctions (NV-junctions) and are formed by a set of proteins. Nvj1 is anchored in the inner and outer nuclear membrane, spans the whole contact site and interacts on the vacuolar membrane with Vac8 (Fig. 9) (Millen, 2008). In *vac8Δ* cells, Nvj1 fails to concentrate into NV-junctions and instead encircled the nucleus. NV-junctions are absent in both *nvj1Δ* and *vac8Δ* cells (Pan, 2000). Therefore *vac8Δ* cells were used as negative-control for all PMN experiments in this study. Under starvation conditions Nvj1 enhances the recruitment of Tsc13 and Osh1. Both proteins are involved in the lipid metabolism of the cell (Kvam and Goldfarb, 2007). GFP-Osh1 has been shown to be a reliable molecular marker to follow nuclear degradation by PMN (Krick, 2008b).

The formation of PMN vesicles depends on these NV-junction proteins and more recently the autophagic machinery has been described to be involved in the PMN process (Krick, 2008b).

4.2.1 Detection of intravacuolar free-floating PMN vesicles

Studies concerning PMN were mainly focused on NV-junction proteins. Their degradation was followed using immunoblots and EM and microscopy.

The nuclear content of PMN vesicles was traced using a NLS-mcherry fusion protein consisting of the nuclear localization sequence of Nab2 and a tandem repeat of the fluorescent mcherry protein. The lipase-like Atg15 protein is required for intravacuolar lysis of autophagic bodies and PMN vesicles. Atg1 is a core autophagic protein required for all known autophagic processes in *S. cerevisiae* (chapter 2.5.5).

Atg15Δ and *atg1Δ atg15Δ* cells expressing NLS-mcherry were starved for 4 h in SD(-N) and examined using videomicroscopy (Fig. 26 (A.)).

Atg15Δ cells expressing NLS-mcherry and the autophagosomal marker GFP-Atg8 (Fig. 26 (B.)) or the cytosolic marker 3-phosphoglycerate kinase (PGK) (Fig. 26 (C.)) were starved for 4 h in SD-(N). Both images (shown in Fig. 26 (B) and Fig. 26 (C)) were taken simultaneously with a Leica TCS SP2 AOBS confocal laser scan microscope.
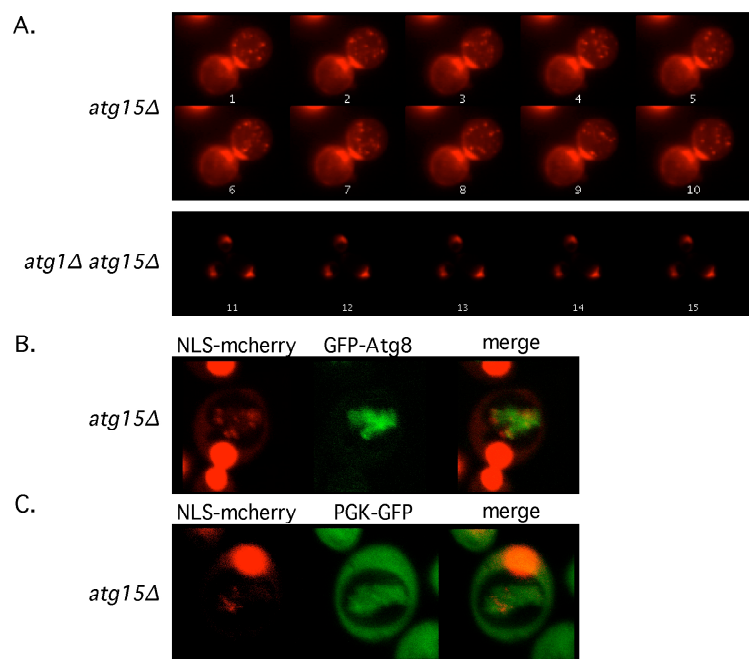
Fig. 26 Detection of intravacuolar free-floating PMN vesicles by fluorescence microscopy.
(A.) Videomicroscopy of *atg15Δ* cells expressing NLS-2mcherry. Cells were starved for 4 h in SD(-N). The imaging of picture 1 - 10 took about 2 sec and pictures 11 - 15 about 1 sec. *Atg15Δ* cells expressing NLS-mcherry and GFP-Atg8 (B.) or PGK-GFP (C.) were starved for 4 h in SD-(N) and imaged using a confocal laser scan microscope.

In *atg15Δ* cells free floating red vesicles accumulated in the vacuole. The red fluorescent vesicles were absent in *atg1Δ atg15Δ* cells (Fig. 26 (A.)).

Fig. 26 (B.) and Fig. 26 (C.) showed significantly more green than red fluorescent intravacuolar vesicles. The red and green vesicles did not overlap.

4.2.2 PMN depends on the autophagic core machinery

Krick et al. showed, using western blot analysis, that the degradation of GFP-Osh1 depends on the core autophagic machinery (Krick, 2008b).

PMN can also be visualized microscopically by NLS-mcherry (Fig. 26). Cells expressing NLS-mcherry and the autophagosome marker GFP-Atg8 were starved for 4 h in SD(-N) medium in the presence of 1 mM proteinase B inhibitor PMSF.
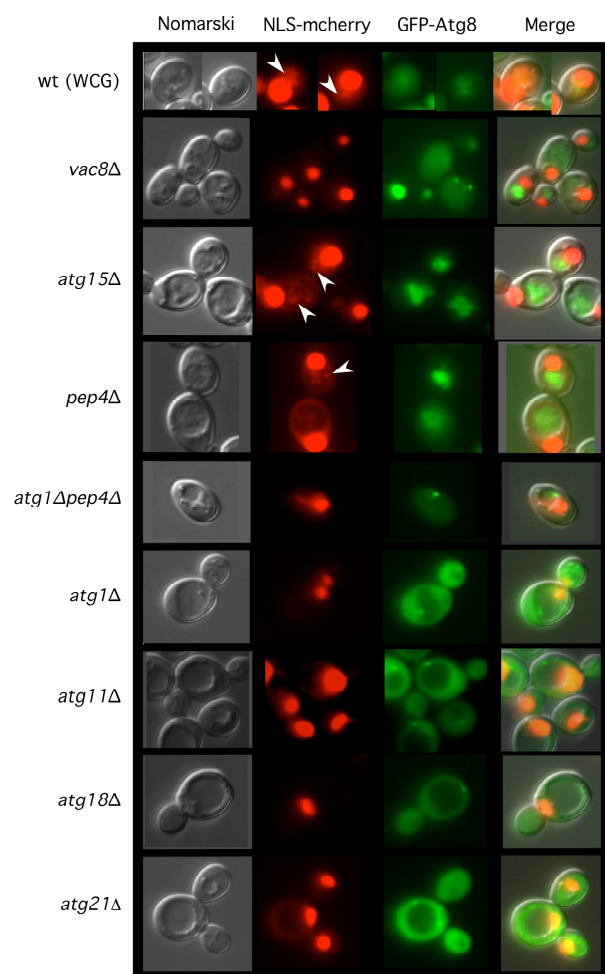
Fig. 27 PMN depends on the autophagic core machinery
The indicated mutant cells coexpressing NLS-mcherry and the autophagic marker GFP-Atg8 were starved for 4 h in SD(-N)-medium in the presence of 1 mM PMSF. White arrowheads indicate vesicles.

In wild type, *atg15Δ* and *pep4Δ* cells red and green fluorescent vesicles accumulated in the vacuole. The *vac8Δ* cells showed green but no red vesicles in the vacuole. All other knockouts neither had a GFP nor a RFP signal in the vacuole, which is in accordance with the western blot analysis of PMN (shown in (Krick, 2008b) (Krick, 2008a)).

4.2.3 Quantification of PMN induction

To find out the best stimulus for PMN induction different starvation media were tested. Stationary (OD_{600} = 6) wild type and *vac8Δ* cells expressing GFP-Osh1 were shifted to different starvation conditions: SD(-N)-media, 1% KAc (potassium acetate), 1% KAc + 2% glucose and CM-medium containing rapamycin (0.2 µg / ml), a TOR (target of rapamycin) inhibitor leading to autophagy induction (chapter 2.5.5).
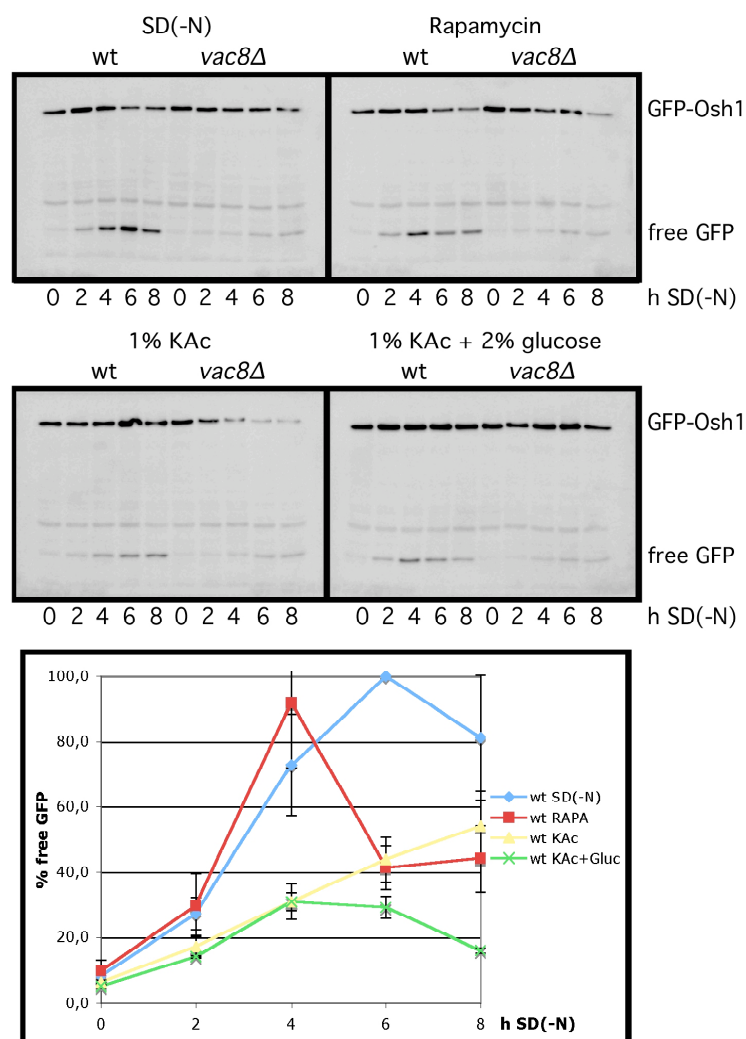
Fig. 28 Quantification of PMN induction
All strains in WCG background. Upper part: Cells expressing GFP-Osh1 were shifted to different starvation conditions, were alkaline lysed at the indicated time points and analyzed by western blot analysis using a monoclonal GFP mouse antibody. Lower part: The free GFP-band of three independent experiments were quantified using the aida software. The 6 h value of the wild type strain in SD(-N) of each experiment was set to 100%. Values are shown with SED.

SD(-N) caused the brightest free GFP signal. Until 4 h induction rapamycin treatment resulted in the same amount of free GFP. Then the GFP signal decreased drastically to 40%. In 1% potassium acetate the results showed a slower increase in free GFP compared to SD(-N) starvation. Addition of 2% glucose decreased the free GFP rate.

4.2.4 Cdc48.3

Cdc48 belongs to the family of AAA$^+$ ATPases. It is involved in many cellular processes like membrane fusion (chapter 2.6.1). The human homologue of Cdc48 is believed to extract ubiquitin conjugated fusion inhibitors out of complexes or lipid membranes and thus mediate fusion events (Schuberth and Buchberger, 2008).

Therefore the involvement of Cdc48 in PMN membrane fusion events was tested. Crossing of the cdc48-3 and WCG4 (wild type in the lab) strain generated the Cdc48.3 temperature sensitive strain in WCG background as described in chapter 3.2.16. The strain did not grow at 38°C which was set as restrictive temperature. The viability at this temperature in SD(-N)-medium for 4 h was not altered compared to wild type cells (data not shown).

In the BY4741 background the Cdc48.3 strain showed a growth defects at 36°C. The restrictive temperature for W303 was 34°C.

The experiments were conducted as described in chapter 3.2.25.2 in these three different backgrounds (WCG (I.); BY4741 (II.); W303 (III.)). The blots were reprobed with antibodies to 3-phosphoglycerate kinase (PGK) as loading control. The samples were loaded again, blotted and the maturation of Ape1 was tested using polyclonal Ape1 antibodies.

I. A.

WCG background GFP-Osh1

I. B.

WCG background GFP-Atg8

Fig. 29 (cont.)

II. A.

BY4741 background GFP-Osh1

II. B.

BY4741 background GFP-Atg8

Fig. 29 (cont.)

III. A.   W303 background GFP-Osh1
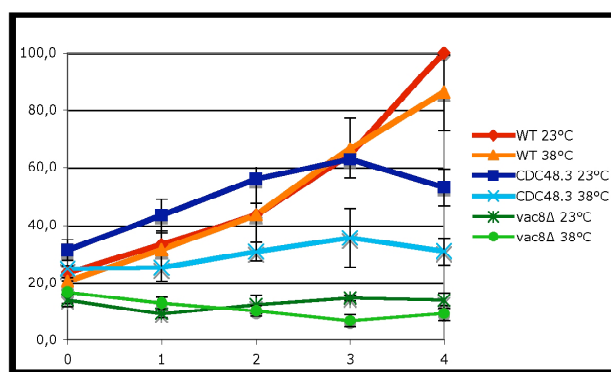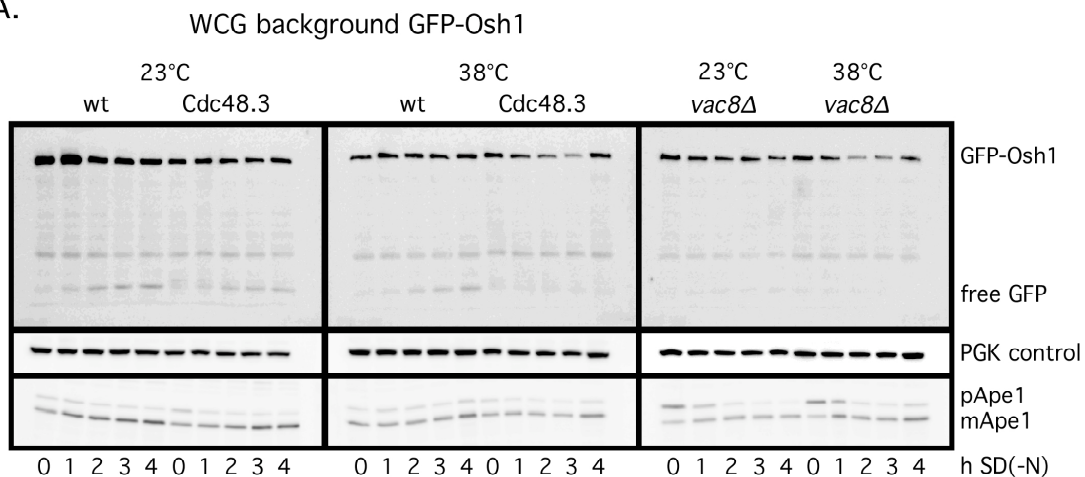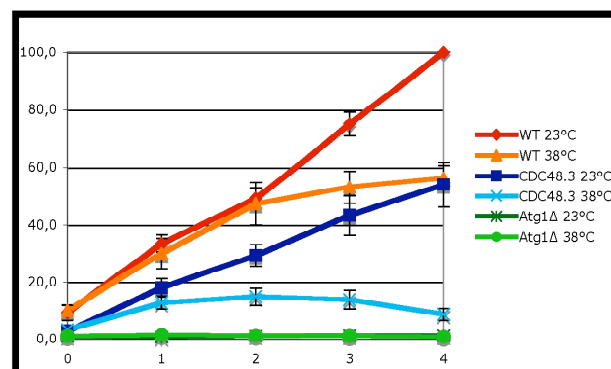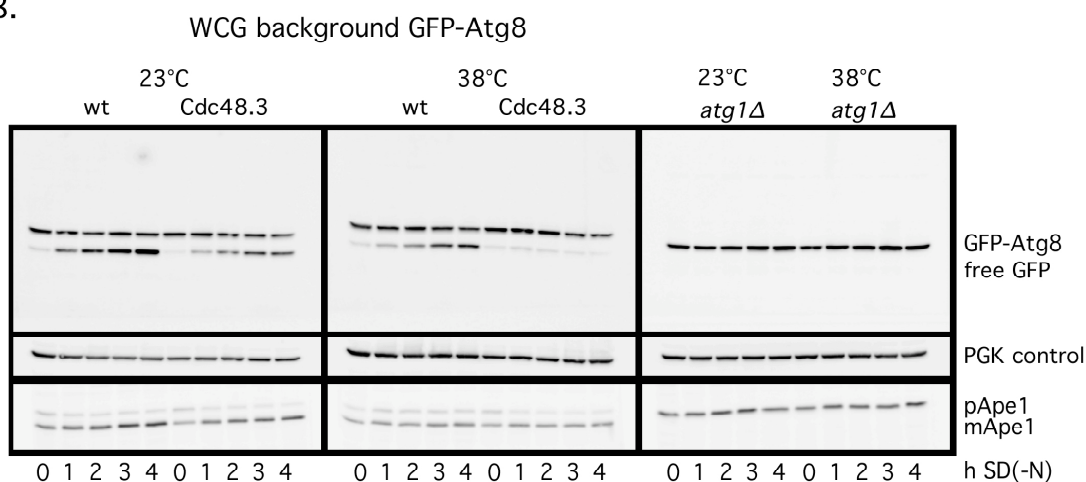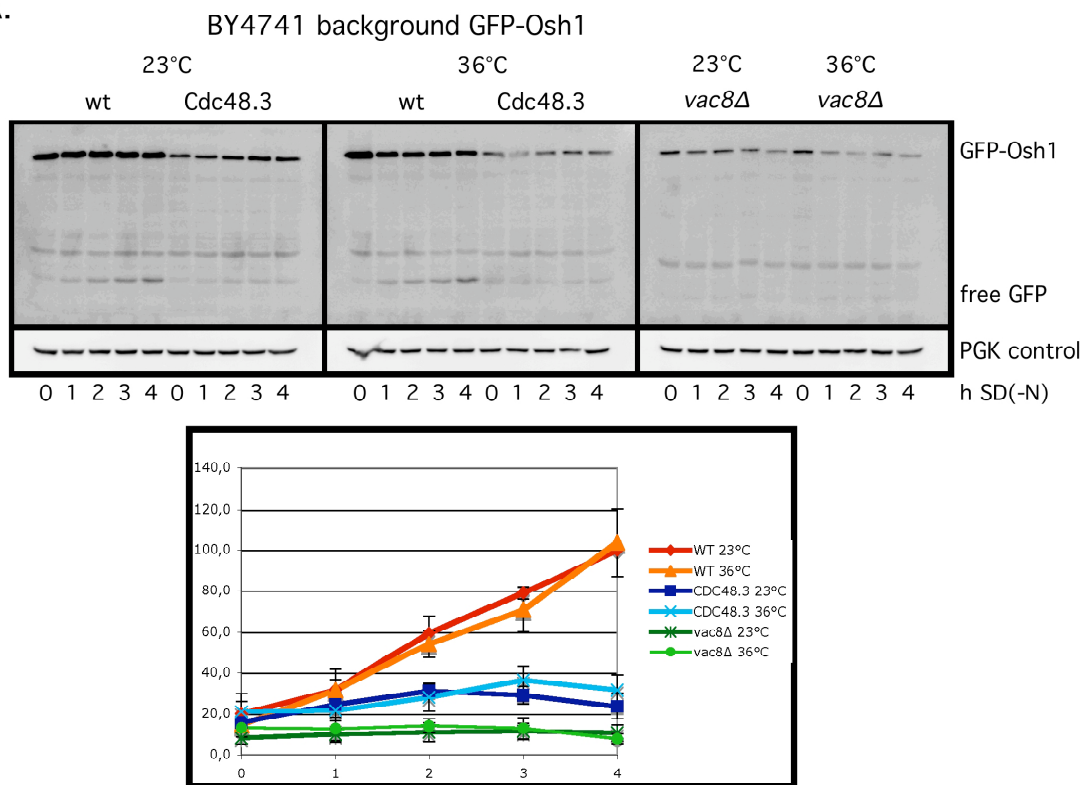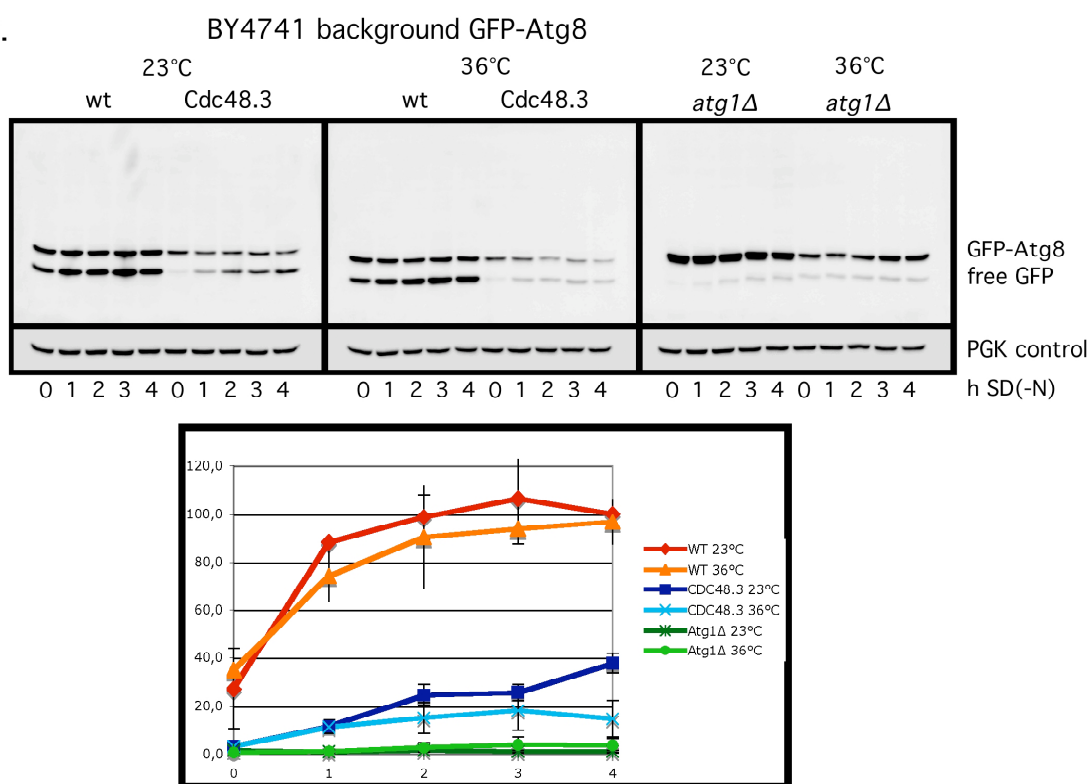
III. B.   W303 background GFP-Atg8
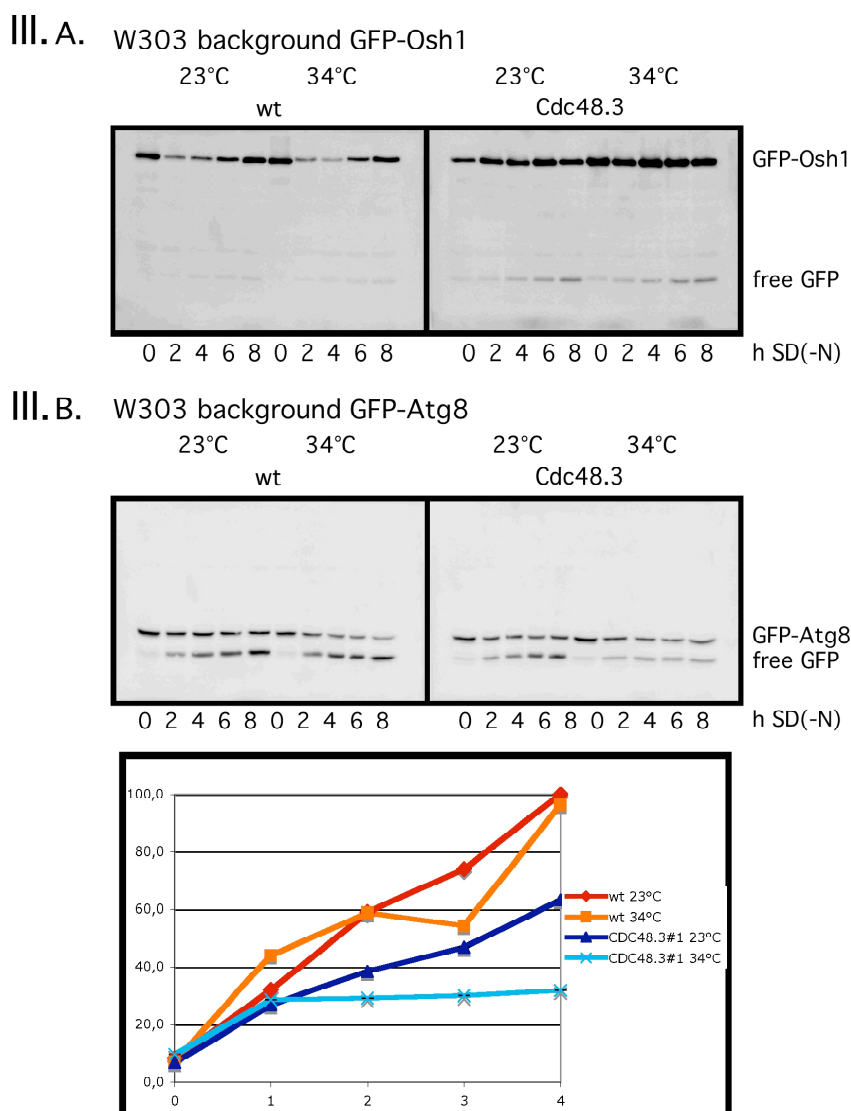
Fig. 29 Cdc48.3 (I.) WCG, (II.) BY4741 and (III.) W303 background
(**I**.) All strains in WCG background. (**II.**) All strains in BY4741 background. (**III.**) All strains in W303 background. Cells expressing GFP-Osh1 **(A.)** or GFP-Atg8 **(B.)**. Cells were pre-cultured at 23°C, shifted to SD(-N)-medium, divided in two equal parts and incubated at 23 or 34°C (W303), 36°C (BY4741) or 38°C (WCG). Western blot analysis of alkaline lysed cells at indicated time points. Blots were probed using a GFP monoclonal antibody and reprobed using a monoclonal PGK antibody **(I. and II.)**. In WCG background **(I.)** the maturation of Ape1p was detected with a polyclonal rabbit Ape1 antibody.
Quantification: The free GFP-signal was quantified: Quantificatin by aida software: **(I.)** three **(A)** or four **(B)** independent experiments; **(II.)** three **(A)** or two **(B)** independent experiments; **(III.)** one experiment **(B)** was quantified.The 4 h value of the wt cells at 23°C was set to 100% in each experiment. Values are shown with SED.

(I.) WCG background:

The degradation of GFP-Osh1 was normal in Cdc48.3 cells at the permissive temperature but a 50% reduction of free GFP was detectable at the restrictive temperature.

The degradation of GFP-Atg8 was slightly reduced at the permissive temperature. This effect was drastically increased at 38°C.

Ape1 maturation was independent on the temperature. Wild type cells produced matured Ape1 and *atg1Δ* cells showed no maturation of Ape1. The PGK loading controls showed no significant difference between samples.

(II.) BY4741 background:

After PMN induction Cdc48.3 cells expressing GFP-Osh1 showed only small amounts of free GFP independent on the temperature. There was no difference in free GFP between 23°C and 38°C, but a significant decrease in free GFP compared to wild type.

GFP-Atg8 degradation was low in Cdc48.3 cells even at the permissive temperature. An increase to the restrictive temperature reduced the free GFP. The PGK controls showed no significant difference between samples.

(III.) W303 background:

GFP-Osh1 showed no free GFP-signal in wild type. Cdc48.3 had a free GFP signal, which did not change between permissive and restrictive temperature. GFP-Atg8 showed a reduction in free GFP at the restrictive temperature.

4.2.5 Cdc48 cofactors

4.2.5.1 The substrate recruiting adaptor Shp1 is required for PMN and macroautophagy

UBX proteins in general are cofactors for Cdc48 / p97 (chapter 3.6.1). In humans the homologues of the substrate recruiting adaptor Shp1 (p47) and Cdc48 (p97) control the fusion of homotypic Golgi membranes (Kondo, 1997). Ubx2 and Ubx5 are described as additional substrate recruiting factors for Cdc48 (Tab. 1) (Schuberth, 2004) (Schuberth and Buchberger, 2008).

Cells were transformed with GFP-Osh1 (Fig. 30 (A.) upper part and (Fig. 30 (B.)) or GFP-Atg8 (Fig. 30 (A.) lower part), grown to stationary phase and starved for up to 8 h. Samples were taken at the indicated time points, alkaline lysed and prepared for immunoblots (chapter 3.2.25.1).
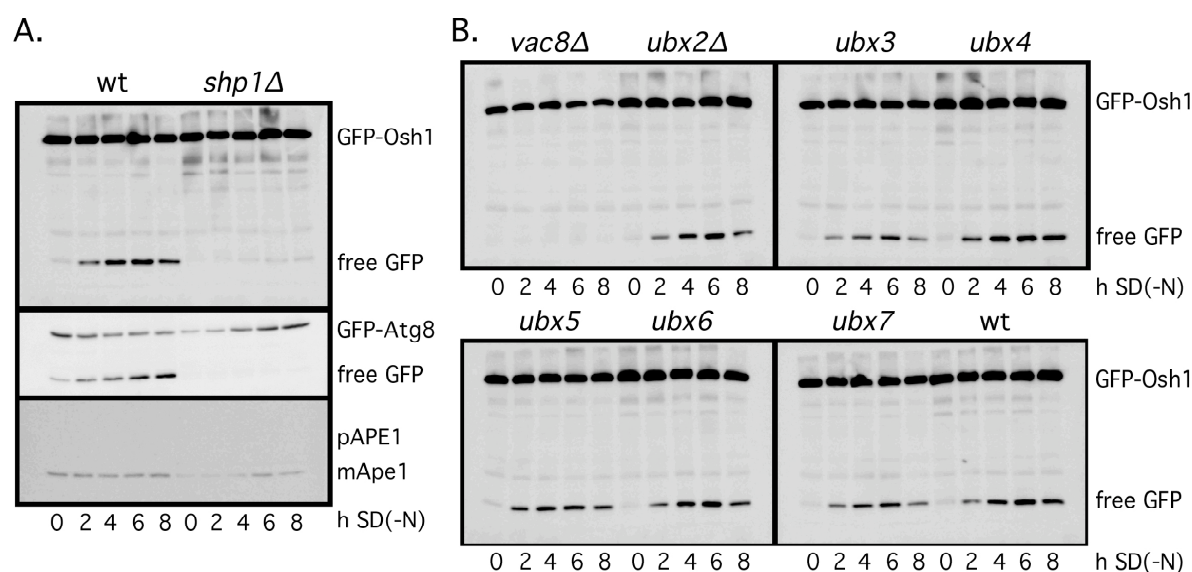
Fig. 30 The Cdc48 substrate adaptor Shp1 is required for PMN and autophagy (A.), but non of the other ubx protein family members (B.)
All strains were BY4741 background. Cells were transformed with GFP-Osh1 **(A)** upper blot and **(B)** or GFP-Atg8 **(A.)** lower two blots. Western blot of alkaline lysed stationary (0 h) and starved (2 – 8 h) SD(-N)) yeast cells. GFP-Osh1, GFP-Atg8 and free GFP were detected using a mouse monoclonal GFP antibody. The maturation of Ape1p was detected with a polyclonal rabbit Ape1 antibody. Three independent experiments showed comparable results.

Ubx2∆, ubx3∆, ubx4∆, ubx5∆, ubx6∆ and *ubx7∆* showed the same amount of free GFP as the corresponding wild type cells expressing GFP-Osh1. The free GFP was drastically reduced in *shp1∆* cells expressing GFP-Osh1 or GFP-Atg8. Ape1 was matured in *shp1∆* cells.

4.2.5.2 Other known complex partners and processing factors of Cdc48

Despite the UBX family there are other known complex partners and processing factors of Cdc48. Der1 and Dfm1 are homologue proteins (Hitt and Wolf, 2004). They both interact with Cdc48 but are part of distinct complexes (Goder, 2008) involved in ER-associated protein degradation (ERAD). The trimeric Cdc48-Ufd1-Npl4 complex is the core component in the export of misfolded ER substrates (ERAD) (Raasi and Wolf, 2007). Ufd1 and Npl4 deletion strains are inviable, therefore a ufd1.1 point mutant lacking the ERAD function was analyzed (Jarosch, 2002). This mutant was also mutated in *prc1* (prc1.1) that codes for the carboxypeptidase Y (CPY; proteinase C). Ufd2 and Ufd3 bind Cdc48 via the same region and compete for Cdc48 binding (Rumpf and Jentsch, 2006). Ufd2 promotes Cdc48 dependent degradation of ubiquitylated substrates whereas Ufd3 stabilizes substrates. The human UBX(-like) protein VCIP135 has been described as the only cofactor that cooperates with the p97-p47 complex in membrane fusion events (Uchiyama, 2002) (Kano, 2005). In contrast to VCIP135, the yeast homologue Otu1 has been characterized in Cdc48 Ufd1-Npl4-dependent degradation processes (Rumpf and Jentsch, 2006), where it participates in the antagonistic interplay of Ufd2 and Ufd3.

Cells were transformed with GFP-Osh1 (Fig. 31 (A.)) or GFP-Atg8 (Fig. 31 (B.)), grown to stationary phase and starved for up to 8 h. Samples were taken at the indicated time points, alkaline lysed and prepared for immunoblots (chapter 3.2.25.1).
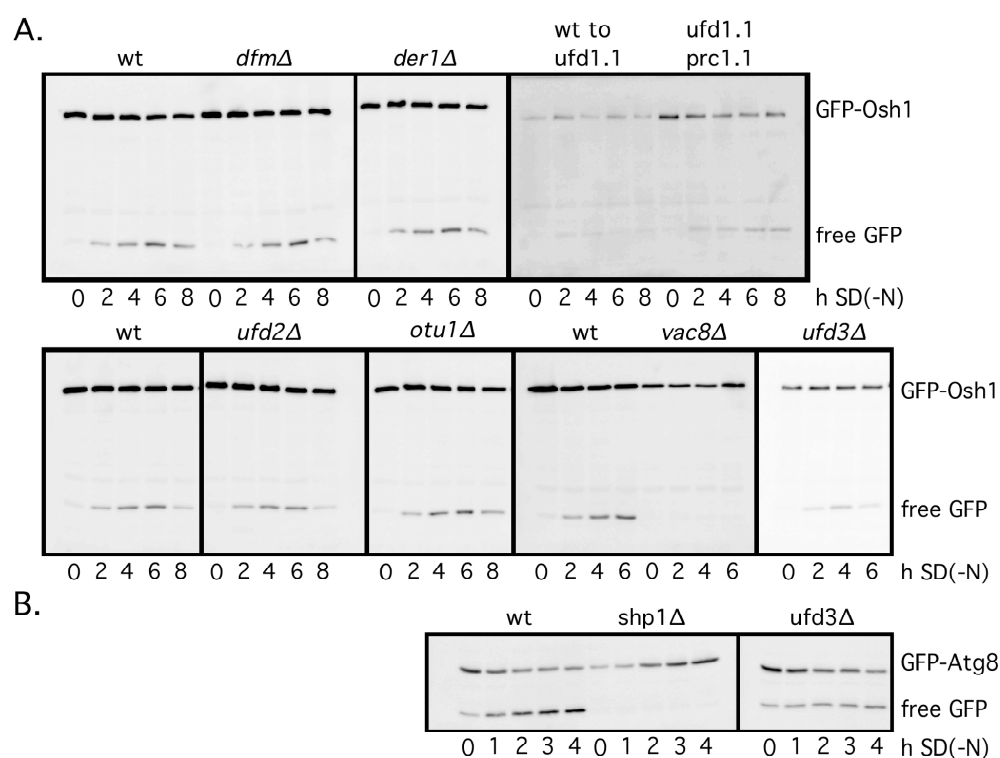
Fig. 31 Complex partners and processing factors of Cdc48
All strains except wt to ufd1.1 and ufd1.1 prc1.1 were BY4741 background. Cells were transformed with GFP-Osh1 **(A.)** or GFP-Atg8 **(B.)**. Western blot of alkaline lysed stationary (0 h) and starved (2 – 8 h SD(-N)) yeast cells. GFP-Osh1, GFP-Atg8 and free GFP were detected using a mouse monoclonal GFP antibody.

Dfm1Δ, der1Δ, ufd2Δ and *otu1Δ* showed the same amount of free GFP as the corresponding wild type cells. The free GFP signal in cells expressing GFP-Osh1 was reduced in *ufd3Δ* cells (this result was reproduced three times) (Fig. 31 (A.)) but only slightly affected in cells expressing GFP-Atg8 (Fig. 31 (B.)). The wild type in BWG1-7a background (wt to ufd1.1) expressed the GFP-Osh1 fusion protein at low level. The strain had hardly any free GFP. The ufd1.1 prc1.1 cells produced free GFP.

4.2.6 Monoubiquitin is required for PMN and autophagy

Cdc48 in combination with Shp1 is described in the literature to interact with ubiquitinated proteins. Doa4 is a ubiquitin isopeptidase, required for recycling of ubiquitin from proteasom-bound polyubiquitinated proteins. Its deletion depletes the cellular ubiquitin level (Swaminathan, 1999) (Ren, 2008).

Wild type and *doa4Δ* cells expressing GFP-Osh1 or GFP-Atg8 were starved in SD(-N). Samples were taken, alkaline lysed and prepared for immunoblots (chapter 3.2.25.1) (Fig. 32 (A.)).

Even monoubiquitin- or polyubiquitin-conjugated proteins can interact with Cdc48 complexes. Ubiquitin is bound on its C-terminal glycine to a target protein. For polyubiquitin chain formation the C-terminus of a free ubiquitin molecule is covalently bound to a intramolecular lysine (one letter code: K) of the target protein bound ubiquitin. Ubiquitin has 7 intracellular lysines, three of them are typically used for polyubiquitination (K29, K48 and K63).

To investigate whether polyubiquitin conjugation is required for PMN, cells were cotransformed with pGFP-Osh1 and plasmids expressing modified ubiquitin molecules under the control of an inducible copper promoter. The ubiquitin molecules contained substitutions of lysines to arginines (one letter code: R) at position 29, 48, 63 or all lysines. The cells were shifted to media containing 100 µM copper sulfate for 3 h. After induction most of the ubiquitin in the cell was modified and used for normal ubiquitination, but could not be polyubiquitin conjugated at the modified position (dependent on the plasmid used). The cells were transferred to SD(-N) starvation medium and samples were collected at the indicated time points, alkaline lysed and prepared for immunoblots (chapter 3.2.25.1) (Fig. 32 (B.)).

A.

Fig. 32 Monoubiquitin is required for PMN and autophagy
(A.) All strains were BY4741 background. **(B.)** All strains were SEY background. Cells were transformed with GFP-Osh1 **(A.)** upper part and **(B.)** or GFP-Atg8 **(A.)** lower part. Western blot of alkaline lysed stationary (0 h) and starved (2 – 8 h SD(-N)) yeast cells. GFP-Osh1, GFP-Atg8 and free GFP were detected using a mouse monoclonal GFP antibody.
(A.) Three independent experiments and **(B.)** two independent experiments showed comparable results.

Doa4Δ cells showed a clear reduction in free GFP signal compared to wild type.

There was no difference in free GFP signal in control cells compared to one of the modified ubiquitins. Even for the ubiquitin molecule without any lysine the free GFP signal showed no decrease. This points to the requirement of monoubiquitin for PMN and autophagy.

4.2.7 Ubp3 and Bre5 are only required for PMN

The ubiquitin protease Ubp3 and its cofactor Bre5 are required for selective autophagic degradation of the large 60S subunit of ribosomes upon starvation (ribophagy). Indeed the catalytic activity of the ubiquitin protease Ubp3 is necessary for its ribophagic function, implying that this process requires the cleavage of ubiquitin from a yet unknown substrate (Kraft, 2008). As ribophagy is a selective variant of autophagy the involvement of Ubp3 or Bre5 was tested in selective degradation of the nucleus.

Wild type, *vac8Δ*, *ubp3Δ* and *bre5Δ* cells were transformed with GFP-Osh1 (Fig. 33 (A.)) or GFP-Atg8 (Fig. 33 (B.)). Stationary cells were shifted to SD(-N) starvation medium and samples were collected at the indicated time points, alkaline lysed and prepared for immunoblots (chapter 3.2.25.1).

Fig. 33 Ubp3 and Bre5 are only required for PMN
All strains were BY4741 background. Cells were transformed with GFP-Osh1 **(A.)** or GFP-Atg8 **(B.)**. Western blot of alkaline lysed stationary (0 h) and starved (2 – 6 h SD(-N)) yeast cells. GFP-Osh1, GFP-Atg8 and free GFP were detected using a mouse monoclonal GFP antibody. **(A.)** Three independent experiments showed comparable results.

In Fig. 33 (A.) *ubp3Δ* and *bre5Δ* cells showed a clear reduction in free GFP compared to wild type cells. In contrast the free GFP signal was comparable to wild type cells when GFP-Atg8 was expressed (Fig. 33 (B.)).

4.2.8 VPS class E genes are only required for PMN

Vps27 and Vps28 belong to class E *vps* genes and are required for formation of multivesicular bodies in late endosomes. In class E mutant strains, the structure of the endosomes is abnormally enlarged and transport and retrieval from this compartment is severely affected. Class E mutants are not required for the Cvt-pathway or autophagy (Reggiori, 2004), but could be involved in micronucleophagy. Wild type, *vac8Δ, vps27Δ* and *vps28Δ* cells were transformed with GFP-Osh1 (Fig. 34 (A.)) or GFP-Atg8 (Fig. 34 (B.)). Stationary cells were shifted to SD(-N) starvation medium and samples were collected at the indicated time points, alkaline lysed and prepared for immunoblots (chapter 3.2.25.1).

Fig. 34 Vps27 and Vps28 are only required for PMN
All strains were BY4741 background. Cells were transformed with GFP-Osh1 **(A.)** or GFP-Atg8 **(B.)**. Western blot of alkaline lysed stationary (0 h) and starved (2 – 8 h SD(-N)) yeast cells. GFP-Osh1, GFP-Atg8 and free GFP were detected using a mouse monoclonal GFP antibody. **(A.)** Three independent experiments showed comparable results.

The *vps27Δ* and *vps28Δ* strains showed a clear reduction in free GFP compared to wild type. In contrast the free GFP signal was comparable to wild type cells when GFP-Atg8 was expressed.

Bsd2 and Tul1 are required for efficient ubiquitination of membrane proteins of the MVB pathway and contribute to the removal of misfolded membrane proteins (Hettema, 2004).
Wild type, *vac8Δ* and bsd2Δ *tul1Δ* cells were transformed with GFP-Osh1. Stationary

cells were shifted to SD(-N) starvation medium and samples were collected at the indicated time points, alkaline lysed and prepared for immunoblots (chapter 3.2.25.1).

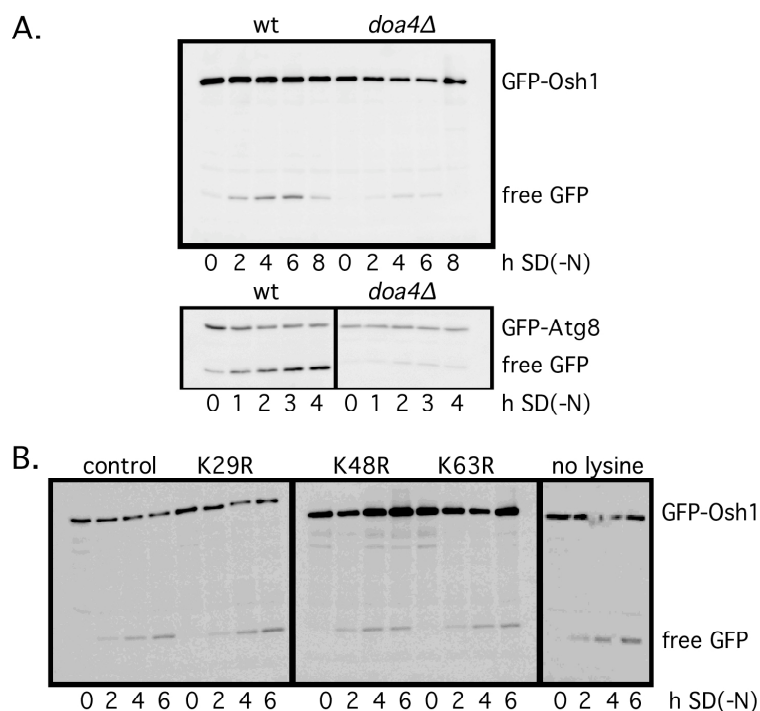**Fig. 35 Further strains involved in MVB transport**
All strains were BY4741 background. Cells were transformed with GFP-Osh1. Western blot of alkaline lysed stationary (0 h) and starved (2 – 6 h SD(-N)) yeast cells. GFP-Osh1 and free GFP were detected using a mouse monoclonal GFP antibody.

Bsd2Δ tul1Δ double mutant cells showed no reduction in free GFP compared to wild type cells.

4.2.9 The Fatty acid elongation machinery is not required for PMN

Fatty acid elongation requires biochemical reactions that are catalyzed by Elo2, Elo3, Tsc13, and Ybr159 (Rössler, 2003). The products of this elongation machinery are so called very-long-chain fatty acids (VLCFAs), which have been proposed to promote highly curved membrane structures (Schneiter and Kohlwein, 1997). Kvam et al. speculated that VLCFAs may be required for the efficient biogenesis of highly curved PMN vesicles. They described a reduced vesicle size in Tsc13-1 mutant cells and Tsc13-1 cells lacking Elo3 (Kvam, 2005).

Tsc13Δ cells are not viable and therefore were not used in this study. Wild type, *vac8Δ, elo2Δ, elo3Δ* and *YBR159Δ* cells were transformed with GFP-Osh1. Stationary cells were shifted to SD(-N) starvation medium and samples were collected at the indicated time points, alkaline lysed and prepared for immunoblots (chapter 3.2.25.1).
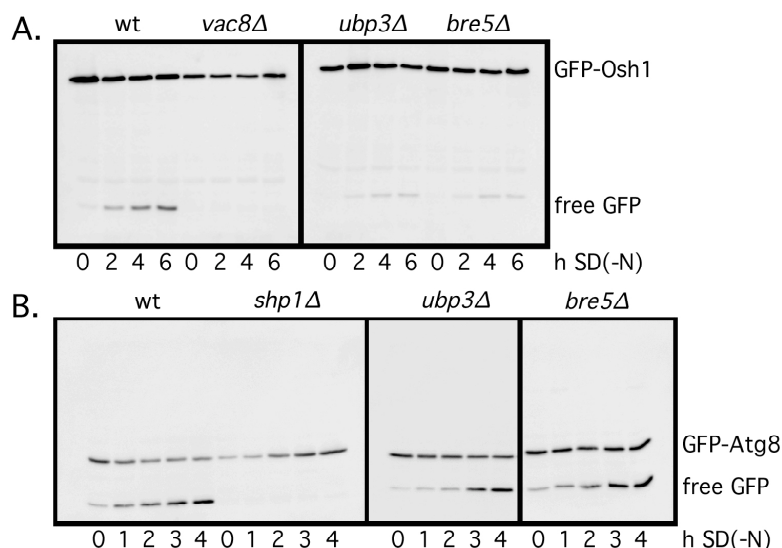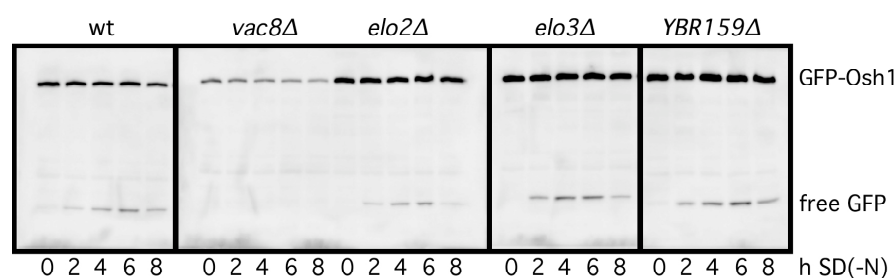

Fig. 36 Fatty acid elongation machinery is not required for PMN
Alls strains were BY4741 background. Cells were transformed with GFP-Osh1. Western blot of alkaline lysed stationary (0 h) and starved (2 – 8 h SD(-N)) yeast cells. GFP-Osh1 and free GFP were detected using a mouse monoclonal GFP antibody.

Elo2Δ, elo3Δ and *YBR159Δ* cells showed no reduction in free GFP compared to wild type cells.

4.2.10 Proteins involved in cortical ER inheritance are not required for PMN

All proteins discussed in this chapter have been described to be involved in the inheritance of the cortical ER. The integral membrane proteins Yop1 and Rtn1 generate the tubular structure of the endoplasmic reticulum (ER) (Hu, 2008).

Scs2 and Ice2 are proteins, which are involved in cortical ER inheritance and in additional perturb septin assembly at the bud neck. Scs2 has a function in targeting Osh1 to NV-junctions, although it is not strictly required for the localization of GFP-Osh1p (Loewen, 2003).

Myo4 is a type V myosin motor protein, which is required for the delivery of cortical ER into daughter cells during bud formation in yeast. She2 and She3 interact with Myo4, but only She2 is required for cortical ER inheritance and acts as a linker between cargo proteins and Myo4 (Du, 2004).

Wild type, *vac8Δ*, *rtn1Δ*, *ice2Δ*, *yop1Δ*, *scs2Δ*, *myo4Δ*, *she2Δ* and she3Δ cells were transformed with GFP-Osh1. Stationary cells were shifted to SD(-N) starvation medium and samples were collected at the indicated time points, alkaline lysed and prepared for immunoblots (chapter 3.2.25.1).
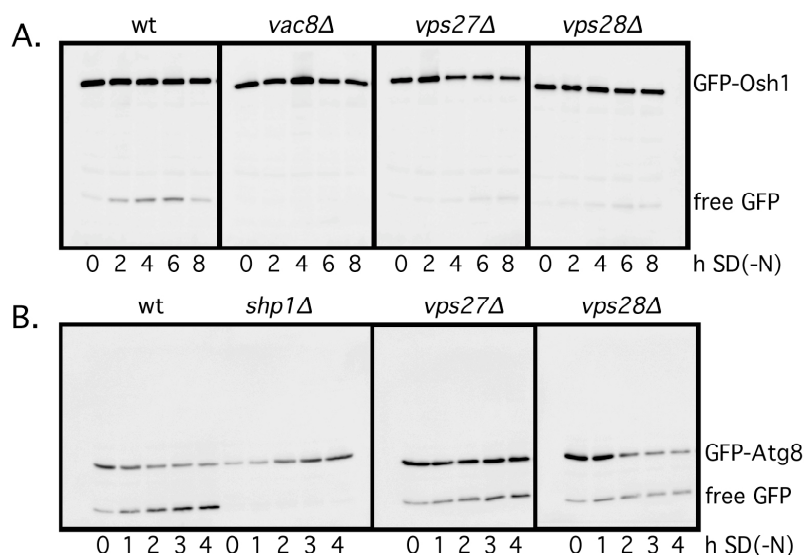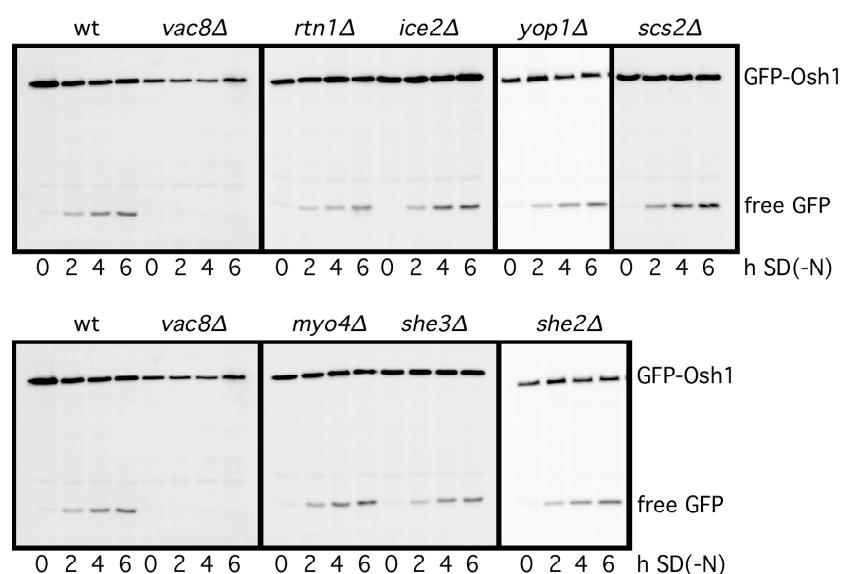

Fig. 37 Proteins involved in cortical ER inheritance are not required for PMN
All strains were BY4741 background. Cells were transformed with GFP-Osh1. Western blot of alkaline lysed stationary (0 h) and starved (2 – 6 h SD(-N)) yeast cells. GFP-Osh1 and free GFP were detected using a mouse monoclonal GFP antibody.

Rtn1Δ, ice2Δ, *yop1Δ*, *scs2Δ*, *myo4Δ*, *she2Δ* and *she3Δ* cells showed no reduction in free GFP compared to wild type cells.

4.2.11 Analysis of a mutant with misshaped nucleus

In *spo7Δ* mutants the nucleus is misshaped exhibiting a single protrusion that may be degraded by PMN. The Spo7 protein is part of a phosphatase complex that represses phospholipid biosynthesis (Campbell, 2006).

Wild type, *vac8Δ* and *spo7Δ* cells were transformed with GFP-Osh1. Stationary cells were shifted to SD(-N) starvation medium and samples were collected at the indicated time points, alkaline lysed and prepared for immunoblots (chapter 3.2.25.1).
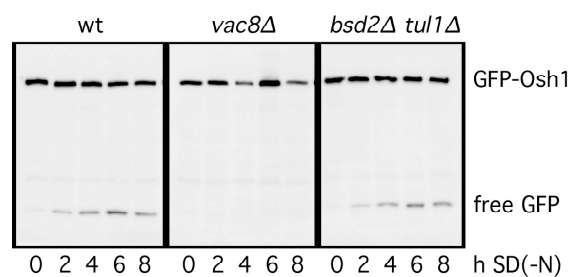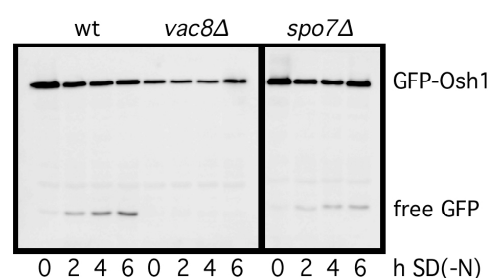

Fig. 38 Analysis of a mutant with misshaped nucleus
All strains were BY4741 background. Cells were transformed with GFP-Osh1. Western blot of alkaline lysed stationary (0 h) and starved (2 – 6 h SD(-N)) yeast cells. GFP-Osh1 and free GFP were detected using a mouse monoclonal GFP antibody.

Spo7Δ cells showed a reduction in free GFP in 2 of 3 experiments compared to wild type cells.

4.2.12 Summary of strains required for PMN identified in this study

Tab. 14 All strains were transformed with GFP-Osh1.

Strain	Free GFP	Times reproduced
Fig. 29 Cdc48.3		
cdc48.3	-	6*

Strain	Free GFP	Times reproduced
Fig. 30 Cdc48 substrate recruiting adaptors		
ubx1Δ / shp1Δ	-	3
ubx2Δ	+	2
ubx3Δ	+	2
ubx4Δ	+	2
ubx5Δ	+	2
ubx6Δ	+	2
ubx7Δ	+	2

Strain	Free GFP	Times reproduced
Fig. 31 complex partners of Cdc48		
der1Δ	+	1

Strain	Free GFP	Times reproduced
dfm1Δ	+	1
otu1Δ	+	1
ufd1_1	+***	1
ufd2Δ	+	1
ufd3Δ / doa1Δ	reduced	1

Fig. 32 Ubiquitin		
doa4Δ	-	3

Fig. 33 Ubp3 and Bre5		
bre5Δ	-	3
ubp3Δ	-	3

Fig.34 VPS class E		
vps27Δ	-	3
vps28Δ	-	3

Fig. 35 Further strains involved in MVB		
bsd2Δ tul1Δ	+	1

Fig. 36 Fatty acid elongation machinery		
elo2Δ	+	1
elo3Δ	+	1
otu1Δ	+	1

Fig. 37 Cortical ER inheritance		
ice2Δ	+	1
myo4Δ	+	1
rtn1Δ	+	1
scs2Δ	+	1
she2Δ	+	1
she3Δ	+	1
yop1Δ	+	1

Fig. 38 Misshaped nucleus		
spo7Δ	reduced**	3

+ = with free GFP   - = blocked / reduced free GFP
* in two backgrounds (WCG4a and BY4741)
** in 2 of 3 experiments
*** problems with background

4.2.13 Summary of strains required for autophagy identified in this study

Tab. 15 All strains were transformed with GFP-Atg8.

Strain	Free GFP
Fig. 29 Cdc48.3	
cdc48.3	-*
Fig. 30 Cdc48 substrate recruiting adaptors	
ubx1Δ / shp1Δ	-
Fig. 31 complex partners of Cdc48	
ufd3Δ / doa1Δ	reduced
Fig. 32 Ubiquitin	
doa4Δ	-
Fig. 33 Ubp3 and Bre5	
bre5Δ	+
ubp3Δ	+
Fig. 34 VPS class E	
vps27Δ	+
vps28Δ	+

+ = with free GFP   - = blocked / reduced free GFP
* in two backgrounds (WCG4a and BY4741)

5. Discussion

5.1. Where are the autophagic membranes coming from?

Autophagy starts at the pre- autophagosomal structure (PAS; phagophore assembly site). Out of this structure double membrane layered vesicles are formed and transported to the vacuole, where their outer membranes fuse with the vacuole, releasing a monolayered vesicle (autophagic body) into the vacuolar lumen. The PAS is believed to be an organelle-like membrane structure. Therefore a membrane source for the PAS itself and the formation of vesicles out of the PAS is required. Different cell compartments have been discussed as potential membrane sources (Ishihara, 2001) (Reggiori, 2004) (Reggiori, 2005) (Young, 2006) (Xie, 2008). The transmembrane protein Atg9 is suggested to be involved in transport of membrane to the PAS (Xie, 2008). It cycles between the PAS and a peripheral pool, which has been proposed to partially colocalizes with mitochondria (Reggiori, 2005) (Reggiori and Klionsky, 2006). Atg27 the second transmembrane protein located at the PAS is involved in the cycling of Atg9 (Yen, 2007). In *atg27Δ* and *atg1Δ atg27Δ* double knockout cells the localization of Atg9 to its peripheral pool is increased (Yen, 2007).

In this study the stability of the peripheral GFP-Atg9 pool as well as the colocalization of this pool to mitochondria was not reproducibly stable (data not shown). But the peripheral GFP-Atg9 dots were completely lost in *atg4Δ atg27Δ* cells resulting in a diffuse signal (Fig. 16 (B.)). As Atg4 is required for the ubiquitin like conjugation of Atg8 to PE (phosphatidylethanolamine) (chapter 2.5.6.1 and Fig. 5) Atg8 is also a suitable candidate to follow the membrane flow.

During autophagy Atg8 localizes to the PAS. In addition to PE conjugation and the Atg12–Atg5-Atg16 complex, its proper localization requires Atg9 and the autophagy-specific phosphatidylinositol 3-kinase (PI3K) complex I (Xie, 2008). Atg8-PE is used as a common marker for autophagy. It is located to the inside and outside of the forming and completed autophagosomes but the coupling of Atg8 to PE is a reversible event. Atg8 is cleaved of from the outer membrane of the completed vesicles by Atg4 and is reused (Fig. 5).

Furthermore, among the core autophagic machinery, Atg8 is the only protein, which has a significant elevated protein level when autophagy is induced (Kirisako, 1999).

The enhanced Atg8 level could somehow trigger an enhanced membrane flow. Legesse-Miller et al. showed that Atg8 plays an additional role in constitutive protein transport pathways from the ER to the Golgi. They demonstrated that overexpression of Atg8 leads to suppression of the temperature sensitive phenotype of the SNARE mutants *bet1-1* and *sec22-2* (Legesse-Miller, 2000).

The results from Legese-Miller et al. were not reproducible in this study (data not shown).

Wild type cells expressing GFP-Atg8 from a CEN plasmid showed a diffuse vacuolar GFP signal and in some cells a PAS dot. In *atg1Δ* cells Atg8 was restricted to the PAS (>75% of cells had a PAS signal). The double knockout strain *atg1Δ atg27Δ*, that has been described to enrich GFP-Atg9 at a peripheral pool, showed also a PAS localization and an additional peripheral pool of GFP-Atg8 (Fig. 17).

The peripheral pool of Atg8 was detected at a ring around the vacuole where PI3P is located (Fig. 20). In *S. cerevisiae* the endomembrane system resides around the vacuole and contains PI3P as a typical lipid component (Di Paolo and De Camilli, 2006) (Gillooly, 2000). The endosomal localization of the peripheral pool of GFP-Atg8 was confirmed by colocalization using the chromosomally tagged endosomal protein Snf7-RFP (Fig. 21 (B.)). In addition *atg1Δ atg27Δ vps4Δ* cells showed an accumulation of GFP-Atg8 at its peripheral pool compared to *atg1Δ atg27Δ* cells (Fig. 21 (A.)). Inactivation of Vps4 results in the enrichment of the ESCRT machinery on the surface of endosomes and enlargement of the compartment (class E compartment) (Babst, 1997).

Thus all three results support a localization of the peripheral pool of Atg8 to endosomes.

The quantification of the peripheral pool of Atg8 showed that 40% of *atg1Δ atg27Δ* cells had more than two clear GFP dots. In contrast only 2% of the *atg1Δ* cells showed this phenotype. The deletion of Atg1 Atg27 and Vps4 additionally increased the number of cells showing a peripheral pool (Fig. 22).

To confirm these microscopic results subcellular fractionation experiments were done as an independent approach.

As control *atg4Δ atg8Δ* double deletion strains expressing either full length GFP-Atg8 or GFP-Atg8*, lacking the C-terminal arginine were analysed. The cells showed the expected shift of GFP-Atg8 from P100 (100000 g pellet) to P13 (13000 g pellet) as previously described by Kirisako et al. (Kirisako, 2000). No shift could be detected in

atg1Δ atg27Δ cells compared to *atg1Δ* cells (Fig. 23 (A.)). An additional experiment using a sucrose gradient to separate the peripheral pool from the PAS pool showed no significant difference between the two strains (Fig. 23 (B.)). The quality of the gradient was tested using the endosomal marker Pep12 that, as expected, primarily located in the same fractions as the main peak of GFP-Atg8.

Both fractionation experiments were unlikely to separate the PAS pool and the peripheral Atg8 pool. But they support the endosomal localization because of the overlap between Pep12 and GFP-Atg8 signal in the sucrose gradient.

Up to now there are no other methods available to clearly separate the PAS from other membranous organelles.

To investigate the involvement of the Atg8 conjugation machinery in the formation of the peripheral pool, two plasmids expressing a full length GFP-Atg8 and a GFP-Atg8*, lacking the C-terminal arginine were analysed. *In vivo* this arginine has to be cleaved of by Atg4 before Atg8 can be coupled to PE in an ubiquitin like reaction (chapter 2.5.6.1 and Fig. 5). In *atg4Δ atg8Δ* cells expressing GFP-Atg8 the GFP signal was mainly cytosolic and only a rare PAS signal was detected because Atg8 could not be coupled to PE (Fig. 18 (A.)). In contrast the GFP-Atg8* construct showed membranous structures colocalizing with the endosomal / vacuolar membrane marker FM4-64 (Fig 18 (B.)).

A GFP-Atg8-cherry protein was created to investigate if the cleavage of Atg8 by Atg4 and therefore the coupling to PE is required for the peripheral localisation of Atg8. The GFP-Atg8-cherry protein was expressed in different knockout cells. The cherry protein at the C-terminus of Atg8 did not influence the cleavage of GFP-Atg8-cherry by Atg4 (Fig. 19 (A.)). In *atg1Δ atg27Δ* cells the GFP signal of GFP-Atg8-cherry was visible at the peripheral pool. This pool vanished in cells additionally lacking Atg4 (Fig. 19 (B.)). But the GFP-Atg8-cherry only showed a diffuse microscopic cherry signal in all strains.

These data suggest that Atg4 and therefore the lipidation of Atg8 is required for the efficient localization of Atg8 to the PAS as well as its peripheral pool.

To show that the slight overexpression of the GFP-Atg8 from a CEN plasmid does not influence its localization, control strains as well as a *atg1Δ atg27Δ* strain expressing a chromosomally GFP-tagged Atg8 were constructed.

Atg1Δ atg27Δ cells often showed membranous GFP structures that did not resemble to endosomal structures but rarely dots (Fig. 24).

The plasmid and chromosomal GFP-Atg8 differ only in three minor points: the expression level, the remaining lox site between promoter and GFP and the linker connecting GFP with Atg8 (Fig. 25).

Only *atg1Δ atg27Δ* double mutant cells, expressing GFP-Atg8 from the plasmid, show a peripheral pool and not *atg1Δ* or *atg27Δ* single mutant cells. This result supports the assumption that the slight overexpression does not influence the localization, because the expression level is the same for all these strains.

The lox site leads to 23 additional amino acids (aa) in front of GFP and therefore may influence the folding of GFP but should not influence the function of Atg8, although this could not be excluded.

The difference between the two linker regions connecting GFP and Atg8 maybe is an explanation for the detected differences in the localization of chromosomally and plasmid expressed GFP-Atg8. Instead of two aa seven aa are inserted. This linker is part of Atg8 and could influence the folding and function of Atg8, which could lead to a mislocalization.

A direct detection of Atg8 with a specific antibody using immunogold EM in *atg1Δ atg27Δ* cells would be the best method to support the localization of Atg8 at endosomes. The antibody available for this study is not suitable for this purpose, because it hardly detects Atg8 in western blot or indirect immunofluorescence and has a high background signal (data not shown). The available antibody could be affinity purified or a new antibody could be generated. Alternatively a GFP monoclonal mouse antibody could be used in cells expressing GFP-Atg8 in immunogold EM, but this GFP-tagging could influence the correct localization of the fusion protein.

In this study GFP-Atg8 expressed from a CEN plasmid showed a peripheral pool colocalizing with endosomes. These results are consistent with the localisation data from Atg9 in mammalian cells pointing to endosomes and TGN (trans Golgi network) (Young, 2006).

Further studies concerning the peripheral pool of Atg8 could answer these questions:

Which proteins are required for the cycling of Atg8? Is the peripheral pool of GFP-Atg8 identical with the GFP-Atg9 pool? How do both cycling events correlate? Is

there more than one membrane source? May one peripheral pool serve as membrane source for the Cvt-pathway and the other for autophagy?

5.2 Micronucleophagy in *S. cerevisiae*

5.2.1 Micronucleophagy in *S. cerevisiae* requires the core autophagic genes

Autophagy is a highly conserved process in eukaryotes. In *S. cerevisiae* the autophagic processes can be divided in two fundamentally different subtypes: microautophagy and macroautophagy. During macroautophagic processes double membrane-layered vesicles are formed, that contain cytosolic material as well as whole organells. Through fusion with the vacuolar membrane a still monolayered autophagic body is released into the vacuole.

During microautophagic processes invaginations of the vacuolar membrane are formed, releasing a monolayered vesicle into the vacuole. The cargo of micro- and macroautophagic processes are degraded, recycled and reused for the synthesis of proteins strictly required for survival.

Micronucleophagy (piecemeal microautophagy of the nucleus, PMN) is a bona fide microautophagic process. In *S. cerevisiae* Nvj1 forms contact sites between the nucleus and the vacuole. This protein spans the outer nuclear ER membrane and interacts with the inner nuclear ER membrane and Vac8 on the vacuolar membrane (Pan, 2000) (Millen, 2008). Micronucleophagy is induced by nutrient depletion. A tethered bleb is formed at the NV-junction, that is limited by three membrane layers: vacuolar membrane, outer nuclear membrane and inner nuclear membrane (Fig. 8 and 9). Upon induction of micronuclophagy Nvj1 recruits two additional proteins to the NV junctions (Kvam, 2005): Tsc13 and Osh1, which are both involved in the lipid metabolism of the cell.

First studies suggested that the autophagic machinery is not required for PMN. The degradation of overexpressed marker proteins coupled to EYFP was measured in different yeast strains by quantifying the fusion protein using immunoblots. *Atg7Δ* cells showed comparable amounts of remaining fusion protein as wild type cells (Roberts, 2003) (Kvam, 2005) (Kvam and Goldfarb, 2006b). Atg7 is part of both

ubiquitin like conjugation systems during autophagy and is therefore strictly required for autophagic processes (Fig. 5). In contrast Krick et al. (Krick, 2008b) showed in a recent publication that PMN requires the core macroautophagy genes including Atg7. They analysed the degradation of the PMN marker protein GFP-Osh1 by quantifying the release of hydrolase resistant free GFP in the vacuole using western blot analysis.

This study supports the latter finding using another molecular approach. To trace the nuclear content *atg15Δ* cells expressing a nuclear resident NLS-2mcherry fusion protein were imaged. Atg15 is a putative lipase, required for the breakdown of intravacuolar vesicles. After starvation *atg15Δ* cells showed intravacuolar free floating cherry vesicles in videomicroscopy. In cells lacking Atg15 and Atg1 no vesicles are formed. This result supported the finding that the core autophagic machinery is required for PMN because Atg1 is essential for autophagosom formation (Fig. 26 (A.)).

The rare red PMN vesicles were clearly distinguishable from the highly enriched autophagosomes in the vacuole of *atg15Δ* cells (Fig. 26 (B.) and (C.)).

To analyze further autophagic mutants to their PMN phenotype, the vesicles had to be stabilized in the vacuole. PMSF inhibits the vacuolar hydrolase proteinase B leading to an accumulation of NLS-2mcherry vesicles and autophagosomes in the vacuolar lumen of wild type cells (Fig. 27). Autophagic mutants showed no free floating vesicles even under these stabilizing conditions (Fig. 27). This is in agreement with the western blot analysis from Krick et al. (Krick, 2008b) showing that the autophagic machinery is indeed required for micronucleophagy.

5.2.2 Induction of micronucleophagy

Different starvation media were tested to identify the best induction conditions for PMN. A quantification of three independent experiments revealed that SD(-N)-medium showed the highest amount of free GFP in western blot analysis. Rapamycin a TOR-kinase (target of rapamycin kinase) inhibitor and known to induce autophagy showed the same amount of free GFP up to 4 h starvation. Afterwards the free GFP signal decreased to 40% (Fig. 28). This indicates that rapamycin is either not stable over longer time periods or it also induces other proteins like hydrolases that increase the degradation of free GFP.

Potassium acetate induces autophagy using other signaling pathways as SD(-N) (unpublished data of the Thumm group) and showed a slower increase in free GFP compared to SD(-N) starvation. The addition of 2% glucose even decreased the free GFP measured.

PMN is highest induced under nitrogen starvation conditions (SD(-N)) and was therefore used for all further experiments in this study.

5.2.3 Membrane fusion in autophagy and PMN

All autophagic processes need membrane fusion events. Little is known about the components required for the different membrane fusions.

To set up a common fusion machinery, the two fusing membranes have to first undergo docking and priming, an ATP-dependent process (Klenchin and Martin, 2000) (Geumann, 2008). The required energy for membrane fusion is delivered by interaction of the SNAREs (soluble *NSF* attachment protein receptor) from opposing membranes and formation of a four-helical bundel in a process termed „zippering". After fusion, all fused SNAREs are located at the same membrane. They have to be disassembled to provide free SNARE molecules for further rounds of fusion, a process carried out by the AAA$^+$ ATPase NSF (*N*-ethylmaleimide-sensitive fusion protein; homologue in *S. cerevisiae*: Sec18) and its cofactor α-SNAP (soluble NSF attachment protein; homologue in *S. cerevisiae*: Sec17), in an energy-dependent process (Jahn and Scheller, 2006).

During PMN three membrane fusion events are necessary: fusion of the vacuolar membrane, the outer nuclear membrane and the inner nuclear membrane (Fig. 8). Krick et al. reported that the standard homotypic vacuolar fusion machinery is not required for the biogenesis of PMN vesicles. Some of the components seemed to be involved in PMN as Sec18 and Sec17, both fundamentally required for membrane fusion mediated by SNAREs, the HOPS complex, and the Rab-GTPase Ypt7, but this phenotype may only be due to the role of these components in vacuolar biogenesis (Krick, 2008b). The molecular composition of the machinery required for all three membrane fusion events is still unclear.

Autophagy also requires several membrane fusion events: membrane transport to the PAS (Atg9 / Atg8 cycling), sealing of the isolation membrane (autophagosome or

Cvt-vesicle formation) and fusion of the autophagosome with the vacuole.

Ishihara et al. showed that Sec18 and Sec17 are required for the fusion of autophagosomes with the vacuole but are not involved in autophagosome formation (Ishihara, 2001). The involvement of these proteins in autophagy could also be indirect due to the role in vacuolar biogenesis as it is proposed for PMN.

Cdc48, which shows significant homology with Sec18, is also an AAA^+ ATPase known to be required for ER homotypic fusion (Latterich, 1995). In yeast the ER membranes also form the nuclear membrane making Cdc48 a likely candidate to mediate at least one membrane fusion event during PMN.

Ishihara et al. showed that *cdc48-3ts* mutant cells cultured in SD(-N) at 34°C showed normal autophagic function compared to wild-type cells although ER fusion has been reported to be affected at this temperature (Latterich, 1995). Thus they concluded that Cdc48 is not required for autophagy (Ishihara, 2001).

In this study Cdc48-3 was crossed into two backgrounds (WCG: standard strain in the lab and BY4741: commercial available and widely used). In parallel the original strain W303 from the Latterich lab was analysed.

The restrictive temperature for each of the Cdc48.3 strains was determined using a growth phenotype. But the viability was not altered during the experiment at this temperature compared to wild type (data not shown). In the WCG background Cdc48.3 cells indeed showed a reduced PMN rate at the restrictive temperature but interestingly also an autophagic phenotype (Fig. 29 (I.)). This result could be reproduced in the BY4741 background even if the PMN and autophagic rate was also reduced at the permissive temperature (Fig. 29 (II.)).

A similar temperature sensitive-phenotype has been reported from Ye et al.. They tested the involvement of Cdc48 in ER protein degradation. They used the membrane protein substrate H-2K[b], a major histocompatibility complex (MHC) class I heavy chain that is quickly degraded in yeast in a proteasome-dependent manner (Casagrande, 2000). They reported that a significant stabilization of H-2K[b] was detected in the Cdc48 mutant (Cdc48-3), even at the permissive temperature. (Ye, 2001).

The wild type strain to the originally described Cdc48-3ts strain from Latterich et al. showed no PMN activity in the GFP-Osh1 assay. But autophagy was also reduced in the Latterich mutant strain at the restrictive temperature compared to wild type and the permissive temperature (Fig. 29 (III.)).

In contrast to Ishihara et al. this study suggests that Cdc48 is required for efficient autophagy and PMN.

Both studies differ in the determination of the restrictive temperature. Probably the temperature chosen from Ishihara et al. had only been too low to show an autophagic phenotype in the Cdc48.3 mutant in the used background.

Cdc48 is involved in many different cellular processes, including ubiquitin-dependent protein degradation and fusion of homotypic membranes (Ye, 2001) (Latterich, 1995) (chapter 2.6.1). The specificity and function of Cdc48 is regulated by different protein complexes (Tab. 1 Classification of Cdc48 cofactors in yeast).

p97 (the human homologue of Cdc48) and p47 (the human homologue of Shp1) control the fusion of homotypic membranes (Kondo, 1997) while ubiquitin-dependent protein degradation pathways require the Cdc48/p97 Ufd1-Npl4 complex (Braun, 2002) (Meyer, 2000) (Ye, 2001) (Jarosch, 2002).

Shp1 (Ubx1) belongs to the UBX protein family, which consists in *S. cerevisiae* of 7 proteins. UBX proteins have been described as general Cdc48 interacting proteins.

This study showed that for autophagy as well as PMN, indeed Shp1, a major substrate-recruiting factor, was essential (Fig. 30). The constitutive Cvt-pathway was unaffected in *shp1Δ* cells as determined by normal Ape1 maturation (Fig 30 (A.) bottom).

In addition to the UBX domain Shp1 possesses a ubiquitin-binding UBA domain that interacts with ubiquitylated proteins *in vivo*.

Binding of the human homologue p47 to ubiquitylated proteins via the UBA domain is required for efficient p97 / p47-mediated Golgi membrane fusion *in vitro* (Meyer, 2002). It has been further hypothesized that this ubiquitylated substrate serves as a fusion inhibitor and has to be extracted out of the membrane by p97 / p47 to mediate membrane fusion. It was postulated that Ufd1 / Npl4 targets multiubiquitylated substrates to Cdc48 destined for proteasomal degradation whereas p47 recruits monoubiquitylated substrates that should not be degraded (Meyer, 2002) (Wang, 2004b).

Loss of Doa4 depletes cellular ubiquitin levels, which causes many cellular defects, including loss of efficient MVB (multi vesicular body) sorting of some integral membrane proteins (Ren, 2008).

Autophagy and PMN were drastically reduced in *doa4Δ* cells (Fig. 32 (A.)). Further

experiments with different ubiquitin mutants showed that polyubiquitination is not necessary for PMN (Fig. 32 (B.)). Therefore free uncoupled ubiquitin is required for both processes (see discussion 5.2.5).

Ufd1 (ubiquitin fusion degradation) and Npl4 are both required for the Cdc48 protein degradation complex. Therefore a point mutant of Ufd1 (Ufd1.1), known to be defective in this function, was tested for PMN. But the corresponding wild type cells expressed the marker protein only at such low level that no free GFP was visible. Maybe the strain was contaminated or harmed during transport. In contrast the Ufd1.1 mutant cells showed free GFP and so Ufd1 may not be required for PMN. The Cdc48 additional substrate recruiting factors Dfm1 and Der1 and the substrate-processing factor Otu1 were also not required for efficient PMN (Fig. 31). The human deubiquitylating enzyme VCIP135 is part of the human mitotic Golgi reassembly machinery and harbors a domain with clear homology to UBX domains (Fig. 39). It is categorised as a substrate processing factor of Cdc48 and its closest *S. cerevisiae* homologue is Otu1. *Ufd3Δ* cells showed a reproducibly reduced free GFP signal and thereby a reduced PMN rate, but only a slight decrease in autophagy (Fig. 31).

Ufd3 (alias Doa1) contains seven WD40 repeats and two other functional domains. The central PFU domain of Ufd3 mediates interaction with ubiquitin whereas the C-terminal PUL domain interacts with Cdc48 (Ren, 2008). Ufd3 as well as Doa4 play a role in sorting of ubiquitinated membrane proteins into multivesicular bodies. It interacts with the Vps27-Hse1 complex. The loss of Ufd3 or Doa4 decreases cellular ubiquitin levels (Ghislain, 1996) (Mullally, 2006), but the Doa4 deletion leads to a more severe phenotype. The defects observed in *ufd3Δ* cells in MVB sorting of ubiquitinated cargo are independent of lower ubiquitin levels, which indicates a more direct role for Ufd3 in controlling the MVB sorting process (Ren, 2008). Ufd3 has the ability to displace Ufd2 from Cdc48 and thereby prevent polyubiquitination (Rumpf and Jentsch, 2006). Ufd3 was required for PMN and autophagy whereas Ufd2 was not required for PMN and not tested for autophagy (Fig. 31).

In contrast to Ufd3, no direct interaction or involvement of Doa4 with Cdc48 has been reported (Ren, 2008).

The requirement of Ufd3 and Doa4 in autophagy and PMN should be verified and the question if the observed reductions in both processes are due to a direct role of one of the proteins or mediated via the low ubiquitin levels should be addressed. Thus *udf3Δ* and *doa4Δ* cells could be transformed with ubiquitin overexpressing plasmids

and then tested for their autophagy and PMN rate in further experiments.

In Fig. 39 the hypothetic components required for membrane fusion of the human system (p97 (A.)) in mitotic Golgi reassembly are compared with the finding from this study concerning autophagy and PMN in *S. cerevisiae* (Cdc48 (B.)).
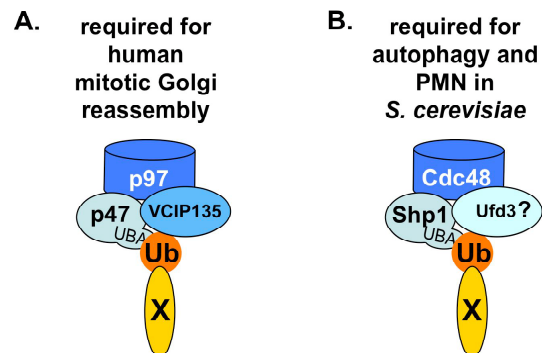
Fig. 39 Composition of CDC48 complexes in membrane fusion events
(A.) Hypothetic model complex for human mitotic Golgi (Meyer, 2005); **(B.)** Hypothetic Cdc48 model complex for *S. cerevisiae* autophagy and PMN; requirement of Ufd3 has to be validated; Ub = ubiquitin; X = unknown fusion inhibitor

The components shown in Fig. 39 (B.) are required for efficient PMN. Further experiments have to confirm their involvement in membrane fusion. One interesting question is which of the membrane fusion events is mediated by the Cdc48 complex. As described earlier in both processes (autophagy and PMN) at least three membrane fusion events have to proceed. Guan et al. published a protease protection assay for autophagy to distinguish between open and closed autophagosomes or fusion with the vacuole using pseudo-maturation of Ape1 via protease K (Guan, 2001) (Strømhaug, 2004). For this purpose a Ape1 maturation assay is not useful, because the Cvt-pathway, which transports Ape1 to the vacuole, is not impaired in Cdc48.3 or *shp1Δ* cells. Instead the pseudo-cleavage of GFP-Atg8 by trypsine could be monitored what has to be first established. Another approach could be electromicrographs to distinguish between wild type, *ypt7Δ* (where the autophagosomal fusion with the vacuole is impaired) and e.g. *shp1Δ* cells. Using these two methods it would be possible to distinguish if autophagosomes are closed in *shp1Δ* cells and still fuse with the vacuolar membrane or accumulate in the cytosol. The latter experiment could also exclude the possibility that the autophagic defect of Cdc48.3 and *shp1Δ* cells is due to an indirect effect like the impairment of the ER itself. Because Reggior et al. showed that in some early secretory mutants no autophagosomes are formed at all (Reggiori, 2004).

5.2.4 Ubp3 and Bre5 are only required for PMN

Kraft *et al.* observed that several GFP-fused ribosomal proteins of both 60S and 40S subunits, which were functional and correctly assembled into ribosomes, were delivered to and degraded in the vacuole of nitrogen starved yeast cells in an autophagy dependent manner. Thus they reported a selective autophagic process for ribosomes. Kraft et al. identified the ubiquitin deconjugation enzyme Ubp3 and its cofactor Bre5 as proteins required for the selective autophagic degradation of the 60S subunit of ribosomes under starvation conditions. The catalytic activity of Ubp3 is needed for ribophagy, implying the involvement of a deubiquination step from a yet unknown protein. Ubp3 and Bre5 are not required for unspecific macroautophagic breakdown of ribosomes (Kraft, 2008).

Micronucleophagy was also significantly reduced in *ubp3Δ* and *bre5Δ* cells whereas macroautophagy was normal (Fig. 33). Thus Ubp3 and Bre5 are involved in two selective autophagic processes. But not all selective autophagic processes require theses proteins, as the Cvt-pathway is not significantly affected in *ubp3Δ* or *bre5Δ* cells (Kraft, 2008). The requirement of Ubp3 and Bre5 additionally supports the involvement of (mono-) ubiquitination for PMN.

5.2.5 VPS class E genes are required for PMN

Vps27 and Vps28 are involved in the formation of multivesicular bodies and belong to the class E subgroup of vacuolar sorting proteins that are supposed to regulate trafficking between endosomes and the vacuole (Piper, 1995). Vps27 contains two putative ubiquitin-interacting motifs and could play a role in the sorting of mono-ubiquitinated proteins at endosomes (Stenmark, 2002) (Ren, 2008). Models suggest that the ubiquitinated cargo is captured by the Vps27-Hse1 complex. At a late stage of the sorting process, ubiquitin is removed from the cargo by the deubiquitinating enzyme Doa4 before incorporation of the cargo into intralumenal vesicles of the MVB pathway (Dupré and Haguenauer-Tsapis, 2001). As Ape1 is normally processed in VPS class E mutant strains, Reggiori et al. concluded that late endosomal functions are not required for the formation of Cvt- vesicles or autophagosomes (Reggiori,

2004).

Autophagy was normal in *vps27Δ* and *vps28Δ* cells, but the PMN rate was clearly reduced in these strains (Fig. 34). Interestingly *doa4Δ* showed a phenotype for both processes (Fig. 32 (A.)), which could be due to the requirement of free ubiqitin for both processes. However this does not explain the involvement of Vps27 and Vps28 exclusively for PMN. It is likely that membrane proteins needed for PMN are transported via the MVB pathway to the vacuole, where they either interact with the vacuolar membrane, participate in one of the membrane fusion events or in the generation of the NV-junction required for PMN vesicle formation.

Hettema et al. showed that Bsd2 and Tul1 are required for efficient ubiquitination of membrane proteins in the MVB pathway and contribute to the removal of misfolded membrane proteins (Hettema, 2004). Both proteins were not required for PMN (Fig. 35).

Other mutant strains exhibiting a MVB phenotype should be analyzed in further experiments.

5.2.6 The fatty acid elongation machinery is not required for PMN

Kvam et al. reported that the lumenal diameters of PMN blebs and vesicles are significantly reduced in *tsc13-1* and *tsc13-1 elo3Δ* mutant cells (Kvam, 2005). Elo2, Elo3, Tsc13 and YBR159 are proteins required for the elongation of very-long-chain fatty acids (VLCFAs) that localize to NV-junctions in *S. cerevisiae* (Kohlwein, 2001). These VLCFAs are enriched in lipid rafts and other detergent-insoluble lipid microdomains (Eisenkolb, 2002) (Dupré and Haguenauer-Tsapis, 2003). VLCFAs have been proposed to promote the formation of highly curved membrane structures (Schneiter and Kohlwein, 1997). Kvam et al. speculate that VLCFAs may be required for the efficient biogenesis of highly curved PMN vesicles (Kvam, 2005). *Tsc13* is an essential gene and was therefore not analyzed in this study. Cells lacking Elo2, Elo3 or YBR159 showed the same PMN rate as wild type cells (Fig. 36).

The structures Kvam et al. reported were visualized using an overexpressing Nvj1-EYFP reporter-construct. However, tagging and overexpression of proteins of the NV-junction apparatus could disturb the normal PMN process and are supposed to influence the size of PMN vesicles. A yeast cell has a diameter of about 5 µm and its nucleus about 1.5 µm. The reported PMN vesicles in wild type cells overexpressing

Nvj1 were 1.44 µm in diameter and therefore as big as the whole nucleus (Kvam, 2005) pointing to an aberrant size of PMN vesicles under these conditions. Kvam et al. further reported a reduction in the size of PMN vesicles to half in *tsc13-1 elo3Δ* mutant cells.

The aberrant size of the PMN vesicles in wild type and mutant cells could be due to overexpression of Nvj1 because in EM (electromicrograph) studies PMN vesicles of wild type cells have a diameter of about 150 µm (a tenth of the size reported by Kvam et al.) (Roberts, 2003) (Krick, 2008b). To investigate if the fatty acid elongation machinery has an influence on the size of these vesicles, cells with native Nvj1 levels should be analyzed. GFP-Osh1 could be used as a non-essential component of the NV-junction (Kvam and Goldfarb, 2004) to monitor the PMN vesicle size in fluorescence microscopy. Another approach to clarify this issue could be EM pictures from the corresponding knockout strains.

5.2.7 Proteins for cortical ER inharitance are not required for PMN

The cortical ER (cER) inheritance can be divided into three different stages: first, cytoplasmic ER tubules move along actin cables into small buds of the mother-bud axis (proteins tested in this study: Myo4, She3); second, the first domain of the cortical ER forms by attachment to the plasma membrane at the bud tip (proteins tested in this study: Yop1 and Rtn1); and third, cER spreads around the entire bud to form a polygonal tubular network (proteins tested in this study: Scs2 and Ice2) (Loewen, 2007).

Scs2, the yeast homolog of mammalian VAMP-associated protein, is further involved in targeting of Osh1 to cellular membranes, although Scs2 is not strictly required for the localization of GFP-Osh1 to NV junctions (Loewen, 2003).

All proteins tested, involved in the inheritance of cortical ER, were not required for the PMN process (Fig. 37).

5.2.8 Analysis of a mutant with misshaped nucleus

Spo7Δ cells are described to have a misshaped nucleus and exhibit a single nuclear protrusion (Campbell, 2006).

These cells showed a reduction in PMN rate in two of three experiments (Fig. 38). The reduction was not drastic and probably an indirect effect. Perhaps the NV-junctions can not be formed correctly as the nucleus is misshaped. The requirement of Spo7 has to be clarified in further experiments.

Further studies concerning PMN could answer these questions:

Is PMN a selective process? Which part of the nucleus is degraded? How specific and efficient is PMN? Which volume of the nucleus is degraded per time? How is the membrane curvature of PMN structures generated? In which step of PMN is the autophagic machinery involved? In which step of PMN is Cdc48 reqired?

6. Bibliography

Abeliovich, H., Zhang, C., Dunn, W.A., Shokat, K.M.und Klionsky, D.J. (2003). Chemical genetic analysis of Apg1 reveals a non-kinase role in the induction of autophagy. Mol Biol Cell *14*, 477-490.

Amar, N., Lustig, G., Ichimura, Y., Ohsumi, Y.und Elazar, Z. (2006). Two newly identified sites in the ubiquitin-like protein Atg8 are essential for autophagy. EMBO Rep *7*, 635-642.

Anderson, D.J.und Hetzer, M.W. (2007). Nuclear envelope formation by chromatin-mediated reorganization of the endoplasmic reticulum. Nat Cell Biol *9*, 1160-1166.

Baba, M., Osumi, M., Scott, S.V., Klionsky, D.J.und Ohsumi, Y. (1997). Two distinct pathways for targeting proteins from the cytoplasm to the vacuole/lysosome. The Journal of Cell Biology *139*, 1687-1695.

Baba, M., Takeshige, K., Baba, N.und Ohsumi, Y. (1994). Ultrastructural analysis of the autophagic process in yeast: detection of autophagosomes and their characterization. The Journal of Cell Biology *124*, 903-913.

Babst, M., Sato, T.K., Banta, L.M.und Emr, S.D. (1997). Endosomal transport function in yeast requires a novel AAA-type ATPase, Vps4p. EMBO J *16*, 1820-1831.

Barth, H., Meiling-Wesse, K., Epple, U.D.und Thumm, M. (2001). Autophagy and the cytoplasm to vacuole targeting pathway both require Aut10p. FEBS Letters *508*, 23-28.

Barth, H., Meiling-Wesse, K., Epple, U.D.und Thumm, M. (2002). Mai1p is essential for maturation of proaminopeptidase I but not for autophagy. FEBS Letters *512*, 173-179.

Braun, S., Matuschewski, K., Rape, M., Thoms, S.und Jentsch, S. (2002). Role of the ubiquitin-selective CDC48(UFD1/NPL4)chaperone (segregase) in ERAD of OLE1 and other substrates. EMBO J *21*, 615-621.

Buchberger, A., Howard, M.J., Proctor, M.und Bycroft, M. (2001). The UBX domain: a widespread ubiquitin-like module. J Mol Biol *307*, 17-24.

Campbell, J.L., Lorenz, A., Witkin, K.L., Hays, T., Loidl, J.und Cohen-Fix, O. (2006). Yeast nuclear envelope subdomains with distinct abilities to resist membrane expansion. Mol Biol Cell *17*, 1768-1778.

Casagrande, R., Stern, P., Diehn, M., Shamu, C., Osario, M., Zúñiga, M., Brown, P.O.und Ploegh, H. (2000). Degradation of proteins from the ER of S. cerevisiae requires an intact unfolded protein response pathway. Mol Cell *5*, 729-735.

Chen, N.und Karantza-Wadsworth, V. (2009). Role and regulation of autophagy in cancer. Biochim Biophys Acta.

Cheong, H., Yorimitsu, T., Reggiori, F., Legakis, J.E., Wang, C.W.und Klionsky, D.J. (2005). Atg17 regulates the magnitude of the autophagic response. Mol Biol Cell *16*, 3438-3453.

Coyle, J.E., Qamar, S., Rajashankar, K.R.und Nikolov, D.B. (2002). Structure of GABARAP in two conformations: implications for GABA(A) receptor localization and tubulin binding. Neuron *33*, 63-74.

Decottignies, A., Evain, A.und Ghislain, M. (2004). Binding of Cdc48p to a ubiquitin-related UBX domain from novel yeast proteins involved in intracellular proteolysis and sporulation. Yeast *21*, 127-139.

Di Paolo, G.und De Camilli, P. (2006). Phosphoinositides in cell regulation and membrane dynamics. Nature *443*, 651-657.

Du, Y. (2004). Dynamics and inheritance of the endoplasmic reticulum. Journal of Cell Science *117*, 2871-2878.

Dunn, W.A., Cregg, J.M., Kiel, J.A., van der Klei, I.J., Oku, M., Sakai, Y., Sibirny, A.A., Stasyk, O.V.und Veenhuis, M. (2005). Pexophagy: the selective autophagy of peroxisomes. Autophagy *1*, 75-83.

Dupré, S.und Haguenauer-Tsapis, R. (2001). Deubiquitination step in the endocytic pathway of yeast plasma membrane proteins: crucial role of Doa4p ubiquitin isopeptidase. Molecular and Cellular Biology *21*, 4482-4494.

Dupré, S.und Haguenauer-Tsapis, R. (2003). Raft partitioning of the yeast uracil permease during trafficking along the endocytic pathway. Traffic *4*, 83-96.

Eisenkolb, M., Zenzmaier, C., Leitner, E.und Schneiter, R. (2002). A specific structural requirement for ergosterol in long-chain fatty acid synthesis mutants important for maintaining raft domains in yeast. Mol Biol Cell *13*, 4414-4428.

Elazar, Z., Scherz-Shouval, R.und Shorer, H. (2003). Involvement of LMA1 and GATE-16 family members in intracellular membrane dynamics. Biochim Biophys Acta *1641*, 145-156.

Epple, U.D., Eskelinen, E.L.und Thumm, M. (2003). Intravacuolar membrane lysis in Saccharomyces cerevisiae. Does vacuolar targeting of Cvt17/Aut5p affect its function? J Biol Chem *278*, 7810-7821.

Epple, U.D., Suriapranata, I., Eskelinen, E.L.und Thumm, M. (2001). Aut5/Cvt17p, a putative lipase essential for disintegration of autophagic bodies inside the vacuole. J Bacteriol *183*, 5942-5955.

Farré, J.C., Manjithaya, R., Mathewson, R.D.und Subramani, S. (2008). PpAtg30 tags peroxisomes for turnover by selective autophagy. Dev Cell *14*, 365-376.

Farré, J.C.und Subramani, S. (2004). Peroxisome turnover by micropexophagy: an autophagy-related process. Trends Cell Biol *14*, 515-523.

Fasshauer, D., Sutton, R.B., Brunger, A.T.und Jahn, R. (1998). Conserved structural features of the synaptic fusion complex: SNARE proteins reclassified as Q- and R-SNAREs. Proc Natl Acad Sci USA *95*, 15781-15786.

Funakoshi, T., Matsuura, A., Noda, T.und Ohsumi, Y. (1997). Analyses of APG13 gene involved in autophagy in yeast, Saccharomyces cerevisiae. Gene *192*, 207-213.

Gasch, A.P., Spellman, P.T., Kao, C.M., Carmel-Harel, O., Eisen, M.B., Storz, G., Botstein, D.und Brown, P.O. (2000). Genomic expression programs in the response of yeast cells to environmental changes. Mol Biol Cell *11*, 4241-4257.

Gauss, R., Trautwein, M., Sommer, T.und Spang, A. (2005). New modules for the repeated internal and N-terminal epitope tagging of genes in Saccharomyces cerevisiae. Yeast *22*, 1-12.

Geumann, U., Barysch, S.V., Hoopmann, P., Jahn, R.und Rizzoli, S.O. (2008). SNARE function is not involved in early endosome docking. Mol Biol Cell *19*, 5327-5337.

Ghislain, M., Dohmen, R.J., Levy, F.und Varshavsky, A. (1996). Cdc48p interacts with Ufd3p, a WD repeat protein required for ubiquitin-mediated proteolysis in Saccharomyces cerevisiae. EMBO J *15*, 4884-4899.

Gillooly, D.J., Morrow, I.C., Lindsay, M., Gould, R., Bryant, N.J., Gaullier, J.M., Parton, R.G.und Stenmark, H. (2000). Localization of phosphatidylinositol 3-phosphate in yeast and mammalian cells. EMBO J *19*, 4577-4588.

Goder, V., Carvalho, P.und Rapoport, T.A. (2008). The ER-associated degradation component Der1p and its homolog Dfm1p are contained in complexes with distinct cofactors of the ATPase Cdc48p. FEBS Letters *582*, 1575-1580.

Goffeau, A., Barrell, B.G., Bussey, H., Davis, R.W., Dujon, B., Feldmann, H., Galibert, F., Hoheisel, J.D., Jacq, C., Johnston, M., Louis, E.J., Mewes, H.W., Murakami, Y., Philippsen, P., Tettelin, H.und Oliver, S.G. (1996). Life with 6000 genes. Science *274*, 546, 563-547.

Guan, J., Stromhaug, P.E., George, M.D., Habibzadegah-Tari, P., Bevan, A., Dunn, W.A.und Klionsky, D.J. (2001). Cvt18/Gsa12 is required for cytoplasm-to-vacuole transport, pexophagy, and autophagy in Saccharomyces cerevisiae and Pichia pastoris. Mol Biol Cell *12*, 3821-3838.

Harding, T.M., Morano, K.A., Scott, S.V.und Klionsky, D.J. (1995). Isolation and characterization of yeast mutants in the cytoplasm to vacuole protein targeting pathway. The Journal of Cell Biology *131*, 591-602.

Hartmann-Petersen, R., Wallace, M., Hofmann, K., Koch, G., Johnsen, A.H., Hendil, K.B.und Gordon, C. (2004). The Ubx2 and Ubx3 cofactors direct Cdc48 activity to proteolytic and nonproteolytic ubiquitin-dependent processes. Curr Biol *14*, 824-828.

He, C., Song, H., Yorimitsu, T., Monastyrska, I., Yen, W.L., Legakis, J.E.und Klionsky, D.J. (2006). Recruitment of Atg9 to the preautophagosomal structure by Atg11 is essential for selective autophagy in budding yeast. The Journal of Cell Biology *175*, 925-935.

Hettema, E.H., Valdez-Taubas, J.und Pelham, H.R. (2004). Bsd2 binds the ubiquitin ligase Rsp5 and mediates the ubiquitination of transmembrane proteins. EMBO J *23*, 1279-1288.

Hitt, R.und Wolf, D.H. (2004). Der1p, a protein required for degradation of malfolded soluble proteins of the endoplasmic reticulum: topology and Der1-like proteins. FEMS Yeast Res *4*, 721-729.

Hu, J., Shibata, Y., Voss, C., Shemesh, T., Li, Z., Coughlin, M., Kozlov, M., Rapoport, T.und Prinz, W. (2008). Membrane Proteins of the Endoplasmic Reticulum Induce High-Curvature Tubules. Science *319*, 1247-1250.

Huang, J.und Klionsky, D.J. (2007). Autophagy and human disease. Cell Cycle *6*, 1837-1849.

Hurley, J.H.und Emr, S.D. (2006). The ESCRT complexes: structure and mechanism of a membrane-trafficking network. Annual review of biophysics and biomolecular structure *35*, 277-298.

Hutchins, M.U.und Klionsky, D.J. (2001). Vacuolar localization of oligomeric alpha-mannosidase requires the cytoplasm to vacuole targeting and autophagy pathway components in Saccharomyces cerevisiae. J Biol Chem *276*, 20491-20498.

Ichimura, Y., Kirisako, T., Takao, T., Satomi, Y., Shimonishi, Y., Ishihara, N., Mizushima, N., Tanida, I., Kominami, E., Ohsumi, M., Noda, T.und Ohsumi, Y. (2000). A ubiquitin-like system mediates protein lipidation. Nature *408*, 488-492.

Ishihara, N., Hamasaki, M., Yokota, S., Suzuki, K., Kamada, Y., Kihara, A., Yoshimori, T., Noda, T.und Ohsumi, Y. (2001). Autophagosome requires specific early Sec proteins for its formation and NSF/SNARE for vacuolar fusion. Mol Biol Cell *12*, 3690-3702.

Jahn, R.und Scheller, R.H. (2006). SNAREs--engines for membrane fusion. Nat Rev Mol Cell Biol *7*, 631-643.

Jarosch, E., Taxis, C., Volkwein, C., Bordallo, J., Finley, D., Wolf, D.H.und Sommer, T. (2002). Protein dislocation from the ER requires polyubiquitination and the AAA-ATPase Cdc48. Nat Cell Biol *4*, 134-139.

Kabeya, Y., Kamada, Y., Baba, M., Takikawa, H., Sasaki, M.und Ohsumi, Y. (2005). Atg17 functions in cooperation with Atg1 and Atg13 in yeast autophagy. Mol Biol Cell *16*, 2544-2553.

Kamada, Y., Funakoshi, T., Shintani, T., Nagano, K., Ohsumi, M.und Ohsumi, Y. (2000). Tor-mediated induction of autophagy via an Apg1 protein kinase complex. The Journal of Cell Biology *150*, 1507-1513.

Kano, F., Kondo, H., Yamamoto, A., Kaneko, Y., Uchiyama, K., Hosokawa, N., Nagata, K.und Murata, M. (2005). NSF/SNAPs and p97/p47/VCIP135 are sequentially required for cell cycle-dependent reformation of the ER network. Genes Cells *10*, 989-999.

Katzmann, D.J., Babst, M.und Emr, S.D. (2001). Ubiquitin-dependent sorting into the multivesicular body pathway requires the function of a conserved endosomal protein sorting complex, ESCRT-I. Cell *106*, 145-155.

Kawamata, T., Kamada, Y., Kabeya, Y., Sekito, T.und Ohsumi, Y. (2008). Organization of the pre-autophagosomal structure responsible for autophagosome formation. Mol Biol Cell *19*, 2039-2050.

Kihara, A., Noda, T., Ishihara, N.und Ohsumi, Y. (2001). Two distinct Vps34 phosphatidylinositol 3-kinase complexes function in autophagy and carboxypeptidase Y sorting in Saccharomyces cerevisiae. The Journal of Cell Biology *152*, 519-530.

Kirisako, T., Baba, M., Ishihara, N., Miyazawa, K., Ohsumi, M., Yoshimori, T., Noda, T.und Ohsumi, Y. (1999). Formation process of autophagosome is traced with Apg8/Aut7p in yeast. The Journal of Cell Biology *147*, 435-446.

Kirisako, T., Ichimura, Y., Okada, H., Kabeya, Y., Mizushima, N., Yoshimori, T., Ohsumi, M., Takao, T., Noda, T.und Ohsumi, Y. (2000). The reversible modification regulates the membrane-binding state of Apg8/Aut7 essential for autophagy and the cytoplasm to vacuole targeting pathway. The Journal of Cell Biology *151*, 263-276.

Kissová, I., Deffieu, M., Manon, S.und Camougrand, N. (2004). Uth1p is involved in the autophagic degradation of mitochondria. J Biol Chem *279*, 39068-39074.

Klenchin, V.A.und Martin, T.F. (2000). Priming in exocytosis: attaining fusion-competence after vesicle docking. Biochimie *82*, 399-407.

Klionsky, D.J., Cregg, J.M., Dunn, W.A., Emr, S.D., Sakai, Y., Sandoval, I.V., Sibirny, A., Subramani, S., Thumm, M., Veenhuis, M.und Ohsumi, Y. (2003). A unified nomenclature for yeast autophagy-related genes. Dev Cell *5*, 539-545.

Klionsky, D.J., Cuervo, A.M.und Seglen, P.O. (2007). Methods for monitoring autophagy from yeast to human. Autophagy *3*, 181-206.

Kohlwein, S.D., Eder, S., Oh, C.S., Martin, C.E., Gable, K., Bacikova, D.und Dunn, T. (2001). Tsc13p is required for fatty acid elongation and localizes to a novel structure at the nuclear-vacuolar interface in Saccharomyces cerevisiae. Molecular and Cellular Biology *21*, 109-125.

Kondo, H., Rabouille, C., Newman, R., Levine, T.P., Pappin, D., Freemont, P.und Warren, G. (1997). p47 is a cofactor for p97-mediated membrane fusion. Nature *388*, 75-78.

Kraft, C., Deplazes, A., Sohrmann, M.und Peter, M. (2008). Mature ribosomes are selectively degraded upon starvation by an autophagy pathway requiring the Ubp3p/Bre5p ubiquitin protease. Nat Cell Biol *10*, 602-610.

Krick, R., Henke, S., Tolstrup, J.und Thumm, M. (2008a). Dissecting the localization and function of Atg18, Atg21 and Ygr223c. Autophagy *4*, 896-910.

Krick, R., Muehe, Y., Prick, T., Bremer, S., Schlotterhose, P., Eskelinen, E.L., Millen, J., Goldfarb, D.S.und Thumm, M. (2008b). Piecemeal microautophagy of the nucleus requires the core macroautophagy genes. Mol Biol Cell *19*, 4492-4505.

Krick, R., Mühe, Y., Prick, T., Bredschneider, M., Bremer, S., Wenzel, D., Eskelinen, E.L.und Thumm, M. (2009). Piecemeal microautophagy of the nucleus: Genetic and morphological traits. Autophagy *5*.

Krick, R., Tolstrup, J., Appelles, A., Henke, S.und Thumm, M. (2006). The relevance of the phosphatidylinositolphosphat-binding motif FRRGT of Atg18 and Atg21 for the Cvt pathway and autophagy. FEBS Letters *580*, 4632-4638.

Kuma, A., Mizushima, N., Ishihara, N.und Ohsumi, Y. (2002). Formation of the approximately 350-kDa Apg12-Apg5.Apg16 multimeric complex, mediated by Apg16 oligomerization, is essential for autophagy in yeast. J Biol Chem *277*, 18619-18625.

Kvam, E., Gable, K., Dunn, T.M.und Goldfarb, D. (2005). Targeting of Tsc13p to nucleus-vacuole junctions: a role for very-long-chain fatty acids in the biogenesis of microautophagic vesicles. Mol Biol Cell *16*, 3987-3998.

Kvam, E.und Goldfarb, D. (2004). Nvj1p is the outer-nuclear-membrane receptor for oxysterol-binding protein homolog Osh1p in Saccharomyces cerevisiae. Journal of Cell Science *117*, 4959-4968.

Kvam, E.und Goldfarb, D. (2006a). Structure and function of nucleus-vacuole junctions: outer-nuclear-membrane targeting of Nvj1p and a role in tryptophan uptake. Journal of Cell Science *119*, 3622-3633.

Kvam, E.und Goldfarb, D. (2007). Nucleus-vacuole junctions and piecemeal microautophagy of the nucleus in S. cerevisiae. Autophagy *3*, 85-92.

Kvam, E.und Goldfarb, D.S. (2006b). Nucleus-vacuole junctions in yeast: anatomy of a membrane contact site. Biochem. Soc. Trans *34*, 340-342.

Laemmli, U.K. (1970). Cleavage of structural proteins during the assembly of the head of bacteriophage T4. Nature *227*, 680-685.

Lang, T., Schaeffeler, E., Bernreuther, D., Bredschneider, M., Wolf, D.H.und Thumm, M. (1998). Aut2p and Aut7p, two novel microtubule-associated proteins are essential for delivery of autophagic vesicles to the vacuole. EMBO J *17*, 3597-3607.

Latterich, M., Fröhlich, K.U.und Schekman, R. (1995). Membrane fusion and the cell cycle: Cdc48p participates in the fusion of ER membranes. Cell *82*, 885-893.

Legesse-Miller, A., Sagiv, Y., Glozman, R.und Elazar, Z. (2000). Aut7p, a soluble autophagic factor, participates in multiple membrane trafficking processes. J Biol Chem *275*, 32966-32973.

Levine, B.und Kroemer, G. (2009). Autophagy in aging, disease and death: the true identity of a cell death impostor. Cell Death Differ *16*, 1-2.

Loewen, C., Young, B., Tavassoli, S.und Levine, T. (2007). Inheritance of cortical ER in yeast is required for normal septin organization. The Journal of Cell Biology *179*, 467-483.

Loewen, C.J., Roy, A.und Levine, T.P. (2003). A conserved ER targeting motif in three families of lipid binding proteins and in Opi1p binds VAP. EMBO J *22*, 2025-2035.

Longtine, M.S., McKenzie, A., Demarini, D.J., Shah, N.G., Wach, A., Brachat, A., Philippsen, P.und Pringle, J.R. (1998). Additional modules for versatile and economical PCR-based gene deletion and modification in Saccharomyces cerevisiae. Yeast *14*, 953-961.

Ma, J., Jin, R., Jia, X., Dobry, C.J., Wang, L., Reggiori, F., Zhu, J.und Kumar, A. (2007). An interrelationship between autophagy and filamentous growth in budding yeast. Genetics *177*, 205-214.

Majeski, A.E.und Dice, J.F. (2004). Mechanisms of chaperone-mediated autophagy. Int J Biochem Cell Biol *36*, 2435-2444.

Mariño, G.und López-Otín, C. (2008). Autophagy and aging: new lessons from progeroid mice. Autophagy *4*, 807-809.

Massey, A., Kiffin, R.und Cuervo, A.M. (2004). Pathophysiology of chaperone-mediated autophagy. Int J Biochem Cell Biol *36*, 2420-2434.

Meyer, H.H. (2005). Golgi reassembly after mitosis:
The AAA family meets the ubiquitin family. Biochimica et Biophysica Acta (BBA) - Molecular Cell Research *1744*, 465-517.

Meyer, H.H., Shorter, J.G., Seemann, J., Pappin, D.und Warren, G. (2000). A complex of mammalian ufd1 and npl4 links the AAA-ATPase, p97, to ubiquitin and nuclear transport pathways. EMBO J *19*, 2181-2192.

Meyer, H.H., Wang, Y.und Warren, G. (2002). Direct binding of ubiquitin conjugates by the mammalian p97 adaptor complexes, p47 and Ufd1-Npl4. EMBO J *21*, 5645-5652.

Millen, J., Pierson, J., Kvam, E., Olsen, L.und Goldfarb, D. (2008). The Luminal N-Terminus of Yeast Nvj1 is an Inner Nuclear Membrane Anchor. Traffic *9*, 1653-1664.

Mizushima, N., Noda, T., Yoshimori, T., Tanaka, Y., Ishii, T., George, M.D., Klionsky, D.J., Ohsumi, M.und Ohsumi, Y. (1998). A protein conjugation system essential for autophagy. Nature *395*, 395-398.

Monastyrska, I.und Klionsky, D.J. (2006). Autophagy in organelle homeostasis: peroxisome turnover. Mol Aspects Med *27*, 483-494.

Mühe, Y. (2007). Mikroautophagischer Abbau von Teilen der Kernhülle und Untersuchungen zum Transport und der Aktivität von Atg15p in der Hefe S. cerevisiae. Doktorarbeit, 132.

Mullally, J.E., Chernova, T.und Wilkinson, K.D. (2006). Doa1 is a Cdc48 adapter that possesses a novel ubiquitin binding domain. Molecular and Cellular Biology *26*, 822-830.

Nakamura, N., Matsuura, A., Wada, Y.und Ohsumi, Y. (1997). Acidification of vacuoles is required for autophagic degradation in the yeast, Saccharomyces cerevisiae. J Biochem *121*, 338-344.

Nakatogawa, H., Ichimura, Y.und Ohsumi, Y. (2007). Atg8, a ubiquitin-like protein required for autophagosome formation, mediates membrane tethering and hemifusion. Cell *130*, 165-178.

Nishida, K., Kyoi, S., Yamaguchi, O., Sadoshima, J.und Otsu, K. (2009). The role of autophagy in the heart. Cell Death Differ *16*, 31-38.

Obara, K., Noda, T., Niimi, K.und Ohsumi, Y. (2008a). Transport of phosphatidylinositol 3-phosphate into the vacuole via autophagic membranes in Saccharomyces cerevisiae. Genes Cells *13*, 537-547.

Obara, K., Sekito, T., Niimi, K.und Ohsumi, Y. (2008b). The Atg18-Atg2 complex is recruited to autophagic membranes via phosphatidylinositol 3-phosphate and exerts an essential function. J Biol Chem *283*, 23972-23980.

Oh-oka, K., Nakatogawa, H.und Ohsumi, Y. (2008). Physiological pH and acidic phospholipids contribute to substrate specificity in lipidation of Atg8. J Biol Chem *283*, 21847-21852.

Orvedahl, A.und Levine, B. (2009). Eating the enemy within: autophagy in infectious diseases. Cell Death Differ *16*, 57-69.

Palmer, G.E., Askew, D.S.und Williamson, P. (2008). The diverse roles of autophagy in medically important fungi. Autophagy *4*, 982-988.

Pan, X., Roberts, P., Chen, Y., Kvam, E., Shulga, N., Huang, K., Lemmon, S.und Goldfarb, D.S. (2000). Nucleus-vacuole junctions in Saccharomyces cerevisiae are formed through the direct interaction of Vac8p with Nvj1p. Mol Biol Cell *11*, 2445-2457.

Paz, Y., Elazar, Z.und Fass, D. (2000). Structure of GATE-16, membrane transport modulator and mammalian ortholog of autophagocytosis factor Aut7p. J Biol Chem *275*, 25445-25450.

Piper, R.C., Cooper, A.A., Yang, H.und Stevens, T.H. (1995). VPS27 controls vacuolar and endocytic traffic through a prevacuolar compartment in Saccharomyces cerevisiae. The Journal of Cell Biology *131*, 603-617.

Raasi, S.und Wolf, D. (2007). Ubiquitin receptors and ERAD: A network of pathways to the proteasome. Seminars in Cell & Developmental Biology *18*, 780-791.

Rabouille, C., Kondo, H., Newman, R., Hui, N., Freemont, P.und Warren, G. (1998). Syntaxin 5 is a common component of the NSF- and p97-mediated reassembly pathways of Golgi cisternae from mitotic Golgi fragments in vitro. Cell *92*, 603-610.

Rapoport, T.A., Rolls, M.M.und Jungnickel, B. (1996). Approaching the mechanism of protein transport across the ER membrane. Curr Opin Cell Biol *8*, 499-504.

Raymond, C.K., Howald-Stevenson, I., Vater, C.A.und Stevens, T.H. (1992). Morphological classification of the yeast vacuolar protein sorting mutants: evidence for a prevacuolar compartment in class E vps mutants. Mol Biol Cell *3*, 1389-1402.

Reggiori, F.und Klionsky, D.J. (2006). Atg9 sorting from mitochondria is impaired in early secretion and VFT-complex mutants in Saccharomyces cerevisiae. Journal of Cell Science *119*, 2903-2911.

Reggiori, F., Shintani, T., Nair, U.und Klionsky, D.J. (2005). Atg9 cycles between mitochondria and the pre-autophagosomal structure in yeasts. Autophagy *1*, 101-109.

Reggiori, F., Wang, C.W., Nair, U., Shintani, T., Abeliovich, H.und Klionsky, D.J. (2004). Early stages of the secretory pathway, but not endosomes, are required for Cvt vesicle and autophagosome assembly in Saccharomyces cerevisiae. Mol Biol Cell *15*, 2189-2204.

Ren, J., Pashkova, N., Winistorfer, S.und Piper, R. (2008). DOA1/UFD3 Plays a Role in Sorting Ubiquitinated Membrane Proteins into Multivesicular Bodies. Journal of Biological Chemistry *283*, 21599-21611.

Roberts, P., Moshitch-Moshkovitz, S., Kvam, E., O'Toole, E., Winey, M.und Goldfarb, D. (2003). Piecemeal microautophagy of nucleus in Saccharomyces cerevisiae. Mol Biol Cell *14*, 129-141.

Rössler, H., Rieck, C., Delong, T., Hoja, U.und Schweizer, E. (2003). Functional differentiation and selective inactivation of multiple Saccharomyces cerevisiae genes involved in very-long-chain fatty acid synthesis. Mol Genet Genomics *269*, 290-298.

Rubinsztein, D.C., DiFiglia, M., Heintz, N., Nixon, R.A., Qin, Z.H., Ravikumar, B., Stefanis, L.und Tolkovsky, A. (2005). Autophagy and its possible roles in nervous system diseases, damage and repair. Autophagy *1*, 11-22.

Rumpf, S.und Jentsch, S. (2006). Functional division of substrate processing cofactors of the ubiquitin-selective Cdc48 chaperone. Mol Cell *21*, 261-269.

Sakai, Y., Oku, M., van der Klei, I.J.und Kiel, J.A. (2006). Pexophagy: autophagic degradation of peroxisomes. Biochim Biophys Acta *1763*, 1767-1775.

Schneiter, R.und Kohlwein, S.D. (1997). Organelle structure, function, and inheritance in yeast: a role for fatty acid synthesis? Cell *88*, 431-434.

Schuberth, C.und Buchberger, A. (2008). UBX domain proteins: major regulators of the AAA ATPase Cdc48/p97. Cell. Mol. Life Sci. *65*, 2360-2371.

Schuberth, C., Richly, H., Rumpf, S.und Buchberger, A. (2004). Shp1 and Ubx2 are adaptors of Cdc48 involved in ubiquitin-dependent protein degradation. EMBO Rep *5*, 818-824.

Scott, S.V., Baba, M., Ohsumi, Y.und Klionsky, D.J. (1997). Aminopeptidase I is targeted to the vacuole by a nonclassical vesicular mechanism. The Journal of Cell Biology *138*, 37-44.

Smith, T.F., Gaitatzes, C., Saxena, K.und Neer, E.J. (1999). The WD repeat: a common architecture for diverse functions. Trends Biochem Sci *24*, 181-185.

Stenmark, H., Aasland, R.und Driscoll, P.C. (2002). The phosphatidylinositol 3-phosphate-binding FYVE finger. FEBS Letters *513*, 77-84.

Strømhaug, P.E., Reggiori, F., Guan, J., Wang, C.W.und Klionsky, D.J. (2004). Atg21 is a phosphoinositide binding protein required for efficient lipidation and localization of Atg8 during uptake of aminopeptidase I by selective autophagy. Mol Biol Cell *15*, 3553-3566.

Sugawara, K., Suzuki, N.N., Fujioka, Y., Mizushima, N., Ohsumi, Y.und Inagaki, F. (2004). The crystal structure of microtubule-associated protein light chain 3, a mammalian homologue of Saccharomyces cerevisiae Atg8. Genes Cells *9*, 611-618.

Suriapranata, I., Epple, U.D., Bernreuther, D., Bredschneider, M., Sovarasteanu, K.und Thumm, M. (2000). The breakdown of autophagic vesicles inside the vacuole depends on Aut4p. Journal of Cell Science *113 (Pt 22)*, 4025-4033.

Suzuki, K., Kirisako, T., Kamada, Y., Mizushima, N., Noda, T.und Ohsumi, Y. (2001). The pre-autophagosomal structure organized by concerted functions of APG genes is essential for autophagosome formation. EMBO J *20*, 5971-5981.

Suzuki, K., Kubota, Y., Sekito, T.und Ohsumi, Y. (2007). Hierarchy of Atg proteins in pre-autophagosomal structure organization. Genes Cells *12*, 209-218.

Swaminathan, S., Amerik, A.Y.und Hochstrasser, M. (1999). The Doa4 deubiquitinating enzyme is required for ubiquitin homeostasis in yeast. Mol Biol Cell *10*, 2583-2594.

Takeshige, K., Baba, M., Tsuboi, S., Noda, T.und Ohsumi, Y. (1992). Autophagy in yeast demonstrated with proteinase-deficient mutants and conditions for its induction. The Journal of Cell Biology *119*, 301-311.

Tal, R., Winter, G., Ecker, N., Klionsky, D.J.und Abeliovich, H. (2007). Aup1p, a yeast mitochondrial protein phosphatase homolog, is required for efficient stationary phase mitophagy and cell survival. J Biol Chem *282*, 5617-5624.

Thumm, M., Egner, R., Koch, B., Schlumpberger, M., Straub, M., Veenhuis, M.und Wolf, D.H. (1994). Isolation of autophagocytosis mutants of Saccharomyces cerevisiae. FEBS Letters *349*, 275-280.

Tsukada, M.und Ohsumi, Y. (1993). Isolation and characterization of autophagy-defective mutants of Saccharomyces cerevisiae. FEBS Letters *333*, 169-174.

Uchiyama, K., Jokitalo, E., Kano, F., Murata, M., Zhang, X., Canas, B., Newman, R., Rabouille, C., Pappin, D., Freemont, P.und Kondo, H. (2002). VCIP135, a novel essential factor for p97/p47-mediated membrane fusion, is required for Golgi and ER assembly in vivo. The Journal of Cell Biology *159*, 855-866.

Wang, Q., Song, C.und Li, C.C. (2004a). Molecular perspectives on p97-VCP: progress in understanding its structure and diverse biological functions. J Struct Biol *146*, 44-57.

Wang, Y., Satoh, A., Warren, G., Meyer, H.H.und Wang, Y. (2004b). VCIP135 acts as a deubiquitinating enzyme during p97-p47-mediated reassembly of mitotic Golgi fragments. The Journal of Cell Biology *164*, 973-978.

Woodman, P.G. (2003). p97, a protein coping with multiple identities. Journal of Cell Science *116*, 4283-4290.

Wurmser, A.E.und Emr, S.D. (2002). Novel PtdIns(3)P-binding protein Etf1 functions as an effector of the Vps34 PtdIns 3-kinase in autophagy. The Journal of Cell Biology *158*, 761-772.

Xie, Z.und Klionsky, D.J. (2007). Autophagosome formation: core machinery and adaptations. Nat Cell Biol *9*, 1102-1109.

Xie, Z., Nair, U.und Klionsky, D.J. (2008). Atg8 controls phagophore expansion during autophagosome formation. Mol Biol Cell *19*, 3290-3298.

Yamada, T., Carson, A.R., Caniggia, I., Umebayashi, K., Yoshimori, T., Nakabayashi, K.und Scherer, S.W. (2005). Endothelial nitric-oxide synthase antisense (NOS3AS) gene encodes an autophagy-related protein (APG9-like2) highly expressed in trophoblast. J Biol Chem *280*, 18283-18290.

Yang, Q., She, H., Gearing, M., Colla, E., Lee, M., Shacka, J.J.und Mao, Z. (2009). Regulation of neuronal survival factor MEF2D by chaperone-mediated autophagy. Science *323*, 124-127.

Yang, Z., Huang, J., Geng, J., Nair, U.und Klionsky, D.J. (2006). Atg22 recycles amino acids to link the degradative and recycling functions of autophagy. Mol Biol Cell *17*, 5094-5104.

Ye, Y., Meyer, H.H.und Rapoport, T.A. (2001). The AAA ATPase Cdc48/p97 and its partners transport proteins from the ER into the cytosol. Nature *414*, 652-656.

Yen, W.L., Legakis, J.E., Nair, U.und Klionsky, D.J. (2007). Atg27 is required for autophagy-dependent cycling of Atg9. Mol Biol Cell *18*, 581-593.

Yorimitsu, T.und Klionsky, D.J. (2005). Autophagy: molecular machinery for self-eating. Cell Death Differ *12 Suppl 2*, 1542-1552.

Young, A.R., Chan, E.Y., Hu, X.W., Köchl, R., Crawshaw, S.G., High, S., Hailey, D.W., Lippincott-Schwartz, J.und Tooze, S.A. (2006). Starvation and ULK1-dependent cycling of mammalian Atg9 between the TGN and endosomes. Journal of Cell Science *119*, 3888-3900.

Yu, L., Wan, F., Dutta, S., Welsh, S., Liu, Z., Freundt, E., Baehrecke, E.H.und Lenardo, M. (2006). Autophagic programmed cell death by selective catalase degradation. Proc Natl Acad Sci USA *103*, 4952-4957.

Yuan, W., Tuttle, D.L., Shi, Y.J., Ralph, G.S.und Dunn, W.A. (1997). Glucose-induced microautophagy in Pichia pastoris requires the alpha-subunit of phosphofructokinase. Journal of Cell Science *110 (Pt 16)*, 1935-1945.

Danksagung

Ein ganz besonderer Dank geht an Prof. Michael Thumm, für die Bereitstellung des sehr interessanten Themas und die Betreuung dieser Arbeit, sowie für die Unterstützung in den letzten drei Jahren.

Prof. Gerhard Braus möchte ich für seine Tätigkeit als Co-Referent meiner Arbeit danken.

Neben Prof. Thumm danke ich den beiden weiteren Mitgliedern meines Thesis Committees, Prof. Gerhard Braus und Dr. Dirk Fasshauer für ihre Anregungen und wertvollen Vorschläge zu meinem Projekt.

Herzlich danken möchte ich Rosi für ihre Unterstützung in allen Situationen und ihre Diskussionsbereitschaft zu dieser Arbeit.

Besonders danken möchte ich Prof. Doenecke für sein Engagement im Graduiertenkolleg 521. Dank geht auch an die anderen Doktoranden des Graduiertenkollegs, für die lehrreichen Seminare und die schöne gemeinsame Zeit.

In den drei Jahren in der Biochemie II habe ich viel Neues gelernt und Schönes erlebt. Besonders bedanken möchte ich mich bei meinen Kolleginnen und Kollegen Anika, Jörn, Sandra, Tanja, Yvonne, Jenny, Tanja, Petra und allen anderen Mitarbeitern der Biochemie II.
Evelyn, Petra und Rosi, die es bis zum Ende mit mir im Keller ausgehalten und für ein angenehmes Arbeitsklima gesorgt haben, sind besonders hervorzuheben!

Ein riesengroßes Dankeschön geht an meine Eltern und meine Schwester für ihren Glauben an mich und ihre immer andauernde Unterstützung.
Dir, Johanna danke ich für Deine liebevolle Unterstützung seit schon fast 7 Jahren!

CURRICULUM VITAE

Persönliche Angaben

Name:	Sebastian Bremer
Geburtsdatum:	13. Februar 1979
Geburtsort:	Hannover
Staatsangehörigkeit:	deutsch

Ausbildung

Seit 03.2006	**Dissertation an der Georg-August-Universität Göttingen** Institut für Biochemie II, Zentrum Biochemie und Molekulare Zellbiologie, Prof. Dr. Michael Thumm **Thema:** Molecular analysis of vesicle biogenesis in autophagy
10.2000 – 02.2006	**Studium der Biologie an der Leibniz Universität Hannover** Hauptfach: Mikrobiologie Nebenfächer: Genetik und Immunologie **Diplomarbeit** an der Medizinischen Hochschule Hannover Klinische Immunologie, Prof. Dr. Roland Jacobs **Thema:** Untersuchungen zur Aktivierbarkeit von Subpopulationen natürlicher Killerzellen des Menschen
08.1999 – 6.2000	**Ausbildung zum Rettungssanitäter** beim Deutschen Roten Kreuz im Rahmen des Zivildienstes
08.1991 – 06.1999	**Gymnasium Bad Nenndorf und Ratsgymnasium Stadthagen**, Humanistischer Zweig
08.1985 – 08.1991	**Grundschule und Orientierungsstufe** in Bad Nenndorf